



**Ernest Orlando Lawrence**  
**Berkeley National Laboratory**  
1 Cyclotron Road, 70R0108B  
Berkeley CA 94720-8168  
(510) 495-2679; fax: (510) 486-4260

May 11, 2014

Mr. Tien Q. Duong  
3V/Forrestal Building  
Office of Vehicle Technologies  
U.S. Department of Energy  
1000 Independence Avenue, S.W.  
Washington D.C. 20585

Dear Tien,

Here is the second quarter FY 2014 report for the Batteries for Advanced Transportation Technologies (BATT) Program. This report and prior Program reports can be downloaded from <http://batt.lbl.gov/reports/quarterly-reports/>.

Sincerely,

Venkat Srinivasan  
Acting Head  
BATT Program

edited by: V. Battaglia  
M. Foure  
S. Lauer  
M. Minamihara

cc: J. Barnes DOE/OVT  
P. Davis DOE/OVT  
D. Howell DOE/OVT  
P. Smith DOE/OVT  
J. Muhlestein DOE-BSO

## Featured Highlights

### *Anodes*

- ✚ Wang (Penn State), Kumta (Pittsburgh), and Cui (Stanford) all developed cyclable Si anodes with low 1<sup>st</sup> cycle capacity loss.

### *Cathodes*

- ✚ Looney and Wang (BNL) used a combination of characterization techniques, including *in situ* synchrotron XRD, to determine how to synthesize single crystal nanoparticles of  $\text{Li}_3\text{V}_2(\text{PO}_4)_3$ .

### *Diagnostics*

- ✚ Yang and Nam (BNL) used *in situ* XAS to show that the Mn-O bond of a Mn-rich layered cathode material changes continuously during a 15 minute hold at 5 V whereas the Ni-O and Co-O bonds stop changing after the first 3 minutes.

### *Modeling*

- ✚ Srinivasan (LBNL) shows that the polarization of the interface between a single ion conductor and an organic electrolyte is around  $400 \Omega\text{cm}^2$  and nearly independent of solvent or concentration of the salt.
- ✚ Ceder (MIT) believes the latest round of calculations of a cation-disordered material with superior Li migration properties may point to a new class of materials with high capacity for Li and high-energy density.

## Task 1.1 - Vincent Battaglia (Lawrence Berkeley National Laboratory)

### Electrode Failure Benchmarking Analysis

**PROJECT OBJECTIVE:** This project is to support the BATT Focus Groups. The emphasis of this work will be on the High-Voltage Cathode Project and the Si Anode Project. If the difference in cycleability of NMO and NCM can be understood through identification of a difference in reaction products, then perhaps the cycleability of NCM at higher voltages can be improved. If differences between the side reactions on graphite and Si can be measured, than perhaps the Si surface can be modified to allow for long-term full cell cycleability comparable to that of cells containing graphite.

**PROJECT IMPACT:** Success with understanding and improving the stability of NCM in the presence of electrolyte at voltages greater than 4.3 V vs. Li/Li+ will translate to an increase in capacity and voltage and hence a compounding improvement in energy density. Improvement in the passivating effects of SEI on Si that allows for long term cycleability, would result in larger fractions of Si in the anode and improved energy density of high-capacity cathode cells.

**OUT-YEAR GOALS:** The goal of this project is to support the High-Voltage Focus Group, which is to understand the limits of cycleability of NCM as the voltage is increased. This project will provide electrochemical and chemical data to support that effort. The other goal of the project is to support the Si Anode Focus Group, which is to effectively use Si in a battery. This project will provide electrochemical and chemical data to support that effort.

**COLLABORATIONS:** None this quarter.

### Milestones

- 1) Make a pouch cell with the same cycling behavior as a coin cell. (Dec. 13) **Complete**
- 2) Go/No-Go: Generate measurable levels of soluble reaction products. Criteria: Evaluate one of the proposed experimental test set-ups for its ability to generate measurable levels of soluble reaction products. (Mar. 14) **Go for generate measureable levels of soluble reaction products**
- 3) Demonstrate a 3-electrode cell where the impedance data of the individual electrodes can be directly assigned to the full cell data. (Jun. 14) **Ongoing**
- 4) Measure the gas composition of a high voltage cell. (Sep. 14) **Ongoing**
- 5) Measure the gas composition of a Si-anode cell. (Sep. 14) **Ongoing**

## Progress Report

The figure to the right shows the amount of dissolution of Mn from a cathode of NCM held at different potentials for a period of two weeks at 25°C. The electrolyte is 1 M LiPF<sub>6</sub> in EC:DEC at 1:2. The Mn lost per gram of cathode material is plotted on the primary axis and the mass of Mn per total mass of Mn in the cathode is plotted on the secondary. One sees from this data that there is a slight dependence of Mn dissolution with potential from 3.6 V up to 4.2 V, increasing slightly as the potential is increased. Above this 4.2 V, there is a rapid increase in the amount of Mn dissolution.

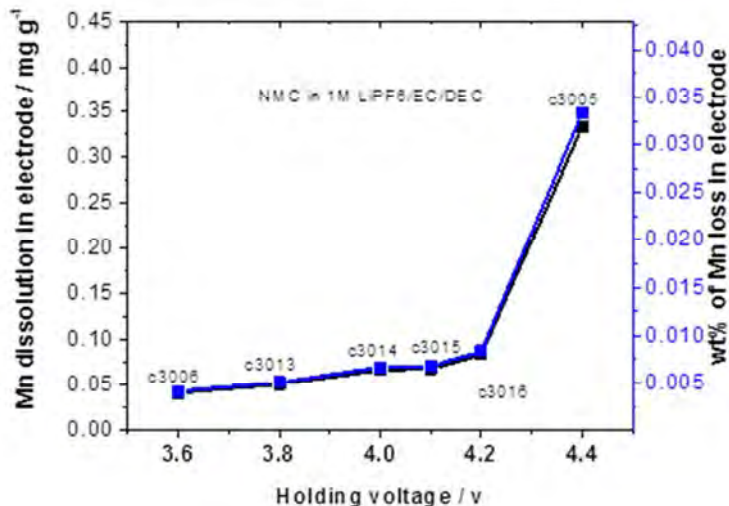


**Figure 1.** Amount of Mn lost from a cathode of NCM held at different voltages for two weeks at 25°C.

Most cells with NCM are not cycled to voltages higher than 4.2 V. It is not absolutely clear why NCM cells are not cycled much higher than this potential, but perhaps this dissolution measurement is a clue. Many of the oxides used in Li-ion batteries are not charged beyond the point where half of the Li is removed. It is generally understood that the material becomes unstable and collapses beyond 50% Li removal. It is possible that the same process occurs for the NCM material and that the collapsing structure also results in the loss of Mn from the material.

This data is one point in time at each potential and hence it is only a snapshot of the Mn dissolution. Little can be inferred about the rate of dissolution, whether it all occurs at once or steadily over the two week period. Thus, more experiments must be performed to determine the reaction mechanism. Overall, this relatively consistent data indicates that this set-up for measuring NCM dissolution is a **Go**.

## Task 1.2 - Karim Zaghib (Hydro-Québec)

### Assembly of Battery Materials and Electrodes

**PROJECT OBJECTIVE:** To develop high-capacity, low-cost electrodes with good cycle stability and rate capability to replace graphite in Li-ion batteries.

The *in situ* analyses of Si based electrodes showed that the bigger particles (*ca.* 13  $\mu\text{m}$ ) start to crack at around 0.1 V. During the charging process, all of the major cracks remained, while some fissures collapsed and others expanded, but the smaller particles (< 2  $\mu\text{m}$ ) did not crack. Furthermore, the *in situ* study revealed that delamination occurred at the interfaces of the particle/binder and the Cu current collector/electrode. These experiments provided a better understanding of the anode cycling mechanism and the failure mode associated with capacity fade. The results will be helpful to redesign the anode architecture. This study will also be beneficial to design the architecture of the high-voltage cathode (LMNO).

**PROJECT IMPACT:** This project will have a major impact on the wide spread adoption of EVs by (i) demonstrating scale-up production of nano-Si powders (to kilogram levels) for advanced EV batteries, and (ii) improving electrode performance by the understanding gained from *in situ* SEM and TEM studies.

The success of the project will contribute to the advancement of EV battery technology by developing batteries with increased energy density and improved cycle life, leading to EVs with longer driving range.

**OUT-YEAR GOALS:** Complete the *in situ* SEM and TEM studies of the Si-anode material during electrochemical cycling and real-time monitoring of structure changes. These analyses will help to understand the failure mode and to guide further improvements in the electrode architecture. These studies will also help to investigate the high-voltage passivation layer to identify the appropriate electrolyte and electrode compositions. The results of this effort will help to identify an alternative supplier of Si powder material as a baseline for the BATT Program.

As a final goal, the optimized Si-anode and LiMnNiO-doped Cr cathode will be evaluated in a laminate 20 Ah Li-ion cell.

**COLLABORATIONS:** Collaborations with BATT members: Vince Battaglia and Gao Liu (LBNL) and John Goodenough (UT Austin.)

### Milestones

- 1) Identify Si-based anode materials that can achieve a capacity of 1200 mAh/g. (Dec. 13) **Complete**
- 2) Supply Si powder (1 Kg) from an alternative supplier as a baseline material for BATT PIs. (Mar. 14) **Complete**
- 3) Go/No-Go: Terminate production of Si powder in anode tests that show more than 20% capacity fade in the initial 100 cycles. Criteria: Supply laminated Si-based electrodes to BATT PIs. (Jun. 14) **Ongoing**
- 4) Supply a 20-Ah Li-ion flat cell based on Si and LiMNO materials to BATT PIs. (Sep. 14) **Ongoing**

## Progress Report

Based on the results obtained in the previous quarter, a suitable electrode composition was identified. The binder type, mixing method, and the loading of the electrodes are key parameters to define the architecture of the anode. Certain characteristics in the anode, such as the porosity and tortuosity, are key to cell performance. Other parameters can also affect the electrochemical performance of the electrode, such as the cut-off voltage, the depth of discharge, and the cycling rate. Electrodes made from an optimum composition (Si:Alginate:carbon with 50:25:25) by weight were evaluated based on cycling. It was found that monitoring the stress on Si-particles is a key parameter that affects the cycling performance. Previously, the upper limit of the stress was defined by the cycled capacity. At 40% DoD, a very stable reversible capacity of  $1670 \text{ mAh g}^{-1}$  with good coulombic efficiency was obtained, but with the cell cycled at 50% DoD, the capacity failed after less than 100 cycles. The discharge/charge curves for the 1<sup>st</sup> and 66<sup>th</sup> cycle show clearly different behavior (Fig. 1). When the cell is cycled at 100% DoD, the capacity fades rapidly and is comparable to the 50% DoD cell after 66 cycles. This result indicates that the capacity buffer is rapidly consumed when the particles experience high stress. Based on the fact that stable cycle life can be obtained, if the threshold of the stress is limited, a longer cycle life, with an acceptable capacity of  $1600 \text{ mAh g}^{-1}$ , can be achieved.

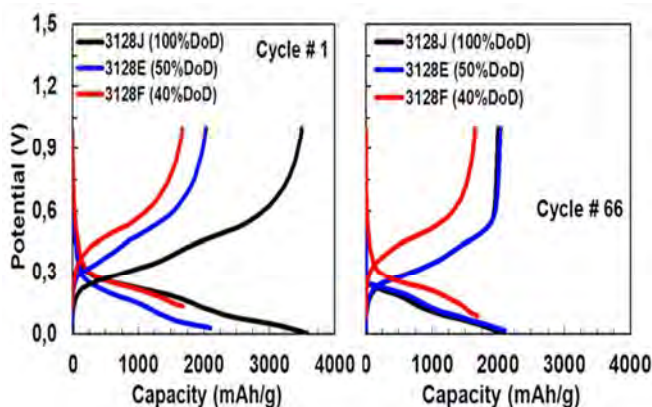


**Figure 1.** Discharge/charge curves at C/6 of Li/EC-DEC-LiPF<sub>6</sub>/Si cells for cycle 1 and 66.

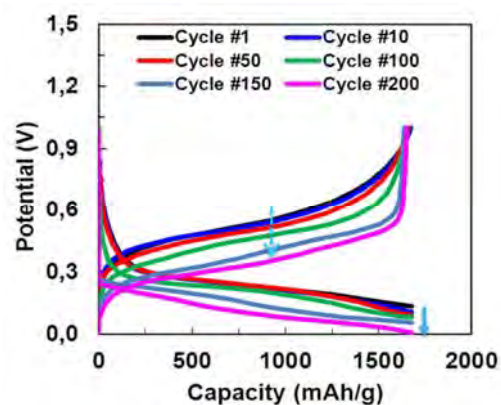


**Figure 2.** Voltage profiles at C/6 of Li/EC-DEC-LiPF<sub>6</sub>/Si cell as a function of cycle life.

The voltage profile of cells that demonstrated stable cycle life was investigated. Cells cycled at less than what may be called the threshold stress, such as the 40% DoD case, yielded stable capacity and an improved end of life. However, when the voltage at the end of discharge was shifted towards the cut-off voltage corresponding to 100% DoD (Fig. 2), a stable capacity was not achieved. The large volume change of the Si particles produced a loss of contact between the particles during cycling, and the residual capacity between 40 to 100% DoD was lost. This finding was confirmed previously by *in situ* SEM; the delamination and cracks were reduced by using smaller particles. With Si-nanoparticles, high reversible capacity is obtained, but in order to achieve much longer cycle life or higher reversible capacity, further work is necessary to understand the failure mode. Impedance spectroscopy will be used to monitor the interfacial resistances changes during the initial cycles to help improve the quality of our electrodes.

HQ has supplied a 20 Ah prototype stacking battery (V. Srinivasan) and 500 g of metallurgical Si material (G. Liu) to BATT PIs.

### Design and Scalable Assembly of High Density Low Tortuosity Electrodes

**PROJECT OBJECTIVE:** Develop a scalable high density binder-free low-tortuosity electrode design and fabrication process to enable increased cell-level energy density compared to conventional Li-ion technology. Characterize and optimize the electronic and ionic transport properties of controlled porosity and tortuosity electrodes as well as densely-sintered reference materials in  $\text{Li}(\text{Ni},\text{Co},\text{Al})\text{O}_2$  (NCA), high capacity  $\text{Li}_2\text{MnO}_3$ - $\text{LiMO}_2$  and high voltage  $\text{LiM}_{1-x}\text{Mn}_2\text{O}_4$  and  $\text{LiM}_{1-x}\text{Mn}_2\text{O}_4\text{F}_y$  spinels in order to elucidate rate limiting steps.

**PROJECT IMPACT:** The high cost (\$/kWh) and low energy density of current automotive Li-ion technology is in part due to the need for thin electrodes and associated high inactive materials content. If successful this project will enable use of electrodes based on known families of cathode and anode actives but with at least 3 times the areal capacity ( $\text{mAh}/\text{cm}^2$ ) of current technology while satisfying the duty cycles of vehicle applications. This will be accomplished via new electrode architectures fabricated by scalable methods with higher active materials density and reduced inactive content, and will in turn enable higher energy density and lower-cost EV cells and packs.

**OUT-YEAR GOALS:** After downselection of cathodes, identify an anode approach that therefore allows full cells in which both electrodes have high area capacity under EV operating conditions. Anode approach will include identifying compounds amenable to same fabrication approach as cathode, or use of very high capacity anodes such as stabilized Li or Si-alloys that in conventional form can capacity-match the cathodes. Use data from best performing electrochemical couple in techno-economic modeling of EV cell and pack performance parameters.

**COLLABORATIONS:** Within BATT, this project collaborates with Antoni P. Tomsia (LBNL) in fabrication of low-tortuosity, high-density electrodes by directional freeze-casting and sintering, and with Gao Liu (LBNL) in the Silicon Anode Focus Group on acoustic emission-based characterization of electrochemically-induced microfracture of Si anodes. Outside of BATT, the project collaborates with Randall Erb (Northeastern U.) on magnetic-alignment based fabrication of low tortuosity electrodes.

#### Milestones

- 1) Measure electronic and ionic conductivities and diffusivity in sintered dense  $\text{Li}(\text{Ni},\text{Co},\text{Al})\text{O}_2$  (NCA) and Fe-doped high voltage spinel  $\text{Li}_{1-x}\text{Mn}_{1.5}\text{Ni}_{0.5}\text{O}_4$  spinel. Fabricate first freeze-cast samples of at least one cathode composition (Dec. 13) **Complete**
- 2) Go/No-Go: Downselect one cathode composition for follow-on work. Criteria: Based on transport measurements and cycling tests of freeze cast and sintered electrodes. (Mar. 14) **Go for downselecting one cathode composition for follow-on work.**
- 3) Demonstrate at least  $5 \text{ mAh}/\text{cm}^2$  capacity per unit area at 1C continuous cycling rate for a freeze-cast cathode (Jun. 14) **Ongoing**
- 4) Demonstrate at least  $10 \text{ mAh}/\text{cm}^2$  capacity per unit area for a 2C 30 sec pulse for a freeze-cast cathode. (Sep. 14) **Ongoing**

## Progress Report

During this quarter, a Go/No-Go milestone was completed, whereby the downselect of a cathode composition for follow-on work was made on the basis of measurement of electronic and ionic transport and the fabrication and testing of freeze-cast electrodes in two candidate systems,  $\text{Li}(\text{Ni},\text{Co},\text{Al})\text{O}_2$  (NCA) and Fe-doped high voltage spinel  $\text{Li}_{1-x}\text{Mn}_{1.5}\text{Ni}_{0.5}\text{O}_4$  spinel.

Previously, under BATT support, it was shown that the introduction of aligned, dual-scale porosity into sintered  $\text{LiCoO}_2$  cathodes where electronic conductivity is not limiting permits *ca.* 3x higher area capacity ( $\text{mAh}/\text{cm}^2$ ) than in conventional electrodes at up to 2C rates. However,  $\text{LiCoO}_2$  is exceptional amongst intercalation cathodes in having unusually high electronic conductivity when delithiated beyond a few percent,  $\sigma_e > 1 \text{ S}/\text{cm}$ . Thus, the measurement of electronic conductivity, and its dependence on state-of-charge, is critical to identifying systems which, as a dense additive-free electrode, can result in very high area capacity electrodes ( $>10 \text{ mAh}/\text{cm}^2$ ) without having electrode polarization become limiting. Ionic conductivity in the solid phase is less concerning since, in the dense, thick electrode limit, salt depletion in the pore space becomes limiting (as shown by porous electrode models). In the work to date,  $\text{LiCoO}_2$ , NMC (1:1:1), NCA, LMNO, and Fe-LMNO have been evaluated (Fe-LMNO being preferred to LMNO for its electrochemical shock resistance.)

Of the candidate cathodes, NMC and the LMNOs appear to have too low electronic conductivity, and have been excluded in the downselect. NCA is also too electronically resistive in the fully dense limit, but as a porous electrode, in which electronic and ionic transport paths can be tuned through microstructure, it is promising. For further work in this project, NCA and LCO are viable candidates in the absence of the addition of a conductive agent.

This quarter, directional freeze-casting of  $\text{LiMn}_{1.5}\text{Ni}_{0.42}\text{Fe}_{0.08}\text{O}_4$  (Fe-LMNO) was completed, bringing the list of cathodes successfully fabricated by this method to LCO, NMC, NCA, and Fe-LMNO. However, as anticipated from the electronic conductivity of Fe-LMNO (reported last quarter), polarization prevents high utilization of single-phase sintered electrodes. In NCA, freeze-cast samples show that at C/50 rate a remarkably high area capacity of  $20 \text{ mAh}/\text{cm}^2$ , which is nearly 10x that of a conventional Li-ion electrode, can be achieved in a sample  $520 \mu\text{m}$  thick (Fig. 1). At C/20 rate, significant polarization has set in, which is consistent in magnitude and SOC dependence with electronic conductivity (being higher at low SOC) limitations. Thus, current efforts are aimed at tailoring the microstructure to shorten electronic path lengths in these electrodes in pursuit of the upcoming milestones.

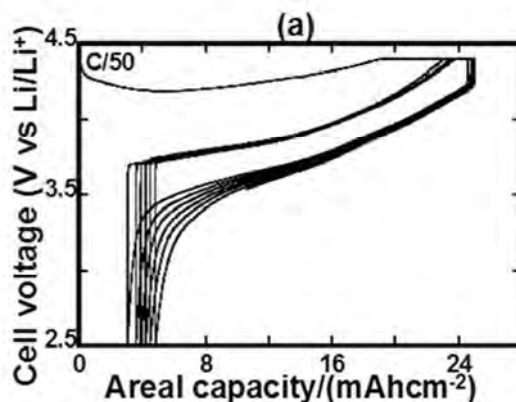


**Figure 1.** NCA freeze-cast electrode with  $20 \text{ mAh}/\text{cm}^2$  capacity at C/50 rate.

### Hierarchical Assembly of Inorganic/Organic Hybrid Si Negative Electrodes

**PROJECT OBJECTIVE:** This proposed work aims to enable Si as a high-capacity and long cycle-life material for negative electrode to address two of the barriers of Li-ion chemistry for EV/PHEV application: insufficient energy density and poor cycle life performance. The proposed work will combine material synthesis and composite particle formation with electrode design and engineering to develop high-capacity, long-life, and low cost hierarchical Si-based electrode. State of the art Li-ion negative electrodes employ graphitic active materials with theoretical capacities of 372 mAh/g. Silicon, a naturally abundant material, possesses the highest capacity of all Li-ion anode materials. It has a theoretical capacity of 4200 mAh/g for full lithiation to the  $\text{Li}_{22}\text{Si}_5$  phase. However, Si volume change disrupts the integrity of electrode and induces excessive side reactions, leading to fast capacity fade.

**PROJECT IMPACT:** This work addresses the adverse effects of Si volume change and minimizes the side reactions to significantly improve capacity and lifetime to develop negative electrode with Li-ion storage capacity over 2000 mAh/g (electrode level capacity) and significantly improve the coulombic efficiency to over 99.9%. The research and development activity will provide an in-depth understanding of the challenges associated with assembling large volume change materials into electrodes and will develop a practical hierarchical assembly approach to enable Si materials as negative electrodes in Li-ion batteries.

**OUT-YEAR GOALS:** There are three aspects of this proposed work - bulk assembly, surface stabilization and Li enrichment, which are formulated into 10 tasks in a four-year period. 1) Develop hierarchical electrode structure to maintain electrode mechanical stability and electrical conductivity. (Bulk assembly). 2) Form *in situ* compliant coating on Si and electrode surface to minimize Si surface reaction (surface stabilization). 3) Use prelithiation to compensate first cycle loss of the Si electrode. (Li enrichment) In the end of the 4th year, the goal is to achieve a Si-based electrode at higher mass loading of Si, and can be extensively cycled cycles with minimum capacity loss at high coulombic efficiency to qualify for vehicle application.

**COLLABORATIONS:** Vince Battaglia and Venkat Srinivasan (LBNL), Xingcheng Xiao (GM), Jason Zhang (PNNL), Chongming Wang (PNNL), Yi Cui (Stanford), and the Si-Anode Focus Group.

#### Milestones

- 1) Design and synthesize 3 more PEFM polymers with different EO content to study the adhesion and swelling properties of binder to the Si electrode performance. (Dec. 13) **Complete**
- 2) Go/No-Go: Down select Si vs. Si alloy particles and particle sizes (nano vs. micro.) Criteria: Down select based on cycling results. (Mar. 14) **Complete**
- 3) Prepare one type of Si/conductive polymer composite particles and test its electrochemical performance. (Jun. 14) **Ongoing**
- 4) Design and synthesize one type of vinylene carbonate (VC) derivative that is targeted to protect Si surface and test it with Si-based electrode. (Sep. 14) **Ongoing**

## Progress Report

Compared to EC, propylene carbonate (PC) is a promising solvent because it offers good ionic conductivity and superior low-temperature performance. This is due to its low-melting temperature of approximately  $-50^{\circ}\text{C}$ , which is far below that of EC ( $30^{\circ}\text{C}$ ). However, instead of forming an effective SEI, PC undergoes a detrimental decomposition process on graphite surfaces during cycling, causing exfoliation of the graphite and cell failure. Vinylene carbonate (VC) has been proven to be an effective additive for LIBs; previous studies indicate that the sacrificial decomposition of VC to form a stable SEI before the carbonate solvents are reduced, enables reversible cycling of graphite in PC-based electrolytes.

This quarter, the use of polymerized vinylene carbonate (polyVC) as a binder for graphite anodes in Li-ion cells was investigated. It functions not only as a traditional binder, but also plays an important role in surface stabilization of graphite in PC-based electrolytes. The polyVC binder enhanced battery performance in an electrolyte with PC content as high as 30 wt%, with a reversible capacity of *ca.*  $170\text{ mAh g}^{-1}$  at a delithiation rate of 1C, whereas a comparable graphite cell, fabricated with a polyvinylidene fluoride (PVDF) binder, failed to cycle.

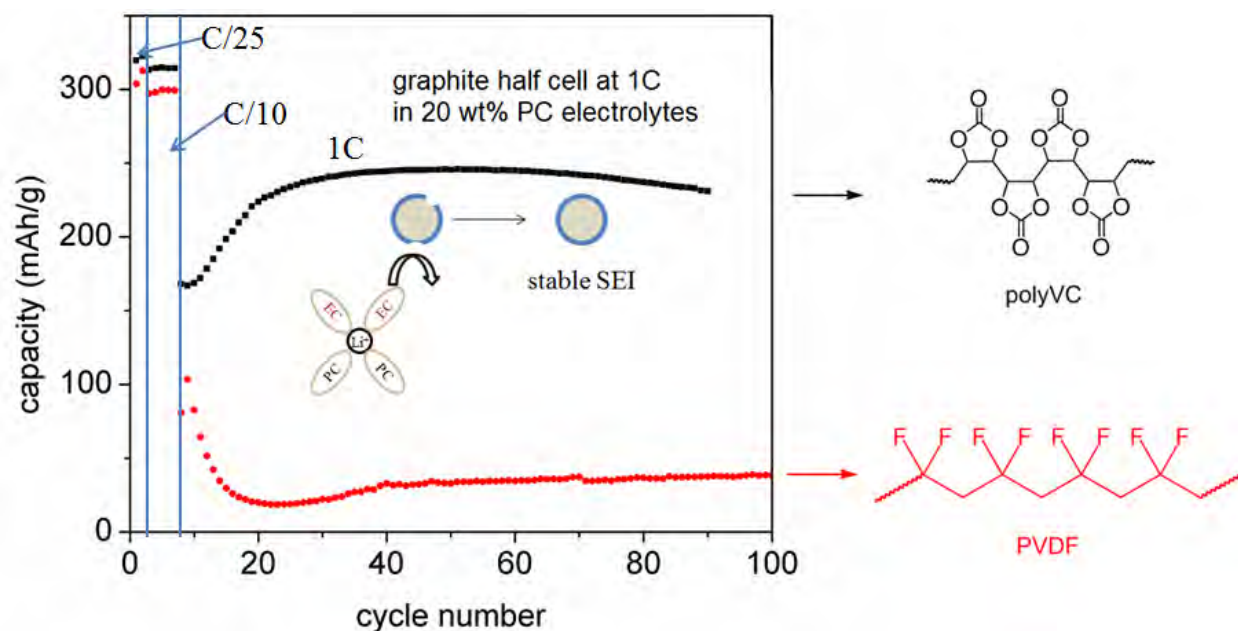


**Figure 1.** Cycling performance of graphite (CGP-G8, ConocoPhillips) half cells based on polyVC or PVDF binder, using 20% PC, 40% EC, 40% DEC and 1 M  $\text{LiPF}_6$ . The cell was put into formation for two cycles C/25, five cycles C/10 before cycling at 1C.

Figure 1 shows cycling performance with a Li counter electrode when the electrolyte was 20 wt% PC with 1 M  $\text{LiPF}_6$ . When 10 wt% PVDF was used as binder, the graphite half-cell cycled at a capacity of *ca.*  $30\text{ mAh g}^{-1}$ . With a stabilized capacity of *ca.*  $250\text{ mAh g}^{-1}$  at 1C for 10 wt% polyVC binder, there was an obvious advantage over the traditional PVDF binder. This new binder, inspired by a performance-enhancing electrolyte additive, could potentially address the undesirable low-temperature performance of state-of-art LIBs.

## Task 1.5 - Vincent Battaglia (Lawrence Berkeley National Laboratory)

### Electrode Fabrication and Materials Benchmarking

**PROJECT OBJECTIVE:** The objective of this task is to bring together a large fraction of the BATT community together to work on a single chemistry. Thus, the best combination of materials we can find will be provided to multiple researchers in the BATT Program for the Focus Groups. The Liu Group will be supplying the Si anodes and our group will develop matching cathodes of  $\text{LiFePO}_4$  that will be used to benchmark the effect of side reactions at the anode on cell capacity fade. For the High Voltage Focus group, our Group will benchmark (i.e. measure reversible capacity, rate performance, cycle efficiency.) the latest NMO material from NEI and an NCM material for comparative testing. This project also serves as a hub for testing new materials developed in the BATT Program.

**PROJECT IMPACT:** This project supports two focus groups. For the Si Focus Group, it is critical that the effect of the side reactions in a full cell are quantified as the side reaction on the Si is considered a major flaw of the material. For the High-Voltage Focus group, it is important to source good materials and to make good cells in order to compare the effects of side reactions on the performance of the active materials that address critical questions for the BATT Program. This project is the key to demonstrating progress within the program against industry standards.

**OUT-YEAR GOALS:** The long-term goal of this project is to support focus groups and identify and provide quality materials, electrodes, and cell performance data. This effort supplies a benchmark for the rest of the BATT Program to build upon. Advancing Li-ion chemistry through proper analysis of state-of-the-art materials.

**COLLABORATIONS:** Gao Liu (LBNL)

#### Milestones

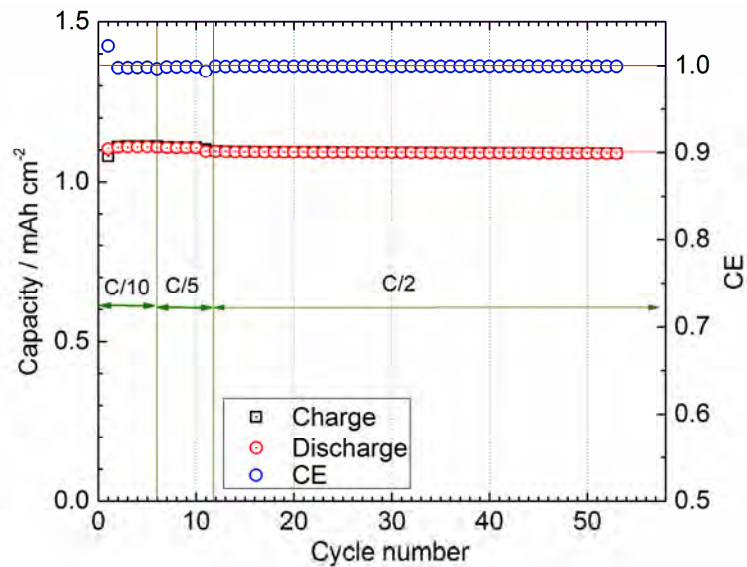
- 1) Go/No-Go: Decide if the newest NMO material from NEI should be the baseline material or not.  
Criteria: Benchmark the newest NMO material from NEI. (Dec. 13) **Go to use NMO.**
- 2) Identify the NCM baseline material. (Mar. 14) **Delayed to Jun. 14**
- 3) Demonstrate a cyclable  $\text{LiFePO}_4$  electrode. (Jun. 14) **Complete**
- 4) Measure the difference in side reactions of graphite and Si when cycled against  $\text{LiFePO}_4$ . (Sep. 14) **Ongoing**

## Progress Report

It took a little longer to receive baseline material than anticipated when the AOP was written last July. The material has been received but is undergoing performance evaluation. Hence, much of the research in this quarter was focused on the next quarter's milestone of producing a cyclable  $\text{LiFePO}_4$  (LFP) electrode with a high enough loading to cycle the Si-based anode of the Si Focus Group against it. That milestone was completed this quarter.

LFP has poor intrinsic electronic conductivity and Li diffusivity, which requires its particle size to be below  $1\ \mu\text{m}$  and electrodes of the material to contain larger than typical quantities of acetylene black to be of value in batteries designed for EVs. This large fraction of small, high-surface area material (the LFP and the carbon additive) favors aggregation during the electrode preparation process. In particular, electrodes constructed of loadings greater than  $1\ \text{mAh}/\text{cm}^2$  typically show large “mud” cracks after casting and drying. Several process changes were attempted to alleviate the formation of cracks: slowing the drying rate, starting with a more viscous slurry by reducing the NMP content, and adding more polymer binder. Of these three, adding more binder was found to stop the formation of large cracks. It is believed that the increased binder content leads to a viscous barrier between particles thereby reducing the surface forces between particles and limiting aggregation.

Initial cycling data at different C-rates is provided in the figure. This data indicates that the electrode cycles well with negligible effects of impedance when cycled at different rates. This cell will be allowed to continue to cycle to failure, which is typically occurs as a result of Li dendrites that short the half-cells.



Cells with higher loadings that display cracks upon drying, can be improved after calendaring. Cycling and impedance data will be taken of cells with different binder contents and those calendared to different porosities. Electrodes with the best overall performance attributes will be defined.

## Task 2.1 - Jack Vaughey (Argonne National Laboratory)

### Novel Anode Materials

**PROJECT OBJECTIVE:** The project seeks to understand how the cycling of elemental silicon in a Li-ion cell configuration affects the local electrode structure and relate the information garnered to counter cell failure mechanisms. By using various types of electrode formulations and diagnostic spectroscopies, we can probe from the surface of the Si to the final complex laminate electrode. Initial work included creation of an all-inorganic electrode that allowed the effects of cycling on the Si to be examined as the electrolyte was the only source of carbon in the cell. This work extended to developing thin film deposition techniques that allow tailoring of the surface chemistry of the Si that influence how the binder and Si interact. In addition to normal cycling, imaging, and impedance spectroscopies we initiated tomography studies of conventional electrodes to examine how electrode porosity and particle size influenced the isolation of Si particles on cycling, a major cause of capacity fade.

**PROJECT IMPACT:** The project utilizes a combination of synthesis and characterization to discern how the cycling of elemental Si in a Li-ion cell affects the surrounding electrode structure and how this can be modified to increase cycle life and stability. Results from these studies will be of interest to cell builders and end-users as degradation of the electrode structure can often be traced as the root cause of inconsistent results and premature cell failure. These goals are in line with EERE and OVT goals of furthering development of novel electrode materials and energy storage systems.

#### **OUT-YEAR GOALS:**

- Using the new BATT standard Si source, design and formulate Si-based electrodes that allow for volume expansion in a less rigid environment than a porous Cu substrate.
- Design and evaluate alternative structures that integrate the role of the current collector with the conductive additive requirement of the electrode to reduce materials requirements

**COLLABORATIONS:** Fikile Brushett (MIT), Lynn Trahey and Fulya Dogan (ANL)

#### Milestones

- 1) Synthesize and evaluate a Si-based electrode that utilizes a multilayer structure to stabilize the active Si. (Dec. 13) **Complete**
- 2) Synthesis and evaluation of at least three alternative electrode structures based on non-Cu porous substrates. (Mar. 14) **Complete**
- 3) Utilize surface sensitive techniques to develop a model of the Si- substrate interface in the alternative electrodes created. (Jun. 14) **Ongoing**
- 4) Evaluate optimized electrode structure against BATT standard Si electrode for rate capability and stability on cycling. Make recommendations to improve BATT standard electrode. (Sep. 14) **Ongoing**

## Progress Report

Studies have continued on the stability and role of Si surfaces on the cycling properties of Si anodes in Li-ion batteries. Surface functional groups interact with the electrolyte and have an effect on the mixture of phases that make up the SEI layer and affect cycling efficiency and capacity fade. In Q1, Cu-Si multilayers were studied to evaluate the role of surface area, conductivity, and reduced electrolyte exposure and noted the protected surface has significantly better capacity retention. Extending these concepts in Q2, additional alternative electrode structures that utilized coating layers on an active Si electrode were analyzed – Si/SiO<sub>2</sub>, Si/Li<sub>x</sub>SiO<sub>2+x/2</sub>, Si/Ti, and an uncoated Si control.

Titanium is an oxophilic metal that is often used in thin film multilayers to increase adherence of the active species to the substrate. Initial work evaluating how Ti interacted with Si in this type of system showed formation of intermetallics under the processing conditions utilized. Similar results were seen in the Cu series studied previously and have been recently reported for Cr adhesion layers. Since these layers are too reactive to stabilize the Si surface, we created a series of Si multilayers with oxide protective coatings. Initial materials were based on an artificial version of the passivation coating of Si, and its lithiated analogue, as reported by Edstrom, *et al.*, in 2013. The three representative samples were synthesized using (1) RF sputtering of a Si target under Ar, (2) the same followed by additional sputtering under an Ar/O<sub>2</sub> mixture to make a layer of SiO<sub>2</sub>, and (3) and taking the multilayer and sputtering Li on the surface and heating, all under vacuum. The samples were then electrochemically evaluated in an electrochemical crystal quartz microbalance (EQCM), which can give us information on weight gain, SEI porosity, and Li content as a function of SOC.

Figure 1 highlights the information gathered from studying the electrochemical response from the unprotected Si film. The data shows SEI formation starting around 1V and lithiation around 350 mV (vs Li). The dashed line represents higher order harmonics from the EQCM balance and relate to film porosity. From initial analysis, the SEI film was relatively dense as formed but as lithiation occurred, notably around 3000 sec, the slope of the dashed blue line increases indicative of a more porous coating as the Si lithiates and the volume expansion starts to disrupt the layer. Initial estimates are that the weight change on the electrode is approximately 20% from Li incorporation and 80% SEI formation on the surface. Similar studies with the SiO<sub>2</sub> coating showed much lower weight gain as the oxide prevented the electrolyte from seeing much of the active Si. The Si was still able to lithiate, but with much less exposure, was sluggish and at lower overall levels. Formation of a surface coating of Li<sub>x</sub>SiO<sub>2+x/2</sub> was also evaluated to check for any reversibility of the lithiation of silica, a possible side reaction that may have an effect on rate capability or cycling efficiency. Under these conditions, the material was found to be stable to electrochemical cycling although electrolyte interactions could not be ruled out at this time.

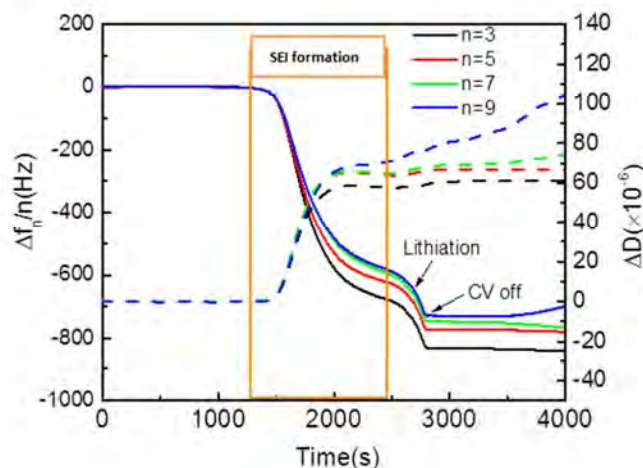


**Figure 1.** EQCM study of a Si film.

## Task 2.2 - Stanley Whittingham (SUNY Binghamton)

### Metal-Based High Capacity Li-Ion Anodes

**PROJECT OBJECTIVE:** To replace the presently used carbon anodes with safer materials that have double the volumetric energy density, and will be compatible with low cost layered oxide and phosphate cathodes and the associated electrolyte.

Specifically, the primary objectives are to:

- Increase the volumetric capacity of the anode by a factor of two over today's carbons
  - 1.6 Ah/cm<sup>3</sup>
- Increase the gravimetric capacity of the anode
  - $\geq 500$  Ah/kg
- Lower the cost of materials and approaches

**PROJECT IMPACT:** The volumetric energy density of today's Li-ion batteries is limited primarily by the low volumetric capacity of the carbon anode. If the volume of the anode could be cut in half, then the cell energy density can be increased by over 50% to approach 1 kWh/liter (actual cell). In addition, alloys with higher Li diffusivity than carbon would minimize the possible formation of cell-shortening dendritic Li under high charging rates or low temperature conditions. Moreover, smaller cells using lower cost manufacturing will lower the cost of tomorrow's batteries.

**OUT-YEAR GOALS:** The long-term goal of this project is to replace the present carbon used in Li-ion batteries with lower cost anodes that have double the volumetric energy density of carbon. This will be accomplished by using Sn and/or silicon based materials. By the end of this project it is anticipated that a new Sn anode will be available that can exceed the charging and discharging rates of carbon thereby making it safer, that will have minimal excess capacity on the first cycle, and that can be cycled at greater than 99% efficiency over 200 cycles.

**COLLABORATIONS:** National Synchrotron Light Source (BNL) and Advanced Photon Source (ANL).

### Milestones

- 1) Identify the two most promising approaches for nano-Si. (Dec. 13) **Complete**
- 2) Reduce the first cycle excess capacity to less than 20% for nano-Sn. (Mar. 14) **Delayed to Sep. 14**
- 3) Go/No-Go: Decision on solvothermal approach for nano-Sn. Criteria: Identify the optimum synthesis approach for nano-Sn anode material. (Jun. 14) **Complete – No-Go on solvothermal**
- 4) Achieve more than 200 cycles on nano-Sn at double the capacity of carbon at the 1C rate. (Sep. 14) **Ongoing**

## Progress Report

The goal of this project is to synthesize Sn- and Si-based anodes that have double the volumetric capacity of the present carbons, without diminishing the gravimetric capacity.

**Milestone (2):** First cycle capacity loss - the impact of varying the graphite/Sn molar ratio used in synthesizing the Sn-Fe-C composite was determined. Figure 1a shows that when the graphite/Sn molar ratio decreases from 10 to 5, a small decrease of both the first capacity loss and the overall capacity is observed. This decrease suggests that although the graphite contributes to the first capacity loss, the overall electrochemical performance does not benefit from reducing the amount of graphite. Moreover, the capacity retention is worse when less graphite is added (Fig. 1a). It is noteworthy that a lower graphite/Sn ratio results in a higher crystallinity of the material (Fig. 1b), which can be associated with the degradation of the capacity retention.

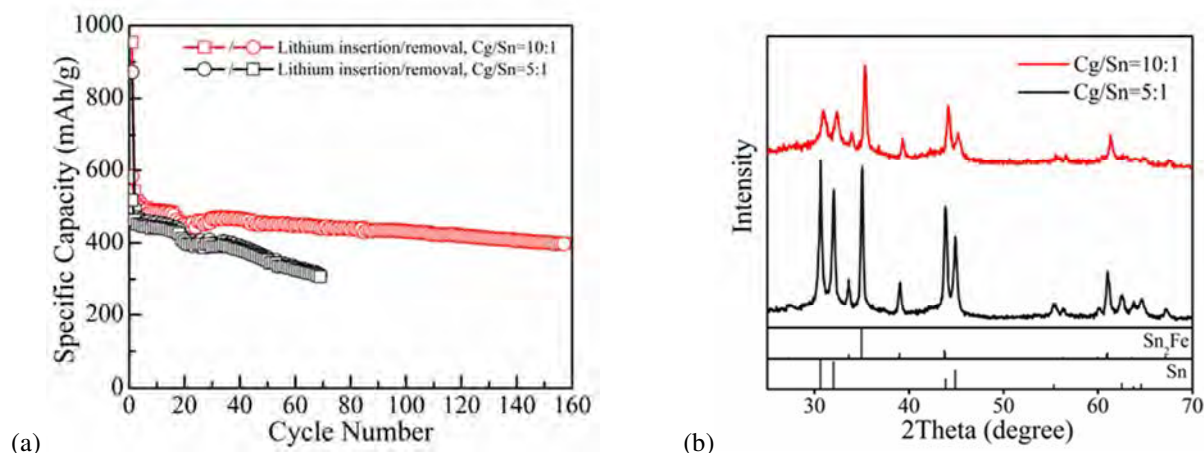


**Figure 1.** (a) Electrochemical performance and (b) XRD patterns of nano-sized Sn-Fe-C synthesized by the mechanochemical method with different graphite/Sn ratios.

**Milestone (3): Complete.** Decision of No-Go has been made for the solvothermal approach preparing nano-Sn, because of poorer results compared with mechanochemical approach.

**Milestone (4):** The nano-sized Sn-Fe-C, synthesized by the mechanochemical method and cycling at the 1C rate, reaches  $2 \text{ Ah/cm}^3$  with relatively less capacity retention compared to the standard graphite (*ca.*  $0.75 \text{ Ah/cm}^3$ ) (Fig. 2). The overall volumetric capacity of the nano-sized Sn-Fe-C is more than twice that of the standard graphite for at least 40 cycles. The material being tested is not optimized (has a graphite/Ti/Sn molar ratio of 10:1:1); the capacity of the optimized nano-sized Sn-Fe-C will be determined in the near future.

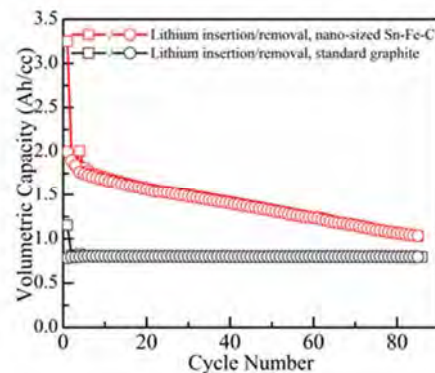


**Figure 2.** Comparison of volumetric capacity of the nano-sized Sn-Fe-C (synthesized by the mechanochemical method) to a standard graphite. The materials are cycled under 1C rate (1C corresponding to a current density value of  $600 \text{ mA g}^{-1}$  for Sn-Fe-C and  $350 \text{ mA g}^{-1}$  for the standard graphite, respectively).

### Nanoscale Composite Hetero-structures and Thermoplastic Resin Binders: Novel Li-ion Anode Systems

**PROJECT OBJECTIVE:** The objective is to identify novel materials and configurations, improved polymeric binders and cost effective scalable strategies to generate these systems to overcome the Si anode limitations. The goals of the present project are to identify an inexpensive nanoscale composites, new class of polymeric binders and electrode configurations displaying higher capacity (>1200 mAh/g) than carbon while exhibiting similar first cycle irreversible loss (<15%), higher coulombic efficiency (>99.9%), and excellent cyclability to replace graphite.

**PROJECT IMPACT:** Identification of new Si based systems displaying higher gravimetric and volumetric energy densities than graphite will likely result in new commercial battery systems that are more robust, capable of delivering better energy and power densities and will be more lightweight than current Li-ion battery packs utilizing graphite anodes for identical performance specifications. New Si anode-based strategies and configurations will also lead to more compact battery designs for the same energy and power density specifications as current Li-ion systems. Commercialization of these new Si anode-based Li-ion battery packs will represent fundamentally, a major hallmark contribution of the BATT Program and the BATT community.

**OUT-YEAR GOALS:** This is a multi-year project comprising of four major phases to be successfully completed in four years. Phase 1: Development of cost effective high energy mechanical milling (HEMM) and direct mechano-chemical reduction (DMCR) approaches to generate nanocrystalline and amorphous Si, and  $\text{Li}_x\text{Si}$  ( $x>3.5$ ) alloys exhibiting capacities in the ~1600 mAh/g range and higher. This phase was completed in year 1. Phase 2: Use of chemical vapor deposition (CVD) to generate amorphous and nanocrystalline Si on vertically aligned carbon nanotubes (VACNT) based nano-scale heterostructures exhibiting specific capacity in the ~2000-2500 mAh/g range. This phase was completed in Year 2. Phase 3: Identify interface control agents (ICA) and surface electron conducting additives (SECA) to lower the first cycle irreversible (FIR) loss (<15%) and improve the coulombic efficiency (CE) (>99.9%). This phase was completed in Year 3. Phase 4: Develop elastic and high strength polymeric binders, to be completed in Year 4.

**COLLABORATIONS:** Ayyakkannu Manivannan (NETL), Spandan Maiti (U. Pittsburgh), and Shawn Litster and Amit Acharya (Carnegie Mellon U)

#### Milestones

- 1) Go/No-Go: Stop microwave approach if it fails to generate nanoscale electrochemically-active architectures of Si and C resulting in capacities greater than or equal to 1200 mAh/g. (Dec. 13) **Discontinued**
- 2) Demonstrate generation of *a*-Si hollow nanotubes using cost effective (< \$65/kg) chemical approaches. (Dec. 13) **Complete**
- 3) Develop interface control agents (ICA) to reduce the first cycle irreversible loss to <15% . (Mar. 14) **Complete**
- 4) Develop surface electron conducting additives (SECA) to improve the coulombic efficiency to >99.9%. (Jul. 14) **Ongoing**
- 5) Develop multilayered *a*-Si/M (M = Matrix) composite films to lower the first-cycle irreversible loss (<15%) and improve the active mass loadings (2-3mg/cm<sup>2</sup>). (Sep. 14) **Ongoing**

## Progress Report

Previously, the electrochemical cycling characteristics of *a*-Si thin films deposited on Cu foil by a pulse-plating technique were reported. It was observed that the electrochemical performance of the *a*-Si films depended on the frequency of deposition, whereas, the capacity fade per cycle and first cycle irreversible loss (FIR) showed a decreasing trend with an increase in the frequency of the pulsing current (report Q1-2014). This quarter, the change of surface morphology on the electrochemically cycled films in comparison to the as-deposited film (pulse frequency: 5000Hz) was studied using the SEM characterization technique to understand the effect of repeated lithiation and delithiation on the film integrity. The as-deposited films show a continuous film morphology (Fig. 1). However, after 10 cycles, cracks seemed to emerge due to the colossal volume changes in Si, resulting in the formation of continuous islands. These islands, once formed, are quite stable even after 50 cycles and did not undergo further cracking or delamination, maintaining integrity, thus, enabling the films to undergo repeated cycling without any capacity fade (report Q1-2014). Efforts are currently directed towards reducing the FIR by carbon coating the *a*-Si surface; the results of these findings will be presented in future quarterlies.

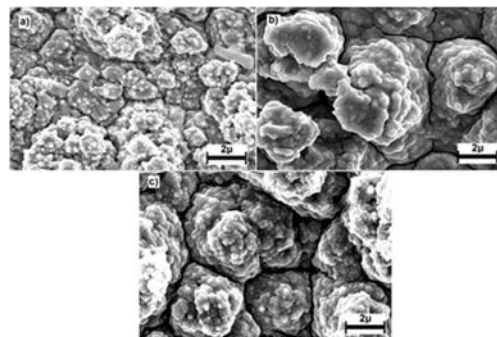


**Figure 1.** SEM images of electrodeposited amorphous Si films at 5000Hz a) before cycling, b) after 10 cycles and c) after 50 cycles.

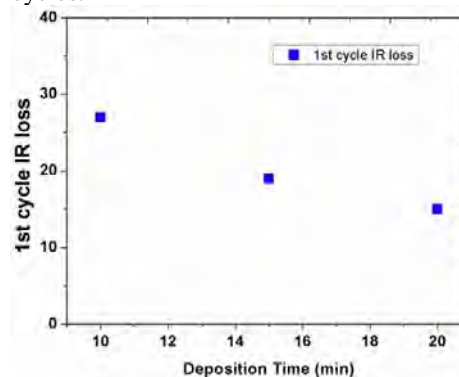


**Figure 2.** First cycle irreversible loss vs. Si-CVD deposition time.

Previously, a novel, scalable approach was reported for generating hollow Si nanotubes (h-SiNT) using a CVD derived sacrificial nanowire template (report Q3-2013.) These h-SiNTs exhibited a FIR of *ca.* 27% and stable reversible capacities of *ca.* 1.5 Ah g<sup>-1</sup> at a 2 A/g charge/discharge rate. In this quarter, novel approaches were explored to lower the FIR and improve the active material loading densities. Accordingly, the time of Si deposition during the CVD process was increased beyond 10 min to obtain a thicker Si shell in the h-SiNTs. This resulted in an increased active material density or higher areal loading on the current collector. Furthermore, the weight fraction of the conductive additive, Super-P, was increased from 10 to 25% at the expense of the natural polymer-based binder to achieve better electronic conduction among the h-SiNTs. As shown in Fig. 2, increasing the deposition time to 15 and 20 min resulted in a significant reduction in FIR of 19% and 15%, respectively. This is probably due to a decrease in the effective specific surface area exposed to the electrolyte, resulting in decreased Li<sup>+</sup> consumption in the SEI layers formed. Figure 3 shows the electrochemical cycling of h-SiNTs implementing the DOE recommended test protocol, obtained using a CVD deposition time of 15 min. A first discharge capacity of 1,814 mAh g<sup>-1</sup> and a first cycle irreversible loss of only 19% were obtained at an areal current density of 0.02 mA/cm<sup>2</sup>. A high loading density of 1.43 mg/cm<sup>2</sup> was achieved for these h-SiNTs. Furthermore, it should be noted that the capacities reported herein are based on the total weight of the dry laminate on the current collector. Extended cycling of these h-SiNTs are currently ongoing and these results will be presented in the next quarterly.

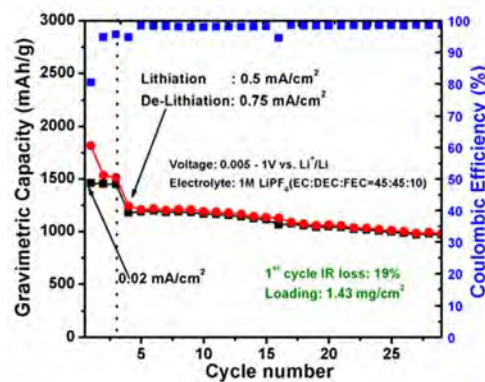


**Figure 3.** Variation of gravimetric specific capacity vs. cycle number of SiNT.

### Development of Silicon-Based High Capacity Anodes

**PROJECT OBJECTIVE:** The objective of this project is to develop high-capacity, low-cost electrodes with good cycle stability and rate capability to replace graphite in Li-ion batteries. The porous Si and the rigid-skeleton supported Si/C composite anode (B<sub>4</sub>C/Si/C) will be further optimized. The optimized B<sub>4</sub>C/Si/C material will be used as the baseline material for both thick electrode fabrication and studies to advance our fundamental understanding of the degradation mechanism in Si based anode. New electrolyte additives, binders, and artificial SEI layers will be investigated to further improve the performance of anodes. New approaches will be developed to pre-lithiate Si-based and other Li-alloy anodes to minimize their first-cycle losses. Fundamental understanding on the formation and evolution of SEI layer, the effect of electrolyte additives and electrode thickness will be investigated by *in situ* microscopic analysis.

**PROJECT IMPACT:** Si-based anodes have much larger specific capacities compared with conventional graphite anodes. However, the cyclability of Si-based anodes is limited because of the large volume expansion that is characteristic of these anodes. This work will develop a low-cost approach to extend the cycle life of high-capacity, Si-based anodes. The success of this work will further increase the energy density of Li-ion batteries and accelerate market acceptance of electrical vehicles (EV), especially for plug-in hybrid electrical vehicles (PHEV) required by the EV Everywhere Grand Challenge proposed by DOE/EERE.

**OUT-YEAR GOALS:** The main goal of the proposed work is to enable Li-ion batteries with a specific energy of >96 Wh/kg (for PHEVs), 5000 deep-discharge cycles, 15-year calendar life, improved abuse tolerance, and less than 20% capacity fade over a 10-year period

#### **COLLABORATIONS:**

Collaboration on anode development will continue with the following battery groups:

- Michael Sailor at UCSD—preparation of porous Si.
- Gao Liu at LBNL—Binders.
- Yi Cui at Stanford—Failure mechanism study.
- Marina Yakovleva at FMC Corp—SLMP
- Chunmei Ben at NREL—surface protection and failure mechanism study.
- David Ji at Oregon State University—Preparation of porous Si by thermite reactions.

#### Milestones

- 1) Identify the fading mechanism in the thick Si electrode vs. thin electrode. (Dec. 13) **Complete**
- 2) Achieve Coulombic charge efficiency of the electrode >90% during the first cycle, through application of SLPs and sacrificial Li electrode to PNNL's B<sub>4</sub>C/Si/C anode. (Mar. 14) **Complete**
- 3) Achieve high loading Si-based anode capacity retention of >1.2 mAh/cm<sup>2</sup> over 150 cycles using new binders/electrolyte additives. (Jun. 14) **Complete**
- 4) Achieve improved cycling stability of thick electrodes (> 3 mAh/cm<sup>2</sup>). (Sep. 14) **Ongoing**
- 5) Achieve a specific energy greater than 30 Wh/kg and the specific power greater than 5 kW/kg, and cycle life greater than 30,000 cycles for Li ion capacitors. (Sep. 14) **Ongoing**

## Progress Report

Nanostructured Si has demonstrated very good cycling stability when the electrode is thin. For a thick electrode or samples with high areal capacity, the interaction between different components (active materials, conductive carbon, and binder) leads to more complicated mechanical/electrical failure of the electrode and, hence, capacity fade. Thick electrodes are easy to peel from the copper current collector. Strong binding among the electrode components and between the electrode and the current collector are critical to ensure stable cycling. A binder with good adhesion and flexibility will help to maintain the integrity of the electrode. Three-dimensional (3D) current collectors such as carbon paper or a carbon nanotube matrix have proved to be helpful in improving the mechanical stability of thick electrodes. Electrodes with 3D current collectors have the advantage of high gravimetric capacity for the cell pack; however, they often lead to lower volumetric capacity because of the open spaces inside of the electrode. High Si-loading in thick electrodes often leads to poor cyclability because of large overall expansion of the electrode and rapid consumption of the electrolyte (which is proportional to the Si loading and the amount of SEI layer formed). Although the electrolyte with FEC additive can lead to improved cyclability because of the thinner and more stable SEI formed in FEC-containing electrolytes, the factors that affect the stability of these SEI layers need to be further investigated.

Further optimized porous Si electrodes show good cycling stability at high loading. Figure 1a shows that the porous Si with a loading of *ca.* 2 mg/cm<sup>2</sup> can have a capacity of *ca.* 1.5 mAh/cm<sup>2</sup> with *ca.* 96% capacity retention over 300 cycles. Good cycling stability was also demonstrated with electrode loadings of *ca.* 3.5 to 4 mg/cm<sup>2</sup>. Figure 1b shows that porous Si electrodes can have a capacity of *ca.* 3 mAh/cm<sup>2</sup> with *ca.* 90% capacity retention over 100 cycles. The battery was cycled using the BATT protocol: 0.005 to 1 V; three formation cycles at 0.06 mA/cm<sup>2</sup>; 0.75 mA/cm<sup>2</sup> for delithiation and 0.5 mA/cm<sup>2</sup> for lithiation.

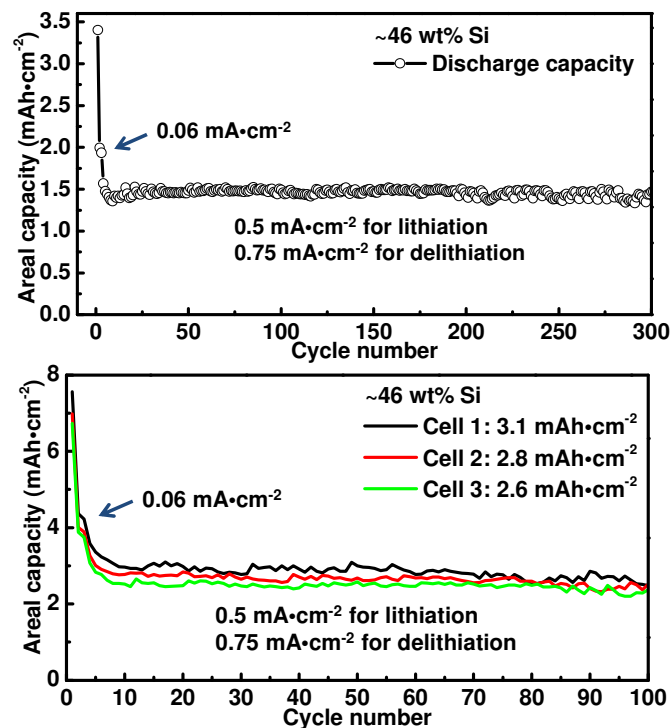


**Figure 1.** (a) Cycling stability of a porous Si electrode of *ca.* 1.5 mAh/cm<sup>2</sup>. (b) Cycling stability of porous Si electrodes of *ca.* 3 mAh/cm<sup>2</sup>.

## Atomic Layer Deposition for Stabilization of Amorphous Silicon Anodes

**PROJECT OBJECTIVE:** The objective of the project is to develop a low-cost, thick, high-capacity Si anode with sustainable cycling performance. Our specific objectives are to develop a novel conductive and elastic scaffold by using Atomic Layer Deposition (ALD) and Molecular Layer Deposition (MLD), demonstrate durable cycling by using the new coating and electrode design, and investigate the effect of atomic surface modification on irreversible capacity loss and cycling performance.

**PROJECT IMPACT:** Due to its high theoretical capacity and natural abundance, silicon has attracted much attention as a promising Li-ion anode material. However, progress towards a commercially-viable Si anode has been impeded by Si's rapid capacity fade caused by large volumetric expansion. In this project, new ALD/MLD conformal nanoscale coatings with desirable elastic properties and good conductivity are developed to accommodate the volumetric expansion and protect the surface from reactive electrolytes, as well as to ensure the electronic paths through the composite electrodes. Successful completion of this project will enable the coated Si anodes to have high coulombic efficiency, as well as durable high-rate capability. This project supports the goals of the DOE *EV Everywhere* Grand Challenge and EERE's Vehicle Technologies Office to develop high-energy batteries for wider adoption of electric vehicles to reduce consumption of imported oil and generation of gaseous pollutants.

### **OUT-YEAR GOALS:**

- Demonstrate durable cycling performance of thick Si anodes (>15  $\mu\text{m}$ ) by using new ALD/MLD coatings and electrode designs
- Explore the importance and mechanism of various coatings via the BATT coating group
- Collaborate within the BATT program with the aim of developing high-rate PHEV-compatible electrodes (both anodes and cathodes)

**COLLABORATIONS:** Phil Ross, Gao Liu and Robert. Kostecki (LBNL), Jason Zhang (PNNL), Yue Qi (MSU), Xingcheng Xiao (GM), Perla Balbuena (Texas A&M), and Kevin Leung (SNL).

### Milestones

- 1) Identify the impact of Alucone MLD coating on the structure and morphology of Si anodes during cycling. (Dec. 13) **Complete**
- 2) Develop  $\text{Al}_2\text{O}_3$ /carbon composite coatings by pyrolysis of Alucone MLD film. (Mar. 14) **Complete**
- 3) Go/No Go: Test coated electrodes in coin cells. Criteria: Stop the development of  $\text{Al}_2\text{O}_3$ /carbon composite coatings if the coating cannot help the performance of Si anodes. (Jun. 14) **Ongoing**
- 4) Synthesize and characterize novel  $\text{AlF}_3$ /Alucone hybrid coating by using ALD and MLD. (Sep. 14) **Ongoing**

## Progress Report

Significantly improved performance has been demonstrated by a Si anode coated with MLD aluminum alkoxide (alucone), as recently published in the *Advanced Materials*, **26**, 2014, p1596. Different from an ALD  $\text{Al}_2\text{O}_3$  layer, an organic group was integrated in the MLD alucone coating from the reaction between trimethyl aluminum and glycerol. The change in chemistry results in a largely reduced elastic modulus from *ca.* 195 GPa in an ALD  $\text{Al}_2\text{O}_3$  coating to *ca.* 39 GPa in the MLD alucone coating. The flexible alucone coating greatly accommodates the massive volume changes in cycling Si anodes, which ensures the highly reversible capacity in the alucone-coated Si anodes. Inspired by previous work on cyclized polyacrylonitrile, sustainable rate performance can be further achieved for Si anodes with electronically conductive and mechanical strong coatings. Therefore, the aluminum oxide/carbon hybrid coating has been synthesized by pyrolysis of the alucone coating, with the aim to increase electronic conductivity of the coating.

A dramatic decrease in resistance was observed upon pyrolysis of the alucone film above 600°C, although structural changes occurred above *ca.* 300°C. The highest electronic conductivity is obtained at *ca.* 850°C. The film displays a resistivity of *ca.* 1.72  $\Omega\text{cm}$ , which is much lower than that of  $\text{Al}_2\text{O}_3$  with a resistance of *ca.*  $10^{14}$   $\Omega\text{cm}$  (Fig. 1a.) The increased electronic conductivity is attributed to the formation of carbon domains in the MLD alucone film. Raman spectra further confirmed the graphitic structure in the pyrolyzed alucone films, see Fig. 1b. Both D and G peaks are observed which represent  $\text{sp}^2$  sites from the perfect graphite structure and the disorder structure, respectively. The graphitic structure is obtained when pyrolysis occurs above 600°C. However, pyrolysis at higher temperatures (>700°C) is required to achieve high electronic conductivity.

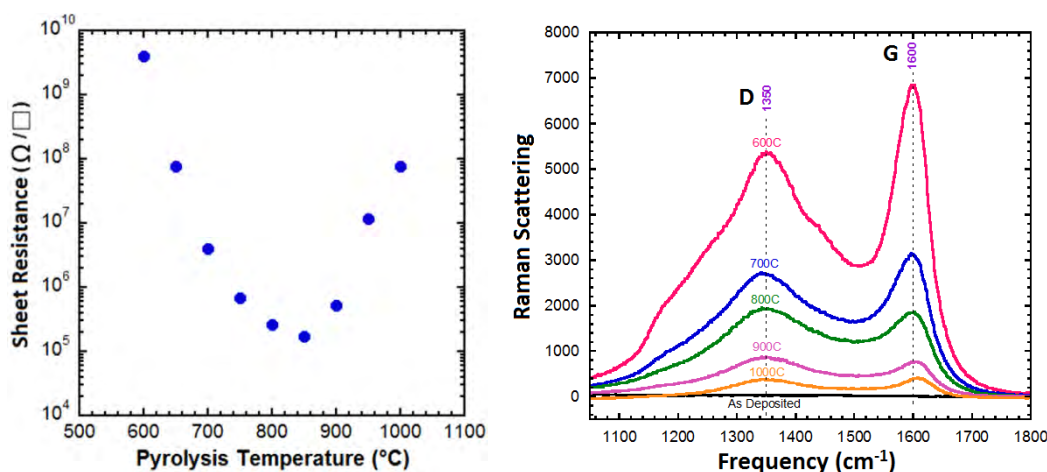


**Figure 1.** (a) Resistance of MLD ALHQ films as a function of pyrolysis temperature; (b) Raman spectra of MLD ALHQ films under different pyrolysis temperatures.

Besides pyrolysis of this alucone coating, a different approach was also developed in the last quarter to fabricate a conductive and elastic coating. Instead of using glycerol in the MLD process, hydroquinone was selected to introduce an aromatic ring in the new MLD ALHQ coating. In this quarter, ALHQ coating was successfully developed on the Si anodes. The coating greatly improved the 1<sup>st</sup> cycle coulombic efficiency from 65% for a bare Si anode to 85% for a coated anode. Improved cycling performance was also demonstrated for the MLD ALHQ coated anode. A sustainable cycling capacity of 1500mAh  $\text{g}^{-1}$  was achieved for the MLD ALHQ coated anode. Electrochemical cycling behavior at elevated rates confirms the capability of this conductive and elastic coating for enhanced rate performance.

## Task 2.6 - Yury Gogotsi and Michel Barsoum (Drexel University)

### New Layered Nanolaminates for Use in Lithium Battery Anodes

**PROJECT OBJECTIVE:** Replace graphite with a new material selected from a group of layered (two-dimensional) binary carbides and nitrides known as MXenes, which may offer combined advantages of graphite and Si anodes with a higher capacity than graphite, less expansion, longer cycle life and a lower cost than Si nanoparticles.

**PROJECT IMPACT:** As a result of this project, a new family of 2D materials (MXenes) was discovered. Using MXenes as anode materials in LIB could lead to higher capacities than graphite with the ability to handle higher cycling rates than graphite anodes. Since each MXene has its own voltage window, considering their rich chemistry and the possibility of solid solutions, MXene compositions can be selected and tuned for certain voltages to produce high-performance batteries with improved safety.

**OUT-YEAR-GOALS:** The project's long term goal is to produce new anode materials (MXenes) that may replace graphite in anodes of Li-ion batteries.

**FY2014** - Improvement of the cycle-life of the anodes. Optimization and modification of the material manufacturing processes to enable large-volume, low-cost production.

#### **COLLABORATIONS:**

- Xiao-Qing Yang and Kyung-Wan Nam, BNL
- Yu Xie and Paul Kent, ORNL
- Jun Lu, Lars Hultman and Per Eklund, Linkoping University, Sweden.
- Jérémy Come, Yohan Dall'Agnese and Patrice Simon, Université Paul Sabatier, Toulouse, France

#### Milestones

- 1) (a) Produce MXene anodes with capability of delivering a stable performance at 10 C cycling rates (Dec. 13). **Complete**  
(b) Complete *in situ* and *ex situ* studies of the lithiation and delithiation of MXenes and determine the most promising materials (Dec. 13). **Delayed to Jun. 14**
- 2) Maximize capacity of MXenes and test newly discovered MXenes that have shown the highest capacity so far (Mo<sub>2</sub>C) (Mar. 14). **Delayed to Jun. 14**
- 3) Predict the theoretical capacity and Li insertion potential of MXenes, and synthesize and test MXenes that are expected to have the largest Li uptake (>600 mAh/g theoretical capacity) and a lithiation/delithiation potential below 1 V (Jun. 14). **Ongoing**
- 4) Demonstrate improved charge/discharge behavior by controlling particle size and surface chemistry of MXenes (Sep. 14). **Ongoing**

## Progress Report

To improve the capacity of multilayer  $\text{Ti}_3\text{C}_2$  by increasing its conductivity, powders were mixed with various weight fractions of carbon black (CB) additives and pressed into 300  $\mu\text{m}$ -thick free-standing discs with loadings of 50 to 60  $\text{mg}/\text{cm}^2$ . The areal capacities vs. cycle number are shown in Fig. 1 for cells with CB loadings of 0, 5, 10, and 15 wt%. For the sample with 10 wt% CB, a reversible areal capacity of 5.9  $\text{mAh}/\text{cm}^2$  was obtained after 50 cycles at a rate of *ca.*  $C/3$ , a value of approximately 5 times higher compared to that obtained for bare  $\text{Ti}_3\text{C}_2$ -pressed discs. This value is well above those currently reported for Si anodes (*ca.* 3.7  $\text{mAh}/\text{cm}^2$ ), Si-graphite composites (2.8 to 4.9  $\text{mAh}/\text{cm}^2$ ),  $\text{Li}_4\text{Ti}_5\text{O}_{12}$  (*ca.* 1.2  $\text{mAh}/\text{cm}^2$ ), and commercial cells (*ca.* 4  $\text{mAh}/\text{cm}^2$ ) and is expected to further increase when other MXenes, which show higher gravimetric capacities (*e.g.*,  $\text{Nb}_2\text{C}$ ,  $\text{Mo}_2\text{C}$ ), are used. At *ca.* 100  $\text{mAh g}^{-1}$ , the gravimetric capacity is moderate, as expected for a 300  $\mu\text{m}$ -thick, dense sample. To maximize gravimetric capacity and improve the rate performance, 5 wt% multi-walled carbon nanotubes, MWCNTs, with a diameter of *ca.* 20 nm were added to delaminated  $d\text{-Ti}_3\text{C}_2$ -based electrodes. The former acted as spacers enhancing the affinity between the MXene layers and electrolyte and as a conductive agent to facilitate electron transfer at higher rates. Two types of electrodes were prepared: 1) by filtering a homogeneous dispersion of  $d\text{-Ti}_3\text{C}_2$  and MWCNT (Fig. 2a), and 2) by repeated filtering of the  $d\text{-Ti}_3\text{C}_2$  dispersion and MWCNT suspension by turns to form sandwich-type structures (Fig. 2b). A reversible capacity of over 150  $\text{mAh g}^{-1}$  was achieved for the  $d\text{-Ti}_3\text{C}_2\text{-MWCNT-mix}$  electrode (prep. 1) during 300 cycles instead of 20  $\text{mAh g}^{-1}$  for pure  $d\text{-Ti}_3\text{C}_2$  at the same cycling rate of 1 C (Fig. 3a). For the  $d\text{-Ti}_3\text{C}_2\text{-MWCNT-sandwich}$  (prep. 2), a reversible capacity over 230  $\text{mAh g}^{-1}$  with good stability was achieved after 200 cycles at 1 C. It should be noted that the capacities for both electrodes tend to increase after tens of cycles. This can be ascribed to the improved wetting of MXene flakes by the electrolyte, which increases the area available for Li adsorption with cycling. Figure 3b shows the charge/discharge profiles of the  $d\text{-Ti}_3\text{C}_2\text{-MWCNT-sandwich}$  at 1 C, which clearly reveals the lithiation/delithiation process during cycling. If this improved capacity for the sandwich-like assembly of the  $d\text{-Ti}_3\text{C}_2\text{/MWCNT}$  nanocomposites is confirmed and maintained for thick samples, it would represent a breakthrough. It is crucial to note here that the gravimetric capacities were still increasing after 300 cycles at 1C (Fig. 3b). As noted above, this can only mean that the theoretical capacity of the composite electrodes has not been reached because not all the MXene area is active. Based on this observation, it is reasonable to conclude that further optimization of the electrode geometry using MWCNT or other conductive spacers should further enhance the gravimetric capacities. This work is ongoing. The remaining challenge is to reduce the overall voltages shown in Fig. 3 to below 1V.

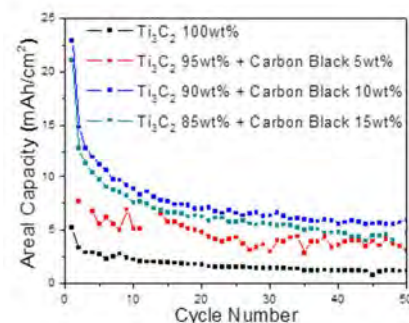


**Figure 1.** Areal capacity vs. cycle number for pressed  $\text{Ti}_3\text{C}_2$  discs with varied carbon black contents at  $C/3$ .

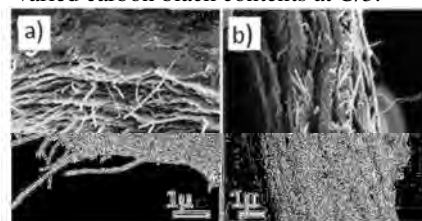


**Figure 2.** SEM images showing the cross section of the  $d\text{-Ti}_3\text{C}_2\text{/MWCNT}$  composite papers: (a)  $d\text{-Ti}_3\text{C}_2\text{-MWCNT-Mix}$ , and (b)  $d\text{-Ti}_3\text{C}_2\text{-MWCNT-sandwich}$ .

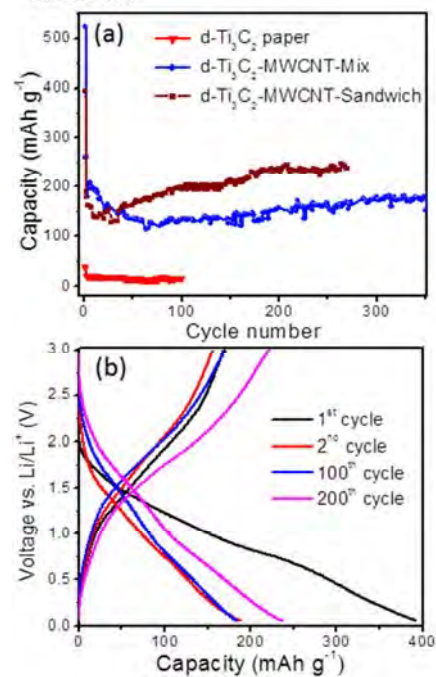


**Figure 3.** (a) Cycling stability of the  $d\text{-Ti}_3\text{C}_2\text{/MWCNT}$  composite electrodes at 1 C; (b) Charge-discharge profile of the  $d\text{-Ti}_3\text{C}_2\text{-MWCNT-sandwich}$  paper at 1 C.

## Synthesis and Characterization of Si/SiO<sub>x</sub>-Graphene Nanocomposite Anodes and Polymer Binders

**PROJECT OBJECTIVE:** Novel structured Si/SiO<sub>x</sub>-carbon nanocomposites and polymer binders will be designed and synthesized to improve Si-based anode electrode kinetics and cycling life, and decrease initial irreversible capacity loss in high capacity Li-ion batteries. By combining the new Si-based anode materials and new polymer binders and investigating their structure-performance relationships, a high performance Si anode can be achieved.

1. Synthesis and characterization of Si/SiO<sub>x</sub>-based nanocomposite Li-ion battery anodes.
2. Identify and evaluate the electrochemical performance of the Si/SiO<sub>x</sub>-based nanocomposite and the polymer binder.
3. Develop understanding of long-lifetime Si anodes for Li-ion batteries by considering both the Si active phase and the polymer binder and surface interactions between the electrode components.

**PROJECT IMPACT:** The proposed collaborative effort closely integrates synthesis of Si-based composite anodes with controlled structure and composition, development of novel functional polymer binders, and materials characterization and electrochemical evaluation. The resulting optimized Si anode electrode will provide electrochemical performances which are essential to achieving higher energy densities in PHEV and EV applications.

**OUT-YEAR GOALS:** According to the accomplishments of the project, several types of Si-based composite with promising electrochemical performance will be developed and demonstrated. New functional polymer binders will be developed. The mechanical and chemical influences of the structure, chemical composition and surface modification on electrochemical performance of those materials will be identified and demonstrated, thus to provide systematic fundamental understanding to guide the Si-based anode material design. The Si-based electrode design, including the selection of materials and polymer binders, will be demonstrated in cell testing at Penn State and with BATT project partners.

**COLLABORATIONS:** Gao Liu (LBNL), Chunmei Ban (NREL), Nissan R&D Center.

### Milestones

- 1) Go/No-Go: Stop the metal composites coating approach and focus on carbon coating approach if the capacities are less than 1500 mAh/g. Criteria: Synthesize, characterize and evaluate Si-based composite with novel coating (e.g. non-oxidic metal composites). (Dec. 13) **Go for carbon coating**
- 2) Identify and demonstrate the optimized composition, structure and surface modification of micro-sized Si/C and porous Si/C composites. (Mar. 14) **Complete**
- 3) Synthesize acidic/semiconducting polymer binders using grafting approach. (Jun. 14) **Ongoing**
- 4) Go/No-Go: Determine if semiconducting polymer approach can generally be applied to Si anodes. Criteria: Synthesis and electrochemical evaluation of Si/Si alloy composites. Fully characterize acidic/semiconducting polymer binders. Supply laminates of the optimized Si/Si alloy electrodes with electrode capacity of 800 mAh/g that cycle 100 cycles to BATT PIs. (Sep. 14) **Ongoing**

## Progress Report

**Si-based anode materials:** Titanium nitride (TiN) coated Si nanoparticles (Si@TiN) were synthesized *via* the reduction of TiO<sub>2</sub>-coated Si nanoparticles (Si@TiO<sub>2</sub>) in nitrogen. The TiO<sub>2</sub> layers were coated on the surface of commercial Si *via* a solution approach, and subsequent thermal annealing in N<sub>2</sub> led to the formation of a Ti nitride coating on Si to obtain TiN-coated Si nanoparticles. The crystalline TiN layer on the Si is composed of TiN nanoparticles with an average particle diameter of around 10 nm, as shown in the TEM image (Fig. 1a). Ti and N elements are uniformly distributed in the Si@TiN particles as shown in the EDS elemental mapping of Si (Fig. 1b), Ti (Fig. 1c) and N (Fig. 1d). The Si@TiN composite shows initial discharge and charge capacities of 2650 mAh g<sup>-1</sup> and 1990 mAh g<sup>-1</sup>, respectively, with an initial coulombic efficiency of 76% (Fig. 2). Si@TiN has a high efficiency of above 99% during cycling. It also shows better cyclability than Si@TiO<sub>2</sub> and Si, with 75% capacity retention (1900 mAh g<sup>-1</sup>) with respect to the first discharge capacity after 100 cycles at 400 mA g<sup>-1</sup>. A capacity of 400 mAh g<sup>-1</sup> can be achieved even at a high current density of 8 A g<sup>-1</sup>, much better than Si nanoparticles. Impedance studies indicate that the TiN coating can enhance the conductivity of the Si@TiN and promote formation of a more stable SEI layer than either the Si or Si@TiO<sub>2</sub>.

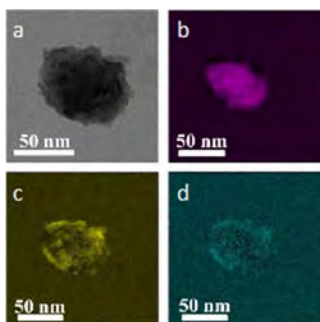


Figure 1.

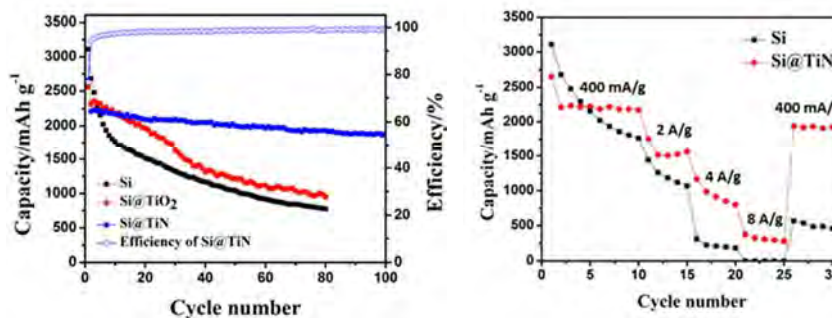


Figure 2.

**Semiconducting binders:** Synthesis of ionic/semiconducting graft binders is continuing; testing of these new binders will occur in the coming quarter. Shown in Fig. 3 is a post-sulfonation route for adding ionic groups to the semiconducting graft structure. Previously, acidic sulfonic acid moieties were identified as an important functional group in thermoplastic sulfone and ketone-based binders. Addition of the sulfonates resulted in binders that gave much higher capacity and less capacity fade with commercial Si nanoparticles when compared to unsulfonated binders. The goal of the current approach is to provide mechanically-robust semiconducting binders with ionic functionality. Aside from sulfonates, carboxylated binders will be explored. The chain growth Suzuki polymerization of 7-bromo-9,9-dialkylfluorene-2-ylboronic acid ester A-B monomer was previously demonstrated. This polymer platform will be used for further modification reactions to create a family of binders to test whether semiconducting motifs can be universally applied to Si-based anodes.

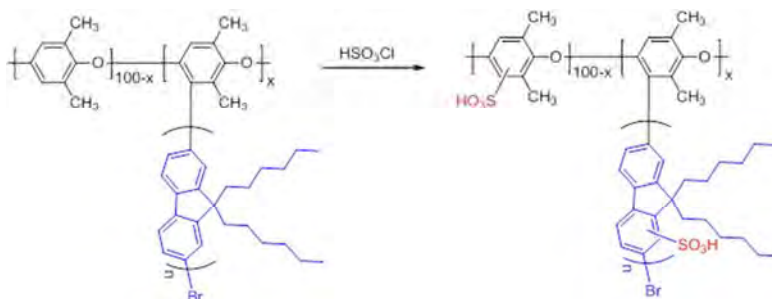


Figure 3.

### Wiring up Silicon Nanoparticles for High Performance Lithium Ion Battery Anodes

**PROJECT OBJECTIVE:** The charge capacity limitations of conventional carbon anodes are overcome by designing optimized nano-architected Si electrodes.

This study pursues two main directions:

- 1) fabricating novel nanostructures that show improved cycle life, and
- 2) developing methods to study the lithiation/delithiation process to understand volume expansion for higher efficiency.

**PROJECT IMPACT:** The Li ion storage capacity, as well as the cycling stability of Si anodes, will be dramatically increased. This project's success will make Si the high performance Li-ion battery anode material toward high energy batteries to power vehicles.

**OUT-YEAR GOALS:** Mass loading, cycling life and first cycle coulombic efficiency (1st CE) will be improved and optimized (over 1 mg/cm<sup>2</sup> and >85%) by varying material synthesis and electrode assembly. Fundamentals of volume expansion as well as SEI formation in Si nanostructures will be identified. A detailed study of inter-particle interactions during electrochemical reaction will be performed by *in situ* and *ex situ* microscopy.

#### **COLLABORATIONS:**

- BATT Program PIs
- SLAC: *In situ* X-ray
- Stanford: Prof. Bill Nix, mechanics; Prof. Zhenan Bao, materials.

#### Milestones

- 1) Utilize Si particles as an anode with capacity > 1000 mAh/g, mass loading of 1mAh/cm<sup>2</sup> and cycle life >100 cycles (Dec. 13) **Complete**
- 2) Go/No-Go: Try other conducting coating materials. Criteria: If the first cycle coulombic efficiency cannot go >80%. (Mar. 14) **Go for try other conducting coating materials.**
- 3) Complete *in situ* and *ex situ* SEM studies of two or multiple Si nanostructures during lithiation/delithiation to understand how neighboring particles affect each other and volume changes. (Jun. 14) **Ongoing**
- 4) Increase mass loading of Si material to achieve 2 mAh/cm<sup>2</sup> and first cycle coulombic efficiency (>85%) and cycle life >300 cycles (Sep. 14) **Complete**

## Progress Report

Inspired by the structure of a pomegranate fruit, a novel secondary structure for Si anodes was designed (Fig. 1). Si nanoparticles (SiNPs) are embedded within a spherical micron-sized porous carbon framework. The porous carbon framework of nanoscale thickness connects all the SiNPs, and also conformally covers the whole secondary particle surface, so that most of the SEI only forms on the outside of the secondary particle. Well-defined void space is engineered around each nanoparticle, allowing the Si to expand without changing the secondary particle morphology or breaking the SEI layer. Such a design has multiple advantageous features, including (i) the nano-sized primary particle size prevents fracture; (ii) the micron-sized secondary structure makes it easier to maintain electrical contact; (iii) the well-defined internal void space allows the SiNPs to expand without destroying the secondary particle morphology; (iv) the carbon framework functions as an electrical highway and a mechanical backbone so that all SiNPs are electrochemically active; (v) carbon also completely wraps the secondary particle surface to limit most of SEI formation to the outer surface, which not only limits the amount of SEI, but also retains the internal void space for Si expansion; and (vi) the dilemma of high surface area and low tap density introduced when using a nano-sized primary feature is partially solved.

The pomegranate design affords remarkable battery performance. As shown in Fig. 2a, its reversible capacity reached  $2350 \text{ mAh g}^{-1}$  at a rate of  $C/20$ . From the second cycle to the 1000th cycle at a rate of  $C/2$ , the capacity retention was more than 97%. After 1000 cycles, over  $1160 \text{ mAh g}^{-1}$  still remained, which is more than three times the theoretical capacity of graphite. Unprecedentedly stable cycling (100 cycles with 94% capacity retention) with high areal capacity ( $3.7 \text{ mAh cm}^{-2}$ ), similar to the areal capacity of commercial Li-ion batteries was demonstrated (Fig. 2b). The SEM images confirm the pomegranate structures remain intact after 100 cycles (Fig. 2c).

The successful design principles developed in this study can be widely applied to other high-capacity Li battery electrodes.

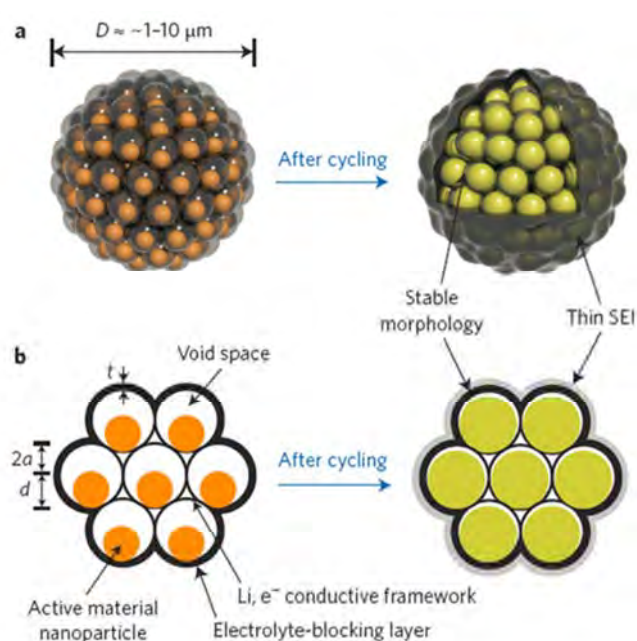


**Figure 1.** Schematic of the pomegranate-inspired design. (a) Three dimensional view and (b) simplified two-dimensional cross-section view of one pomegranate microparticle before and after electrochemical cycling (in the lithiated state).

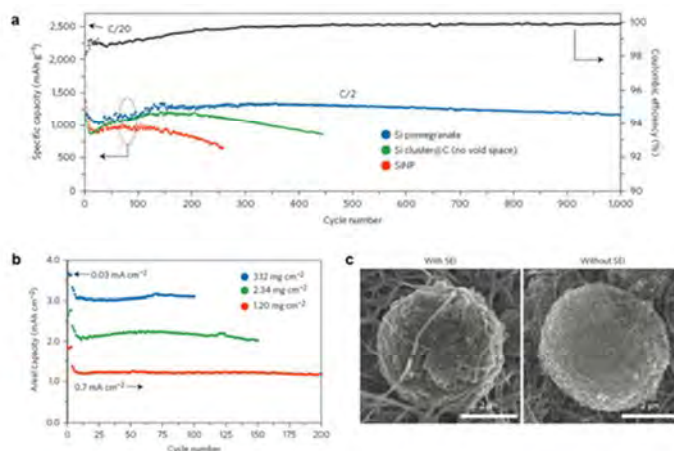


**Figure 2.** (a) Reversible delithiation capacity for the first 1000 galvanostatic cycles of Si pomegranate and other structures tested under the same conditions. (b) High areal mass loading test (up to  $3.12 \text{ mg cm}^{-2}$  active material) of Si pomegranate anodes. (c) Typical SEM images of Si pomegranates after 100 cycles.

The SEM images confirm the pomegranate structures remain intact after 100 cycles (Fig. 2c).

### Fluorinated Electrolyte for 5-V Li-ion Chemistry

**PROJECT OBJECTIVE:** The objective of this project is to develop a new advanced electrolyte system with outstanding stability at high voltage and high temperature and improved safety characteristic for an electrochemical couple consisting of the high voltage  $\text{LiNi}_{0.5}\text{Mn}_{1.5}\text{O}_4$  (LNMO) cathode and graphite anode. The specific objectives of this proposal are the design, synthesis and evaluation of (1) non-flammable high voltage solvents to render intrinsic voltage and thermal stability in the entire electrochemical window of the high-voltage cathode materials, and (2) electrolyte additives to enhance the formation of a compact and robust solid electrolyte interphase (SEI) on the surface of the high voltage cathode. A third objective is to gain fundamental understanding of the interaction between electrolyte and high voltage electrode materials, the dependence of SEI functionality on electrolyte composition, and the effect of high temperature on the full Li-ion cells using the advanced electrolyte system.

**PROJECT IMPACT:** This innovative fluorinated electrolyte is intrinsically more electrochemically stable due to the fluorine substitution; therefore it would be applicable to cathode chemistries based on TM oxides other than LNMO. Therefore, the results of this project can be further applied to a wide spectrum of high-energy battery systems oriented for PHEVs that operate at high potentials, such as  $\text{LiMPO}_4$  (M=Co, Ni, Mn), or battery systems that require a high-voltage activation process, such as the high-capacity Li-Mn-rich  $x\text{Li}_2\text{MnO}_3 \cdot (1-x)\text{Li}[\text{Ni}_x\text{Mn}_y\text{Co}_z]\text{O}_2$ . Therefore, this electrolyte innovation will push the U.S. supply base of batteries and battery materials past the technological and cost advantages of foreign competitors, thereby increasing economic value to the USA. ANL's new fluorinated electrolyte material will enable the demand for more PHEVs and EVs, which directly transforms to much less gasoline consumption and less pollutant emissions.

**OUT-YEAR-GOALS:** The goal of this project for the 2<sup>nd</sup> year is to deliver a new fluorinated electrolyte system with outstanding stability at high voltage and high temperature with improved safety characteristic for an electrochemical couple consisting of 5-V Ni-Mn spinel  $\text{LiNi}_{0.5}\text{Mn}_{1.5}\text{O}_4$  (LNMO) cathode and graphite anode. The specific objectives of this proposal are the design, synthesis, and evaluation of (1) non-flammable high voltage fluorinated solvents to attain intrinsic voltage stability in the entire electrochemical window of the high-voltage cathode material and (2) effective electrolyte additives that form a compact and robust solid-electrolyte interphase (SEI) on the surfaces of the high voltage cathode and graphitic anode.

**COLLABORATIONS:** Kang Xu, Co-PI, U.S. ARL; Xiao-Qing Yang, Co-PI, BNL; Ganesh Skandan, NEI Corporation; Brett Lucht, University of Rhode Island; Libo Hu, Andrew Jansen, Ira Bloom, and Gregory Krumdick, ANL.

#### Milestones

- 1) Complete theoretical calculation of electrolyte solvents (fluorinated carbonate, fluorinated ether) and additives (fluorinated phosphate, fluorinated phosphazene); Validate the electrochemical properties of the available fluorinated solvents by CV and leakage current experimnt. (Dec. 13) **Complete**.
- 2) Synthesize and characterize the Gen-1 electrolyte (3 linear/cyclic F-carbonate solvents + 1 additive) by NMR, FT-IR, GC-MS, DSC. (Mar. 14) **Ongoing**.
- 3) Evaluate the LNMO/graphite cell performance of Gen-1 electrolyte [Solvent(s) + Additive(s)]. (Jun. 14) **Ongoing**.
- 4) Optimize the Gen-1 high voltage F-electrolyte; Deliver 10 baseline pouch cells. (Sep. 14) **Ongoing**.

## Progress Report

In the second quarter of FY14, the team continued to synthesize and characterize several fluorinated carbonate compounds as high voltage electrolyte candidates and evaluated their electrochemical performance in LNMO/graphite cells. The molecules that have currently been synthesized, characterized and purified are listed in Fig. 1a. The reactions involved in the synthesis are illustrated in Fig. 1b.

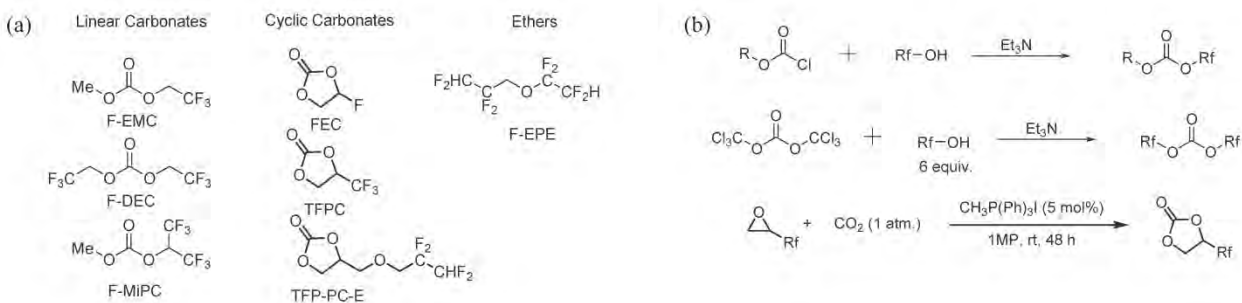


**Figure 1.** (a) Structures of currently synthesized fluorinated carbonates; (b) General synthetic schemes of the fluorinated carbonates.

The first generation high voltage F-electrolyte HVE1 (1.0 M LiPF<sub>6</sub> in FEC/F-EMC/F-EPE=3/5/2 v/v/v with 1% LiDFOB) was formulated. Tremendous improvement in LNMO/A12 cell performance over the SOA electrolyte was observed by using HVE1 (Fig. 2a) with minimal electrode morphology change (Fig. 2b, 2c). The coulombic efficiency of HVE1 is stabilized at around 99.5% after 20 cycles while the SOA cell never reached 98%, demonstrating the improved oxidation stability of HVE1.

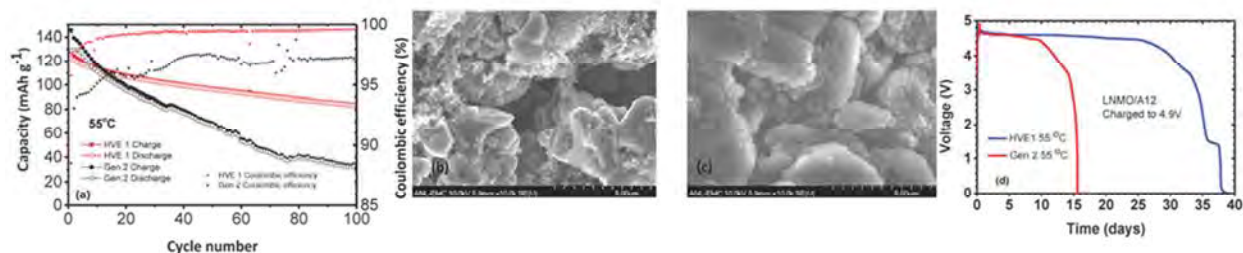


**Figure 2.** (a) Capacity retention of LNMO/graphite cells cycled between 3.5-4.9 V, C/3 using Gen 2 and HVE 1 electrolyte at 55°C; SEM of LNMO (b) and graphite (c) electrode after 100 cycles at 55 °C; (d) Self-discharge property of HEV1 and Gen 2 at 55°C.

FT-IR spectra (not shown) of the harvested LNMO showed no obvious organic species for the HVE1 cell cycled at 55°C while a prominent peak at 1720 cm<sup>-1</sup> was observed for the SOA cell. From RT to 55°C, the graphite anode with Gen 2 electrolyte underwent a significant increase in the level of decomposition products. This finding points to a significant morphology change of the SEI layer under high temperature operation. In comparison, the HVE anode showed less organic residues in the IR spectrum and the presence of more inorganic species on the graphite surfaces, which was supported by images from the SEM. No visual difference was observed between the RT and 55 °C data. SEM, FT-IR, and GC-MS data for the graphite anode and the harvested electrolyte confirmed that HVE1 could tolerate high voltage charging and formed a robust SEI comprising of more inorganic species, which is more stable at high temperature during the high voltage charging and discharging.

In this quarter, the self-discharge of the LNMO/graphite cells with HVE1 was compared to that of Gen 2 electrolytes. From a fully charged state (4.9 V) at 55°C, the cell with the fluorinated HVE1 electrolyte lasted more than twice as long (38 days) as the Gen 2 cell (15 days) before rapid capacity fade, which is another indicator of the excellent stability of the fluorinated electrolyte. This data is shown in Fig. 2d.

## Task 3.2 – Joe Sunstrom and Hitomi Miyawaki (Daikin America, Inc.)

### Daikin America High Voltage Electrolyte

**PROJECT OBJECTIVE:** Development of a stable (300 – 1000 cycles), high-voltage (at 4.6 volts), and safe (self-extinguishing) formulated electrolyte.

Exploratory Development (Budget Period #1 – October 1, 2013 to January 31, 2015)

- Identify promising electrolyte compositions for high-voltage (4.6 v) electrolytes via the initial experimental screening and testing of selected compositions

Advanced Development (Budget Period #2 – February 1, 2015 to September 31, 2015)

- Detailed studies and testing of the selected high-voltage electrolyte formulations and the fabrication of final demonstration cells

**PROJECT IMPACT:** Fluorinated small molecules offer the advantage of low viscosity along with high chemical stability due to the strength of the C-F bond. Due to this bond strength, Daikin fluorochemical materials are among the most electrochemical stable materials that still have the needed performance attributes for a practical electrolyte. Such an electrolyte will allow routine operating voltages to be increased to 4.6 volts. This technological advance would allow significant cost reduction by reducing the number of cells needed in a particular application and/or allow for greater driving range in PHEV applications.

**OUT-YEAR-GOALS:** This project has a clearly defined goals for both temperature and voltage performance which are consistent with the deliverables of this proposal. Those goals are to deliver an electrolyte capable of 300 - 1000 cycles at 3.2 - 4.6 V at nominal rate with stable performance. An additional goal is to have improved high temperature (> 60°C) performance. An additional safety goal is to have this electrolyte be self-extinguishing.

**COLLABORATIONS:** At present, the team is collaborating with and receiving great advice from Vince Battaglia's group at LBNL. In addition, there are plans to collaborate with another group (TBD) for electrode surface analysis.

### Milestones

Budget Period #1 – Oct. 1, 2013 to Jan. 31, 2015

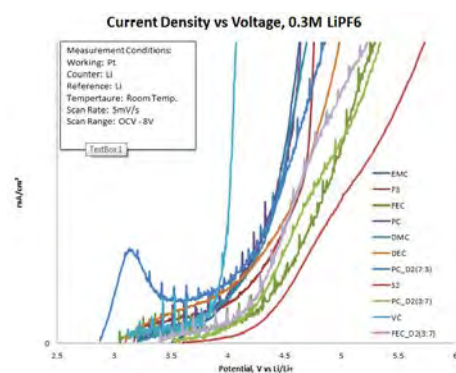
- 1) Complete identification of promising electrolyte formulations. Experimental design completed with consistent data sufficient to build models. Promising electrolyte formulations are identified which are suitable for high-voltage battery testing. **Ongoing**
- 2) Fabricate 10 interim cells and deliver cells to DOE laboratory to be specified. **Ongoing**
- 3) Electrochemical and battery cycle tests are completed and promising results are obtained which demonstrate stable performance at 4.6 volts. **Ongoing**

## Progress Report

The technical approach to achieve the milestones is based on an iterative plan following a sound scientific method, also sometimes referred to as a Plan-Do-Check-Act (PDCA) cycle, which has been described in detail in last report.

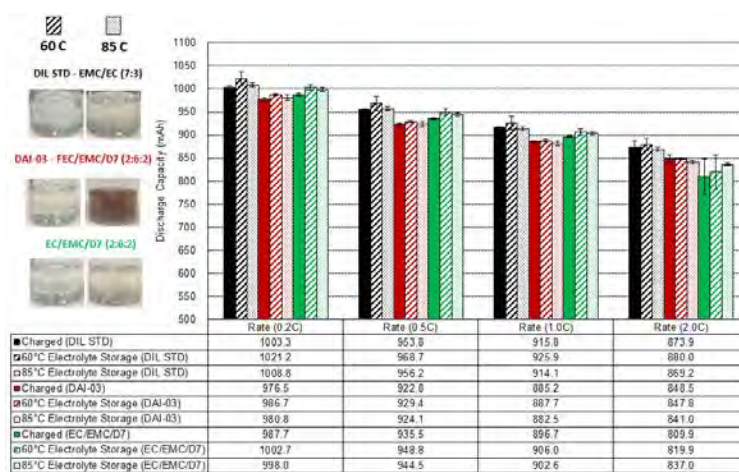
**Status:** The first PDCA cycle is nearing completion. The initial project plan outlines this cycle as the first stage of optimization of the base solvent mixtures for the target electrolytes. Base property measurements of the candidate solvents and mixtures have been completed. The voltage and temperature stability has been determined for the materials. The conductivity of the mixtures has been measured with respect to the solvent identities and proportions.

The first set of experiments was to determine voltage stability of the hydrocarbons and fluorocarbons to be used in the study. The linear scan voltammetry (LSV) of several of the candidate materials is shown below. The scans are completed using a platinum working electrode against lithium metal counter and reference electrodes. The materials scanned are hydrocarbons (PC, EMC, DEC, DMC, VC) fluorocarbons (FEC, S2, D2, F3) and mixtures thereof. In all cases, the fluorocarbon/fluorocarbon mixtures have a higher decomposition voltage. The noise in the signals is due to contact resistance of the alligator clips.



Additional LSV scans show a comparison of the conventional additive vinylene carbonate with a fluorocarbon additive mixture (FEC/D2) which has higher voltage stability.

A temperature stability investigation was completed on the two baseline compositions which were identified in the previous quarter. The baseline electrolytes are one hydrocarbon (EMC/EC 7:3) and one fluorocarbon (FEC/EMC/D7 2:6:2). These were compared to a third electrolyte which contained fluoroether D7 but with EC instead of FEC to delineate thermal stabilities of hydrocarbon, FEC, and the fluoroether.



The three compositions were prepared then stored neat at RT, 60°C, and 85°C. The composition containing FEC had a noticeable color change at 85°C (see graph). NMC/graphite cells were then filled with these electrolytes and the performance was measured. The results in the graph show no difference in rate or capacity when discharged from 4.2 V, even with apparent decomposition of the FEC electrolyte. However, after the fully charged cells are stored at 85°C for 72 hrs, there is pronounced gassing in cells containing FEC electrolyte, regardless of the electrolyte aging protocol. This enhanced gassing leads to diminished cell performance in capacity retention, recovery, and rate capability. It is suggested that all oven aging protocols do not exceed 60°C to get true performance characteristics of FEC containing electrolytes. Conductivity of the chosen baseline electrolytes was measured and compared to variations of the same. The parameters for the conductivity study include hydrocarbon identity, fluoroether content, FEC vs. EC, and salt concentration. The objective of this measurement is to understand magnitude of conductivity change by affecting simple parameters. Finally, high voltage (3.0 to 4.6 V) cycling has begun for the baseline electrolytes (1.0 M LiPF<sub>6</sub> EMC/EC 7:3, 1.2 LiPF<sub>6</sub> FEC/EMC/D7 2:6:2). Initial data shows the advantage of the fluorinated solvents compared to conventional solvents when cycling at high voltage.

## Task 3.3 – Dee Strand (Wildcat Discovery Technologies)

### Novel Non-Carbonate Based Electrolytes for Silicon Anodes

#### **PROJECT OBJECTIVE:**

The objective of this project is to develop non-carbonate electrolytes that form a stable solid electrolyte interphase (SEI) on silicon alloy anodes, enabling substantial improvements in energy density and cost relative to current lithium ion batteries (LIBs). These improvements are vital for mass market adoption of electric vehicles. At present, commercial vehicle batteries employ cells based on  $\text{LiMO}_2$  ( $M = \text{Mn, Ni, Co}$ ),  $\text{LiMn}_2\text{O}_4$ , and/or  $\text{LiFePO}_4$  coupled with graphite anodes. Next generation cathode candidates include materials with higher specific capacity or higher operating voltage, with a goal of improving overall cell energy density. However, to achieve substantial increases in cell energy density, a higher energy density anode material is also required. Silicon anodes demonstrate very high specific capacities, with a theoretical limit of 4200 mAh/g and state-of-the-art electrodes exhibiting capacities greater than 1000 mAh/g. While these types of anodes can help achieve target energy densities, their current cycle life is inadequate for automotive applications. In graphite anodes, carbonate electrolyte formulations reductively decompose during the first cycle lithiation, forming a passivation layer that allows lithium transport, yet is electrically insulating to prevent further reduction of bulk electrolyte. However, the volumetric changes in silicon upon cycling are substantially larger than graphite, requiring a much more mechanically robust SEI film.

#### **PROJECT IMPACT:**

Silicon alloy anodes enable substantial improvements in energy density and cost relative to current lithium ion batteries. These improvements are vital for mass market adoption of electric vehicles, which would significantly reduce  $\text{CO}_2$  emissions as well as eliminate the US dependence on energy imports.

#### **OUT-YEAR-GOALS:**

Development of non-carbonate electrolyte formulations that

- form stable SEIs on 3M silicon alloy anode, enabling coulombic efficiency > 99.9% and cycle life > 500 cycles (80% capacity) with NMC cathodes;
- have comparable ionic conductivity to carbonate formulations, enabling high power at room temperature and low temperature;
- are oxidatively stable to 4.6V, enabling the use of high energy NMC cathodes in the future; and
- do not increase cell costs over today's carbonate formulations.

#### **COLLABORATIONS:**

Wildcat is working with 3M on this project. To date, 3M is supplying the silicon alloy anode films and NMC cathode films for use in Wildcat cells.

#### Milestones

- 1) Assemble materials, establish baseline performance with 3M materials (Dec. 13) **Complete**
- 2) Develop initial additive package using non-SEI forming solvent. (Mar. 14) **Complete**
- 3) Screen initial solvents with initial additive package. (Jun. 14) **Ongoing**
- 4) Design/build interim cells for DOE (Sep. 14) **Ongoing**

## Progress Report

The second quarter of this project focused on identification of an initial SEI additive package that can be used in an EC-free electrolyte formulation. A total of 82 additives were tested at two concentrations in NMC//Si alloy full cells in a PC:EMC (1:4), 1M LiPF<sub>6</sub> baseline electrolyte. The first-cycle discharge capacities and coulombic efficiencies for the formulations of additives sorted by chemistry category of the additives are shown in Fig. 1. Each category (labelled Cat # on graph) contains multiple additives in a particular chemistry family (*e.g.*, anhydrides, boron containing molecules, etc.) In both figures, the gray band is +/- one standard deviation about the mean of the PC/EMC control electrolyte with no additives. The pink band is the similar quantity for the EC/EMC (EC:EMC (1:2), 1M LiPF<sub>6</sub> control electrolyte with no additives. Standard deviations of the PC/EMC controls are large as the performance of the non-EC containing electrolyte with no additive is very poor on silicon. Many of the additives improve both first cycle specific capacity and coulombic efficiency relative to the PC/EMC control. Several of the additives perform similarly to the EC/EMC control in the NMC//Si alloy full cells.

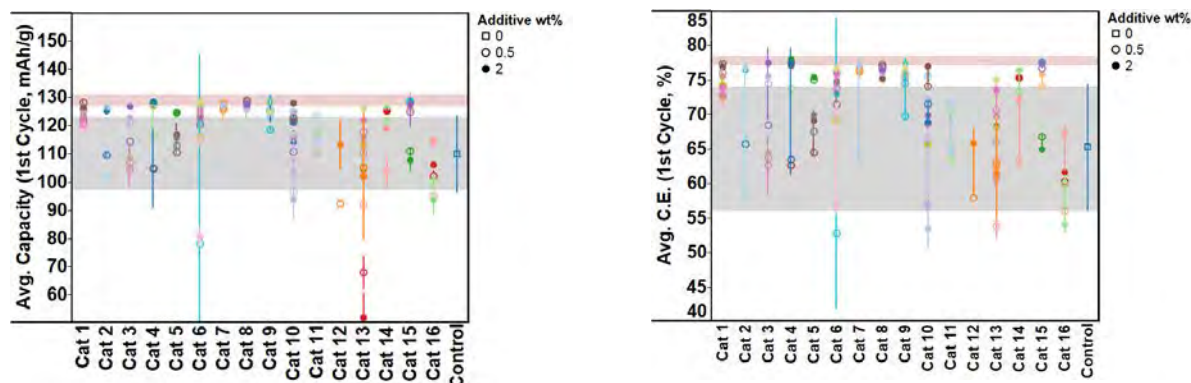


**Figure 1.** Full cell first cycle discharge capacities of additives in PC/EMC base electrolyte are improved over the control (gray band)

The capacity retentions at cycle 50 for the additives in PC/EMC full cells are shown in Fig.2, where several of the additives perform similarly to the EC/EMC control.

Since the PC/EMC base solvent shows poor cycle life, presumably due to poor SEI formation, the additives circled in Fig. 2 must account for improved SEI. The improved SEI provides performance similar to that obtained with an EC/EMC electrolyte. Therefore, these additives provide the basis for evaluation of alternative, non-carbonate solvents – which defines the next phase of the project.

Activities in the next quarter will focus on two main efforts. First, screening non-carbonate solvents and formulations with the initial additives identified in 1Q14 will begin. Second, screening of new additives will continue, based on hypotheses described in the original Wildcat proposal for effectiveness in a PC/EMC based electrolyte. As new, promising additives are identified, these will be incorporated into formulations of new solvents.

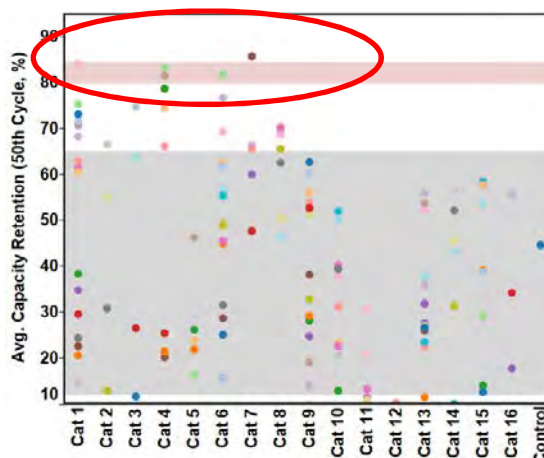


**Figure 2.** Cycle lives of several additives in PC/EMC are similar to the EC/EMC control in NMC//Si alloy full cells.

## Task 4.1 – Michael Thackeray (Argonne National Laboratory)

### Novel Cathode Materials and Processing Methods

**PROJECT OBJECTIVE:** The end-goal of this project is the development of low-cost, high-energy and high-power, Mn-oxide-based cathodes for PHEV and EV vehicles. Improvement of design, composition and performance of advanced electrodes with stable architectures, facilitated by an atomic-scale understanding of electrochemical and degradation processes, is a key objective of this work. New processing routes as well as Argonne National Laboratory's comprehensive characterization facilities will be used to explore novel, surface and bulk structures both *in situ* and *ex situ* in the pursuit of advancing Li-ion battery cathode materials.

**PROJECT IMPACT:** Standard Li-ion technologies are currently unable to meet the demands of next-generation PHEV and EV vehicles. Battery developers and scientists alike will take advantage of the knowledge, both applied and fundamental, generated from this project to further advance the field. In particular, it is expected that this knowledge will significantly enable progress towards meeting the DOE goals for 40-mile, all-electric range, PHEVs.

#### **OUT-YEAR-GOALS:**

- Identify composite electrode structures that mitigate or eliminate voltage fade.
- Identify and characterize surface chemistries and architectures that allow fast Li-ion transport, are stable to ~5 V, and mitigate or eliminate transition-metal dissolution.
- Scale-up, evaluate and verify promising cathode materials using Argonne National Laboratory's Scale-up and Cell Fabrication facilities.
- Take advantage of Argonne National Laboratory's user facilities (e.g., the Advanced Photon Source (APS), the Center for Nanoscale Materials (CNM), the Electron Microscopy Center (EMC) and the Argonne Leadership Computing Facility (ALCF) to build on the fundamental knowledge gained to promote and implement the rational design of new electrode materials.
- Use complementary theoretical approaches to further the understanding of electrode structures and electrochemical processes to accelerate the progress of materials development.

**COLLABORATIONS:** Jason Croy, Brandon Long, Joong Sun Park, Kevin Gallagher, Mahalingam Balasubramanian (APS), Dean Miller (EMC), and William David (Rutherford Appleton Laboratory, UK).

#### Milestones

- 1) Evaluate the stabilization and performance of near end-member,  $\text{Li}_2\text{MnO}_3$ -containing composite electrodes. Specifically, high and low  $\text{Li}_2\text{MnO}_3$ -content electrodes. (Dec. 13) **Go for low  $\text{Li}_2\text{MnO}_3$ ; No-go for high  $\text{Li}_2\text{MnO}_3$**
- 2) Evaluate new synthetic routes using layered  $\text{LiMO}_2$  (M = Mn, Ni, Co) precursors to prepare composite electrode materials. (Mar. 14) **Complete**
- 3) Synthesize and characterize unique surface architectures that enable  $>200$  mAh/g at a  $>1\text{C}$  rate with complementary theoretical studies of surface structures. (Jun. 14) **Ongoing**
- 4) Identify structures and compositions, including surface and bulk, that can deliver *ca.* 230 mAh/g at an average discharge voltage of *ca.* 3.5 V on extended cycling. (Sep. 14) **Ongoing**

## Progress Report

Past reports indicate that transformations in composite, layered-layered (LL) electrodes might be mitigated with the incorporation of a stabilizing spinel component. This component, ideally with a transition metal (TM) occupancy of 25% in the Li layers, may serve as a stabilizing unit against further TM migration. In addition, due to the 3D pathways in the spinel structure, enhanced rate performance can also be realized over pure LL materials. However, control over both elemental and structural composition is difficult when integrating layered and spinel components by traditional syntheses routes; hindering the systematic optimization of targeted materials. Recently, an exploratory study was undertaken to evaluate several different synthesis methods for their effectiveness in creating LL electrodes with integrated spinel components, noted as layered-layered-spinel (LLS).

Recent research has shown that the intermediate, low-temperature firing of precursor materials, often employed in the synthesis of cathode materials, results in a non-uniform distribution of lattice parameters in the final products, yielding secondary phases not otherwise observed. This suggests that a low-temperature “spinel precursor” might promote the formation of LLS composites. A systematic study was conducted by synthesizing a targeted  $\text{LiMn}_{1.5}\text{Ni}_{0.5}\text{O}_4$  precursor at temperatures between 450-850°C. These precursors were thoroughly mixed with LL,  $\text{Li}_{1.2}\text{Mn}_{0.6}\text{Ni}_{0.2}\text{O}_2$  precursors, also fired at various temperatures, and fired at final temperatures of 850 and 900°C. XRD and electrochemical cycling (not shown), however, revealed poor integration of the two components and no electrochemical advantages were found. These results suggest that high-energy ball milling may be of some advantage to this approach. This line of research has been stopped and given a “no-go” decision.

Layered  $\text{Li}_2\text{MnO}_3$  precursors have been successfully used to produce composite structures. Using this novel method a study was conducted to ascertain its effectiveness for synthesizing LLS electrodes. Figure 1(a) shows the first-cycle electrochemical discharge (prior to charging) from a series of  $x[\text{Li}_{1.2}\text{Mn}_{0.6}\text{Ni}_{0.2}\text{O}_2] \cdot (1-x)\text{LiMn}_{1.5}\text{Ni}_{0.5}\text{O}_4$  electrodes. The increasing capacities with decreasing  $x$  follow the expected trend for uptake of Li in vacant octahedral sites of the incorporated spinel structures. Figure 1(b) shows the XRD evolution with  $x$ ; the appearance of spinel peaks are evident with minor NiO-like impurities for  $x=0.5$  and 0.75 (dashed lines). Figure 1(c) shows high resolution TEM of a  $0.85[0.25\text{Li}_2\text{MnO}_3 \cdot 0.75\text{LiMn}_{0.375}\text{Ni}_{0.375}\text{Co}_{0.25}\text{O}_2] \cdot 0.15\text{LiMn}_{1.5}\text{Ni}_{0.5}\text{O}_4$  particle. Clearly observable within the image are layered (A and C) and spinel (B) regions. EDX analysis on the spinel region (B) revealed a Mn and Ni rich composition; indicating the intended  $\text{LiMn}_{1.5}\text{Ni}_{0.5}\text{O}_4$  composition may in fact be present.

This novel synthesis method utilizing  $\text{Li}_2\text{MnO}_3$  will continue to be used to explore LLS electrodes.

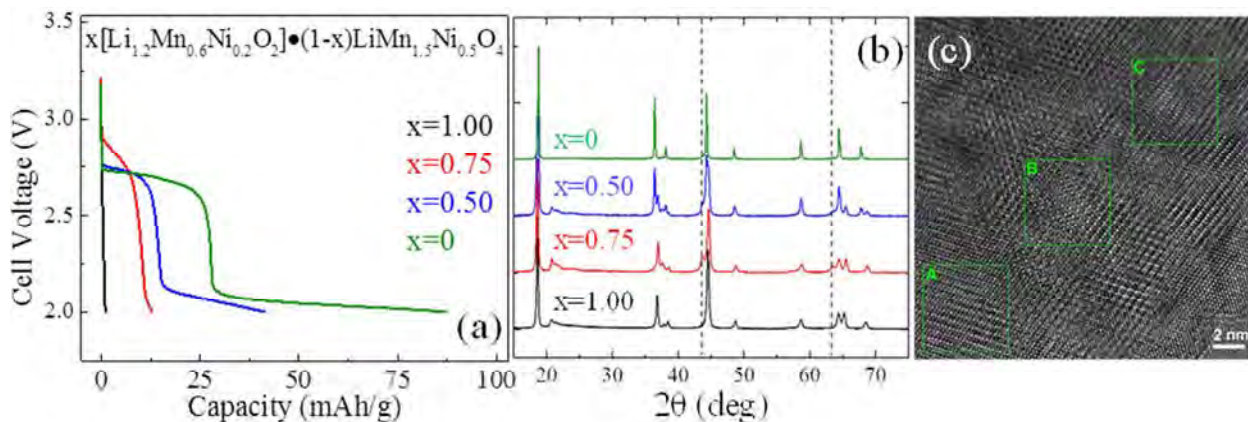


**Figure 1.** (a) Initial discharge capacities for various  $x$  values in  $x[\text{Li}_{1.2}\text{Mn}_{0.6}\text{Ni}_{0.2}\text{O}_2] \cdot (1-x)\text{LiMn}_{1.5}\text{Ni}_{0.5}\text{O}_4$  electrodes and the corresponding XRD patterns, (b) Dashed lines mark NiO-like impurities, (c) High resolution TEM image of  $0.85[0.25\text{Li}_2\text{MnO}_3 \cdot 0.75\text{LiMn}_{0.375}\text{Ni}_{0.375}\text{Co}_{0.25}\text{O}_2] \cdot 0.15\text{LiMn}_{1.5}\text{Ni}_{0.5}\text{O}_4$  particle showing integrated, layered (regions A and C) and spinel (region B) components.

### Design of High Performance, High Energy Cathode Materials

**PROJECT OBJECTIVE:** To develop high energy, high performance cathode materials including composites and coated powders, using spray pyrolysis and other synthesis techniques. The emphasis is on two systems; modified NMC materials and the high voltage spinel,  $\text{LiNi}_{0.5}\text{Mn}_{1.5}\text{O}_4$  (LNMO). Partial substitution of Ti for Co in NMCs results in higher discharge capacities (up to 225 mAh/g) without the need for a formation reaction and without risk of structural change during cycling. Experiments are directed towards optimizing the synthesis, improving cycle life, and understanding the effect of Ti substitution. For LNMO, particle size and morphology are controlled during spray pyrolysis synthesis by varying residence time, temperature, precursors and other synthetic parameters. By exploiting differences in precursor reactivity, coated materials can be produced, and composites can be prepared by post-processing techniques such as infiltration. These approaches are expected to improve cycling due to reduced side reactions with electrolytes.

**PROJECT IMPACT:** To increase the energy density of Li ion batteries, cathode materials with higher voltages and/or higher capacities are required, but safety and cycle life cannot be compromised. In the short term, the most promising materials are based on high voltage spinels or modified NMCs that do not require formation cycles or undergo structural transformations during cycling. Ti-substituted NMCs exhibit increased discharge capacity, due to improved first cycle efficiencies and are not expected to undergo structural changes or voltage decay during cycling. Optimizing LNMO particle morphologies, utilizing coatings and composites are expected to improve coulombic efficiencies and safety as well as cycle life.

**OUT-YEAR GOALS:** Two high-energy cathode systems will have been optimized for this work; LNMO and high capacity Ti-substituted NMC cathodes, which do not require activation via charge to high potentials. Materials will be synthesized by a simple, low cost spray pyrolysis method, which has potential for commercialization. This technique produces phase-pure, unagglomerated powders and allows for excellent control over particle morphologies, sizes and distributions. Coated materials will also be produced in either one or two simple steps by exploiting differing precursor reactivities during the spray pyrolysis procedure, or by first preparing hollow spheres of an electroactive material, infiltrating the spheres with precursors of the high voltage cathodes, and subsequent thermal treatment. The final result is expected to be a high energy density cathode material with good safety and cycling characteristics suitable for use in vehicular applications, which can be made by a low-cost process that is easily scalable.

**COLLABORATIONS:** Huolin Xin (BNL), Dennis Norlund, Tsu-Chien Weng, and Dimosthenis Sokaras (SLAC National Accelerator Laboratory), Mark Asta (U.C. Berkeley)

#### Milestones

- 1) Complete optimization of Ti-NMC synthesis with  $\text{TiOSO}_4$  precursor. (Dec.13) **Discontinued. This effort has been transferred to the ABR program**
- 2) Go/No-Go: Decision on infiltration of  $\text{LiFePO}_4$  into LNMO. Criteria: A “no go” decision will be made if attempts to prevent reaction of  $\text{LiFePO}_4$  with LNMO during processing fail (Mar.14) **No go. Effort will be redirected towards composites with spray pyrolyzed NMCs.**
- 3) Complete soft XAS experiments on Ti-NMCs (Jun.14) **Completed**
- 4) Go/No-Go: Decision on spray pyrolysis of NMCs. Criteria: A “no go” decision will be made if the electrochemical performance of the spray-pyrolyzed material does not equal that of the material made by co-precipitation. (Sep. 14). **Ongoing**

## Progress Report

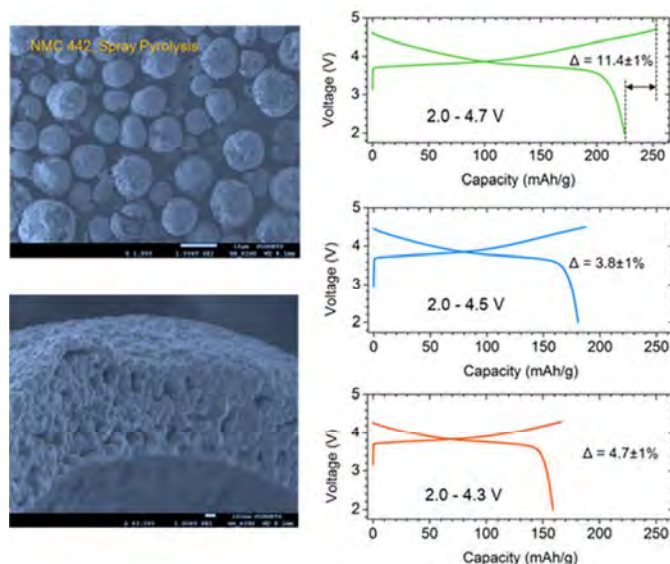


**Figure 1.** SEM images of NMC-442 prepared by spray pyrolysis (left, top and bottom). Electrochemical cycling in Li half cells was performed with different voltage cutoffs: 2.0-4.7 V (top right), 2.0-4.5 V (middle right) and 2.0-4.3 V (bottom right).

Spray pyrolysis synthesis of cathode materials was resumed this quarter. For synthesis of NMCs, a wide range of synthetic parameters were screened, including stock solution concentration, gas flow rate, and Ni/Mn/Co ratios. NMC-442 and NMC-622 samples were successfully prepared. Electrochemical cycling has been performed on these materials and representative results are shown in Fig. 1. The SEM images in Fig. 1 show the typical morphology of the NMC-442 materials; hollow structures with shells consisting of nanoscale primary particles, strongly connected to each other. Further efforts are being implemented to achieve dense solid secondary particles by controlling synthesis parameters. Hollow particles will be used in the fabrication of composites *via* an infiltration process (this effort will replace milestone 2, for which a “no go” decision has been made). Electrochemical testing shows that the spray pyrolyzed NMC materials have higher discharge capacities and improved coulombic efficiencies compared to NMCs produced by co-precipitation reactions, prompting a “go” decision for milestone 4. Further efforts are ongoing to determine the rate capability and cycling stability, as well as to include Ti in the compositions.

Synchrotron X-ray Raman spectroscopy has also been used this quarter to characterize NMC materials. Several unexpected phenomena have been observed and the data are being processed.

### High-capacity, High-voltage Cathode Materials for Lithium-Ion Batteries

**PROJECT OBJECTIVE:** A significant increase in capacity and/or operating voltage is needed to make the Li-ion technology viable for vehicle applications. This project addresses this issue by focusing on the design and development of cathode materials based on polyanions that have the possibility for reversibly inserting/extracting more than one Li ion per transition-metal ion and/or operating above 4.3 V. Specifically, high-capacity and/or high-voltage Li transition-metal phosphate, silicate, and carbonophosphate cathodes are investigated. The major issue with the phosphate and silicate cathodes is the poor electronic and ionic transport, which limits the practical capacity, energy density, and power density. To overcome these difficulties, novel microwave-assisted solvothermal, microwave-assisted hydrothermal, and template-assisted synthesis approaches are pursued to realize controlled morphology with smaller particle size and to integrate conductive additives like graphene in a single synthesis step.

**PROJECT IMPACT:** The critical requirements for the widespread adoption of Li-ion batteries for vehicle applications are high energy, high power, long cycle life, low cost, and acceptable safety. The currently available cathode materials do not adequately fulfill these requirements. The polyanion cathodes with the novel synthesis approaches pursued in this project have the potential to significantly increase the energy and power. More importantly, the covalently bonded polyanion groups can offer excellent thermal stability and enhanced safety. The microwave-assisted synthesis approaches pursued also lower the manufacturing cost of the cathodes through a significant reduction in reaction time and temperature.

**OUT-YEAR GOALS:** The overall goal is to enhance the electrochemical performances of high-capacity, high-voltage polyanion cathode systems and to develop a fundamental understanding of their structure-composition-performance relationships. Specifically, the project is focused on enhancing the electrochemical performance of systems such as  $\text{LiMPO}_4$ ,  $\text{Li}_2\text{MP}_2\text{O}_7$ ,  $\text{Li}_2\text{MSiO}_4$ ,  $\text{Li}_3\text{V}_2(\text{PO}_4)_3$ ,  $\text{Li}_9\text{V}_3(\text{P}_2\text{O}_7)_3(\text{PO}_4)_2$ ,  $\text{Li}_3\text{M}(\text{CO}_3)(\text{PO}_4)$ , and their solid solutions with  $\text{M} = \text{Mn, Fe, Co, Ni, and VO}$ . Advanced structural, chemical, surface, and electrochemical characterizations of the materials synthesized by novel approaches are anticipated to provide in-depth understanding of the factors that control the electrochemical properties of the polyanion cathodes. For example, the possible segregation of certain cations to the surface in solid solution cathodes consisting of multiple transition-metal ions and the role of conductive graphene integrated into the polyanion cathodes can help design better-performing cathodes.

**COLLABORATIONS:** None this quarter.

#### Milestones

- 1) Establish whether or not  $\text{LiMnPO}_4$  can be aliovalently doped with  $\text{V}^{3+}$  and determine its effect on electrochemical performance. (Dec-13) **Complete**
- 2) Demonstrate  $> 200$  mAh/g capacity with  $\text{LiVOPO}_4$  prepared by novel synthesis approaches. (Mar-14) **Complete**
- 3) Establish whether or not  $\text{LiCoPO}_4$  can be aliovalently doped with  $\text{V}^{3+}$  and determine its effect on electrochemical performance. (Jun-14) **Ongoing**
- 4) Go/No-Go: Stop the microwave-assisted synthesis if capacities are  $< 150$  mAh/g. Criteria: demonstrate  $> 150$  mAh/g capacity with  $\text{Li}_3\text{M}(\text{CO}_3)(\text{PO}_4)$  prepared by microwave-assisted synthesis. (Sep-14) **Ongoing**

## Progress Report

This quarter's efforts focused on the synthesis of  $\text{LiVOPO}_4$  polymorphs and the optimization of their microstructures. First,  $\alpha_1$ - $\text{LiVOPO}_4$ /graphene nanocomposite was synthesized by a microwave-assisted solvothermal (MW-ST) process at  $210^\circ\text{C}$  in a mixed solvent consisting of water and ethanol. The  $\alpha_1$ - $\text{LiVOPO}_4$  (tetragonal) sample exhibits a "flower-balls" morphology with an average particle size of *ca.*  $5\ \mu\text{m}$ , as shown in the scanning electron microscopy (SEM) image in Fig. 1a. Each "flower ball" is composed of uniform 80 to 100 nm "nanopetals" (see the inset in Fig. 1a). Graphene sheets were incorporated to form  $\alpha_1$ - $\text{LiVOPO}_4$ /graphene nanocomposite by the thermal reduction of graphene oxide (GO) during the microwave synthesis. As seen in Fig. 1b, cyclic voltammetry (CV) of the  $\text{LiVOPO}_4$ /graphene nanocomposite at  $0.01\ \text{mV s}^{-1}$  shows two reduction peaks at 2.3 and 3.9 V and two oxidation peaks at 2.5 and 4.1 V. The two peaks correspond to the reversible insertion/extraction of two Li (between  $\text{VOPO}_4$  and  $\text{Li}_2\text{VOPO}_4$ ), analogous to that found previously with both  $\alpha$ - $\text{LiVOPO}_4$  (triclinic) and  $\beta$ - $\text{LiVOPO}_4$  (orthorhombic), although the lower-voltage (*ca.* 2 V) profile is more sloping in  $\alpha_1$ - $\text{LiVOPO}_4$  compared to those in  $\alpha$ - $\text{LiVOPO}_4$  and  $\beta$ - $\text{LiVOPO}_4$ . Figure 1c shows the first charge-discharge profiles at C/20 rate of  $\alpha_1$ - $\text{LiVOPO}_4$ /graphene cathodes. The first charge capacity of  $160\ \text{mAh g}^{-1}$  at *ca.* 4 V corresponds to the extraction of 1.0 Li per formula. The first discharge capacity of  $220\ \text{mAh g}^{-1}$  corresponds to the insertion of 1.4 Li per formula, with the sloping voltage profile below 2.4 V corresponding to the insertion of the second Li into  $\text{LiVOPO}_4$ . These results are consistent with the CV data. Figure 1d shows the cyclability of the  $\alpha_1$ - $\text{LiVOPO}_4$ /graphene cathodes at C/20 and C/10 rates; further optimization is needed to improve the cyclability.

In addition,  $\beta$ - $\text{LiVOPO}_4$  by a sol-gel method was synthesized. Since the particle size of this  $\text{LiVOPO}_4$  sample is large, as seen in in Fig. 2a, it delivered a capacity of  $< 50\ \text{mAh g}^{-1}$  (not shown), indicating the criticality of reducing the particle size to overcome the poor ionic and electronic conductivity limitations. A macroporous carbon as a hard-template was employed to confine the growth of  $\text{LiVOPO}_4$  during the calcination process. The templated- $\text{LiVOPO}_4$  sample has a much smaller particle size, as seen in Fig. 2b, but the XRD pattern in Fig. 2c indicates this sample to be more like  $\alpha$ - $\text{LiVOPO}_4$  rather than  $\beta$ - $\text{LiVOPO}_4$ . Since the microwave process resulted in large (5 to  $10\ \mu\text{m}$ ) particles of  $\alpha$ - $\text{LiVOPO}_4$ , the  $\alpha$ - $\text{LiVOPO}_4$  with smaller particle size in Fig. 2b is anticipated to show better electrochemical performance, which will be pursued in the future.

In other work, the focus was also on suppressing the voltage decay in Li-rich layered oxide cathodes through compositional control and an understanding of the factors leading to voltage decay.

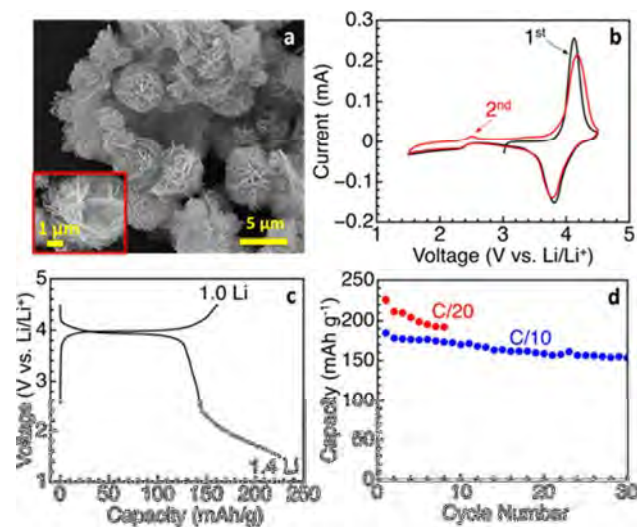


**Figure 1.** (a) SEM image, (b) CV plots, (c) first charge-discharge profiles at C/20 rate, and (d) cyclability at C/20 and C/10 rates of  $\alpha_1$ - $\text{LiVOPO}_4$ /graphene cathodes.

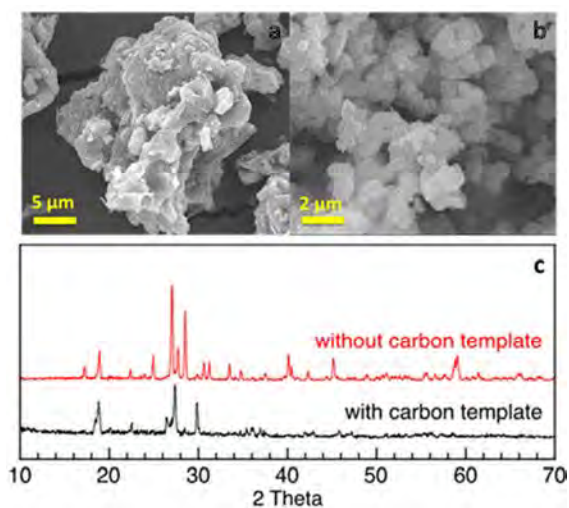


**Figure 2.** SEM images of  $\beta$ - $\text{LiVOPO}_4$  prepared (a) without and (b) with a carbon hard-template and (c) XRD patterns of the two samples.

### Development of High Energy Cathode Materials

**PROJECT OBJECTIVE:** The objective of this project is to develop high-energy, low-cost, and long-life cathode materials. Synthesis of Li-Mn-rich (LMR) layered composite cathodes will be further optimized by using the novel approaches we developed for high-voltage spinel in FY 2013. The working mechanism of the identified electrolyte additive will be systematically explored to reveal key factors that enable stable cycling of the LMR cathode. Advanced characterization techniques will be combined with electrochemical measurements to understand and mitigate the challenges in the LMR cathode.

**PROJECT IMPACT:** Although state-of-the-art cathode materials such as LMR layered composites have very high energy densities, their voltage fade and long-term cycling stability still need to be further improved. In this work, we will investigate the fundamental fading mechanism of LMR cathodes and develop new approaches to reduce the energy loss of these high-energy cathode materials. The success of this work will increase the energy density of Li-ion batteries and accelerate market acceptance of electrical vehicles (EV), especially for plug-in hybrid electrical vehicles (PHEV) required by the EV Everywhere Grand Challenge proposed by DOE/EERE.

**OUT-YEAR GOALS:** The long-term goal of the proposed work is to enable Li-ion batteries with a specific energy of >96 Wh/kg (for PHEVs), 5000 deep-discharge cycles, 15-year calendar life, improved abuse tolerance, and less than 20% capacity fade over a 10-year period.

#### **COLLABORATIONS:**

- Bryant Polzin (ANL)- LMR electrode supply
- X.Q. Yang (LBNL): *in situ* XRD characterization during cycling
- Karim Zaghib (Hydro-Quebec): material synthesis
- Kang Xu (ARL): new electrolyte

#### Milestones

- 1) Preparatory work on stable cycling of 80% capacity retention after 150 cycles high energy cathode based on  $x\text{Li}_2\text{MnO}_3 \cdot (1-x)\text{LiMO}_2$  ( $M = \text{Mn, Ni, Co}$ ;  $0 \leq x \leq 1$ ) (Dec. 13). **Complete**
- 2) Obtain stable cycling of 80% capacity retention after 150 cycles from high energy cathode based on  $x\text{Li}_2\text{MnO}_3 \cdot (1-x)\text{LiMO}_2$  ( $M = \text{Mn, Ni, Co}$ ;  $0 \leq x \leq 1$ ). (Mar. 14) **Complete**
- 3) Identify the fundamental mechanism responsible for electrolyte-additive-induced performance improvement of LMR cathode. (Jun. 14) **Ongoing**
- 4) Demonstrate the effects of elemental doping to improve the cycling stability of >200 cycles. (Sep. 14) **Ongoing**

## Progress Report

Last quarter, the working mechanism of tris (pentafluorophenyl) borane ( $(C_6F_5)_3B$ , TPFPB) as an electrolyte additive was proposed based on the improved electrochemical performance of LMR. This quarter, the effect of TPFPB on the long-term cycling of LMR was further investigated. The testing protocol proposed by ANL was adopted to evaluate the TPFPB additive.

Figure 1a compares the cycling ability of  $Li[Li_{0.2}Ni_{0.2}Mn_{0.6}]O_2$  cathode with and without the TPFPB additive. The cycling data of all three samples almost overlapped with each other for the first 100 cycles. After 100 cycles, however, LMR degraded quickly in the electrolyte without the TPFPB additive. Because TPFPB had the capability to modify the interfacial reaction between LMR and electrolyte, as discussed in last quarter's report, very stable cycling of LMR was demonstrated in the electrolyte with TPFPB (Fig. 1a). After 500 cycles, the capacity retention of LMR is high at 74.2% with a 0.1 M TPFPB as additive. Further increasing TPFPB to 0.2 M in the electrolyte slightly increased the capacity retention to 76.8% after 500 cycles. The Q2 milestone (e.g., stable cycling of 80% capacity retention after 150 cycles from LMR) was reached during this quarter.

A thick electrode (Toda HE5050 LMR-NMC) prepared by ANL also was used to further evaluate TPFPB. At a high active material loading of  $12.5 \text{ mg/cm}^2$ , the first discharge capacity was still  $>200 \text{ mAh g}^{-1}$  in all the cells (Fig. 1b). The addition of TPFPB did not change the voltage profiles during charging, which is consistent with the TPFPB effect reported last quarter. During cycling, the thick LMR electrode decayed rapidly after only 50 cycles (Fig. 1c). Of note, based on the  $12.5 \text{ mg/cm}^2$  loading, C/3 translated to  $1.11 \text{ mA/cm}^2$ , which is detrimental to the Li side during repeated cycling. In other words, the shortened cycling of the thick LMR electrode was partially caused by the anode side. However, with addition of 0.1M TPFPB, the stable cycling was extended to nearly 100 cycles. With addition of 0.2 M TPFPB to the electrolyte, the capacity retention was further improved to 76.7% after 125 cycles, indicating that TPFPB is a promising additive that could improve LMR performance in practical applications.

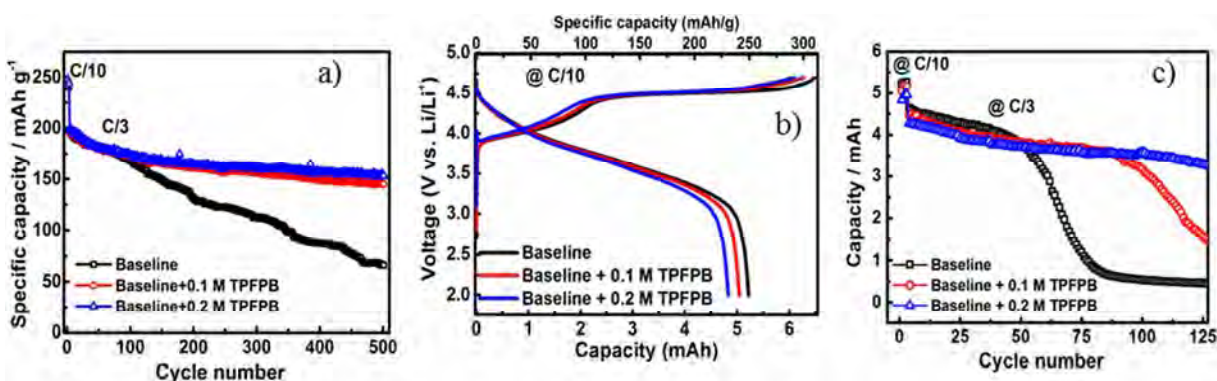


**Figure 1.** a) Long-term cycling performance of PNNL-made  $Li[Li_{0.2}Ni_{0.2}Mn_{0.6}]O_2$  (LMR loading:  $2\text{-}3 \text{ mg/cm}^2$ ) at C/3; b) Charge-discharge curves corresponding to the samples shown in a); c) cycling stability of thick LMR electrodes (loading of active material (Toda HE5050 LMR-NMC):  $12.5 \text{ mg/cm}^2$ ) prepared by ANL. Voltage range: 2.0 to 4.7 V; current: C/10 for three formation cycles followed by C/3 in the subsequent cycling ( $1C = 250 \text{ mA g}^{-1}$ ).

### *In situ* Solvothermal Synthesis of Novel High Capacity Cathodes

**PROJECT OBJECTIVE:** Develop low-cost cathode materials that offer high energy density ( $\geq 660$  Wh/kg) and electrochemical properties (cycle life, power density, safety) consistent with USABC goals.

**PROJECT IMPACT:** Present-day Li-ion batteries are incapable of meeting the 40-mile all-electric-range within the weight and volume constraints established for PHEVs by DOE and the USABC. Higher energy density cathodes are needed for Li-ion batteries to be widely commercialized for PHEV applications. This effort will focus on increasing energy density (while maintaining the other performance characteristics of current cathodes) using synthesis methods that have the potential to lower cost. The primary deliverable for this project is a reversible cathode with an energy density of about 660 Wh/kg or higher.

**OUT-YEAR GOALS:** In FY14, work on Cu-V-O cathodes will be concluded, and efforts will be directed to the synthesis and electrochemical characterization of V-based (fluoro)phosphates. Hydrothermal-based synthesis techniques for preparing ternary and/or quaternary Li-V-PO<sub>4</sub>(-X) type cathodes will be explored, either via direct chemical reaction or through ion exchange. By the end of FY14, structural and electrochemical characterization of two different types of Cu-V-O compounds will be completed, as well as the preparation of multiple Li-V-PO<sub>4</sub>(-X) cathodes. *In situ* x-ray analysis will be used to determine the precursors and reaction conditions for optimal synthesis procedures. Electrochemical testing, along with material characterization (*in situ* and *ex situ*), will be used to identify Li reaction mechanisms and limitations to cycling stability of synthesized cathodes.

**COLLABORATIONS:** Jianming Bai, Lijun Wu, and Yimei Zhu (BNL), Arumugam Manthiram (UT Austin), Brett Lucht (U. Rhode Island), Zaghbir Karim (Hydro-Québec), Jason Graetz (HRL), Peter Khalifah (StonyBrook U.), Kirsuk Kang (Seoul Nat. U., Korea).

#### Milestones

- 1) Complete the structural and electrochemical characterization of  $\epsilon$ -Cu<sub>x</sub>V<sub>2</sub>O<sub>5</sub> cathodes. (Dec. 13) **Complete**
- 2) Develop synthesis procedures to prepare Li-V-PO<sub>4</sub> cathodes. (Mar. 14) **Complete**
- 3) Optimize the synthesis and characterize the structural and electrochemical properties of 2<sup>nd</sup> class of Cu-V-O cathode. (Jun. 14) **Ongoing**
- 4) Develop synthesis procedures to prepare Li-V-PO<sub>4</sub>-X cathodes, and electrochemically characterize at least one Li-V-PO<sub>4</sub>-X compound. (Sep. 14) **Ongoing**

## Progress Report

Following extensive investigation of Cu-V-O cathodes, effort has moved onto the synthesis of polyanion-type cathodes. They are of particular interest given the open, while stable, framework, as well as high voltage induced by phosphate groups and the possibility of accessing multiple redox states of transition metals (eventually enabling high-energy density). The current focus is on synthesis of ternary and quaternary lithium vanadium phosphates,  $\text{Li-V-PO}_4(-X)$ , either *via* hydrothermal ion-exchange (as demonstrated for making  $\text{Li}(\text{Na})_{1+x}\text{VPO}_5\text{F}_x$ ) or direct chemical reactions. This quarter, results are reported on solvothermal-assisted synthesis of monoclinic  $\text{Li}_3\text{V}_2(\text{PO}_4)_3$  (LVP), a promising cathode with a theoretical capacity of  $197 \text{ mAh g}^{-1}$ .

Direct solvothermal synthesis of LVP, *via* heat treatment of precursors in ethylene glycol solution at different temperatures was attempted, but only amorphous intermediates (along with residual  $\text{Li}_3\text{PO}_4$  from the precursors) were observed. An additional calcination step was needed to obtain the monoclinic LVP phase (Fig. 1).

Additional efforts were focused on investigating and tuning the synthesis process. A combination of x-ray absorption spectroscopy (XANES and EXAFS) of the V K-edge, along with electron diffraction and high-resolution TEM imaging were used to identify the local structure and chemical states of V in the intermediate and final reactant products, and *in situ* synchrotron XRD was applied for tracking the detailed phase evolution during calcination. Some of the diffraction patterns from *in situ* XRD measurements are given in Fig. 2a which clearly indicates no formation of the crystalline LVP phase at low temperatures. At elevated temperatures,  $630^\circ\text{C}$  and above, LVP was detected while  $\text{Li}_3\text{PO}_4$  precursor was simultaneously consumed. Eventually the pure, monoclinic LVP phase was obtained at about  $730^\circ\text{C}$ . This investigation shows that LVP may not be synthesized *via* a “one-pot” solvothermal process. However, the solvothermal step was found to play the role of reducing V (to the valence 3+) and reaching a similar local ordering in the intermediate as that of the final product (identified *via* XANES and EXAFS of V K-edge), and thus is essential to eventual formation of the final LVP phase (after calcination).

Based on the investigation of synthesis reactions, a solvothermal-assisted procedure was developed for making the pure phase of LVP with monoclinic structure (cell parameters  $a=8.808\text{\AA}$ ,  $b=8.598\text{\AA}$ ,  $c=12.048\text{\AA}$ ,  $\beta=90.547^\circ$ ; Fig. 2b). The as-synthesized material is composed of single-crystalline nanoparticles coated with a thin layer of carbon. In the initial electrochemical tests, excellent rate capability and cycling stability were observed in the electrodes made from these materials (to be published).

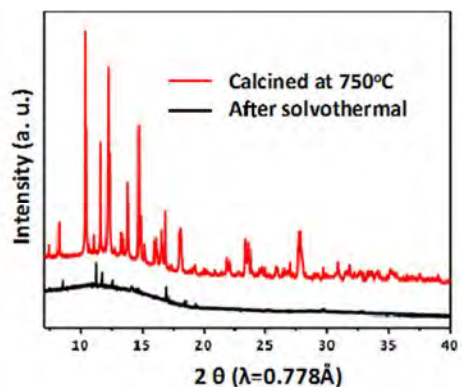


**Figure 1.** Synchrotron XRD patterns recorded from intermediate (black curve) and final product (red; after calcination).

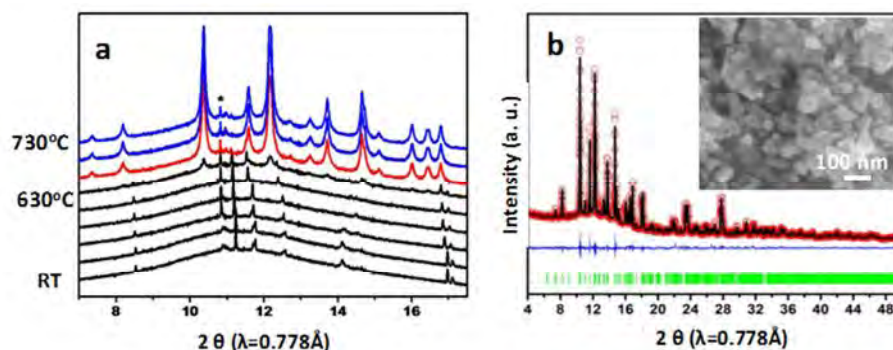


**Figure 2.** (a) *In situ* synchrotron XRD studies of synthesis reactions in preparing  $\text{Li}_3\text{V}_2(\text{PO}_4)_3$ , (b) XRD, structure refinement, and SEM image (inset) of as-synthesized LVP (monoclinic;  $P2_1/n$ ).

### Lithium-bearing Mixed Polyanion (LBMP) Glasses as Cathode Materials

**PROJECT OBJECTIVE:** Develop mixed polyanion glasses as potential cathode materials for lithium ion batteries with superior performance to lithium iron phosphate for use in electric vehicle applications. Modify compositions of mixed polyanion glasses to provide higher electrical conductivities, specific capacities, and specific energies than similar crystalline polyanionic materials. Test mixed polyanion glasses in coin cells for electrochemical performance and cycleability. The final goal is to develop mixed polyanion glass compositions for cathodes with specific energies up to near 1,000 Wh/kg.

**PROJECT IMPACT:** The projected performance of glass cathode materials addresses the Vehicle Technology Multi-Year Plan goals of higher energy densities, excellent cycle life, and low cost. Mixed polyanion glasses offer the potential of exceptional cathode energy density up to 1,000 Wh/kg, excellent cycle life from a rigid polyanionic framework, and low cost conventional glass processing.

**OUT-YEAR GOALS:** The composition of successful mixed polyanion glasses with multivalent transitions will be used as the basis to model, produce, and electrochemically test glasses from multiple polyanion systems (ex. phosphates, borates, silicates), polyanion substitutions (ex. vanadate, molybdate), and transition metal contents. The electrochemical performance of these compositionally varied glasses will be used to develop optimized glass compositions to obtain maximum specific energy within a desirable voltage window. Cathode processing of the most promising mixed polyanion glasses will be refined to obtain desired cycling and rate performance. Complex mixed polyanion glasses will be modeled, and those glasses with excellent predicted properties will be produced and tested. In-depth electrochemical testing will be performed on the most successful mixed polyanion glasses. The predicted and experimentally verified electrochemical performances from computational thermodynamic models for different glass systems will be used to develop a summary perspective on the design of mixed polyanion glasses for use as cathodes.

**COLLABORATIONS:** Chris Wolverton's group at Northwestern University utilized their Open Quantum Materials Database to model the equilibrium voltages of glass-state conversion reactions in hundreds of potential polyanion glass cathode materials.

#### Milestones

- 1) Synthesize, characterize, and perform electrochemically testing on a mixed polyanion glass that is theoretically capable of a multi-valent transition. (Dec. 13) **Complete**
- 2) Demonstrate the effect of submicron particle size on the electrochemical performance of mixed polyanion glass cathodes. (Mar. 14) **Complete**
- 3) Measure the electrical conductivities of a series of mixed polyanion glasses as a function of polyanionic substitution. (Jun. 14) **Ongoing**
- 4) Synthesize, characterize, and perform electrical testing on at least four different glass cathode compositions with theoretical specific energies exceeding lithium iron phosphate. (Sep. 14) **Ongoing - completed 2 out of 4 glass cathode materials.**

## Progress Report

In a new collaboration, Chris Wolverton's group at Northwestern University has utilized their Open Quantum Materials Database (OQMD) to model the discharge voltages of glass-state conversion reactions. The thermodynamic discharge voltages of hypothetical conversion reactions of crystalline polyanionic materials were modeled to estimate the discharge voltages of glass-state conversion reactions. Utilizing their vast OQMD database, they were able to estimate the discharge voltages of over a thousand possible polyanion glass cathode materials. Some examples of Cu, Fe, and manganese phosphate glasses are provided in Table 1. While the experimentally observed discharge voltages of glass-state conversion reactions in Fe, Mn, and copper phosphate/vanadate glasses (1.3 to 1.5 V, 1.9 V, 2.5 V, respectively) are lower than modeled values, galvanostatic intermittent titration technique (GITT) tests are underway to experimentally measure near thermodynamic discharge voltages of mixed polyanion glass cathodes. A preliminary GITT result on copper phosphate/vanadate glass (*ca.* 3.1 V glass-state conversion reaction measured) has shown good agreement with voltages from thermodynamic modeling (2.8 V copper vanadate, 3.2 V copper phosphate).

The effect of particle size on the electrochemical performance of mixed polyanion glass cathodes was studied using coarse and fine milled  $\text{Fe}_4(\frac{1}{2}\text{P}_2\text{O}_7 * \frac{1}{2}\text{V}_2\text{O}_7)_3$  glass. The coarse milled glass powder had a surface area of  $4 \text{ m}^2 \text{ g}^{-1}$  and an approximate average particle size of 550 nm. The fine milled glass powder had a surface area of  $25 \text{ m}^2 \text{ g}^{-1}$  and an approximate average particle size of 95 nm. The cathodes with fine-milled powder showed substantially higher capacities at high discharge rates when discharged down to 1.75V (Fig. 1).

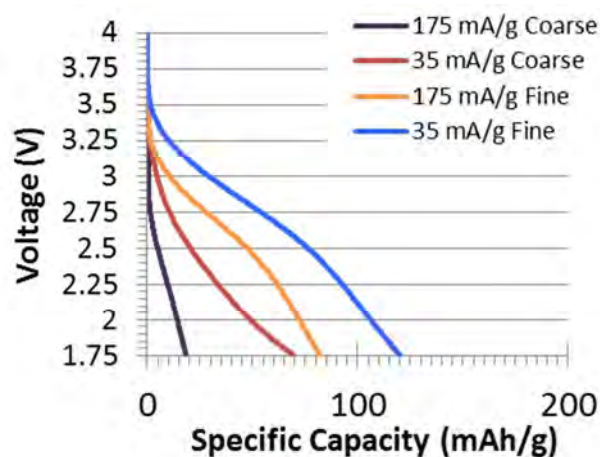


**Figure 1.** Discharge curves of fine and coarse milled  $\text{Fe}_4(\frac{1}{2}\text{P}_2\text{O}_7 * \frac{1}{2}\text{V}_2\text{O}_7)_3$  glass cathodes

	Valence	Predicted Voltage	Specific Capacity (mAh/g)	Energy density (mWh/g)
$\text{Cu}_3(\text{PO}_4)_2$	$\text{Cu}^{2+}$	3.31 V	380	1258
$\text{Cu}_2(\text{P}_2\text{O}_7)$	$\text{Cu}^{2+}$	3.21 V	326	1045
$\text{Cu}_3(\text{VO}_4)_2$	$\text{Cu}^{2+}$	2.97 V	347	1030
$\text{Cu}_2(\text{PO}_4)$	$\text{Cu}^{2+/1+}$	3.3 V	331	1079
$\text{Fe}(\text{PO}_4)$	$\text{Fe}^{3+}$	2.53 V	468	1183
$\text{Fe}(\text{VO}_4)$	$\text{Fe}^{3+}$	2.40 V	419	1007
$\text{Fe}(\text{PO}_3)_2$	$\text{Fe}^{2+}$	2.19 V	235	514
$\text{Fe}_3(\text{PO}_4)_2$	$\text{Fe}^{2+}$	2.16 V	402	867
$\text{Mn}(\text{PO}_4)$	$\text{Mn}^{3+}$	2.36 V	470	1109
$\text{Mn}(\text{PO}_3)_2$	$\text{Mn}^{2+}$	1.79 V	236	423
$\text{Mn}_3(\text{PO}_4)_2$	$\text{Mn}^{2+}$	1.68 V	405	680
$\text{Mn}_2(\text{P}_2\text{O}_7)$	$\text{Mn}^{2+}$	1.48 V	344	509

**Table 1.** Predicted voltages of glass-state conversion reactions from thermodynamic modeling by Chris Wolverton's group at Northwestern University.

## Task 4.7 - John Goodenough (University of Texas at Austin)

### Lithium Batteries of Higher Capacity and Voltage

**PROJECT OBJECTIVE:** To develop a solid  $\text{Li}^+$  electrolyte that (1) can block dendrites from a  $\text{Li}^0$  anode, (2) has a  $\text{Li}^+$  conductivity  $\sigma_{\text{Li}} > 10^{-4} \text{ S cm}^{-1}$ , (3) is stable in different liquid electrolytes at anode and cathode, (4) has a low impedance for  $\text{Li}^+$  transfer across a solid/liquid electrolyte interface, (5) is capable of low-cost fabrication as a thin, mechanically robust film.

**PROJECT IMPACT:** A solid  $\text{Li}^+$ -electrolyte separator would permit use of a  $\text{Li}^0$  anode, thus maximizing energy density for a given cathode, and liquid flow-through and air cathodes of high capacity as well as high-voltage solid cathodes given two liquid electrolytes having different windows.

**OUT-YEAR-GOALS:** Prepare an oxide/polymer composite  $\text{Li}^+$  electrolyte having a  $\sigma_{\text{Li}} > 10^{-4} \text{ S cm}^{-1}$  that can be fabricated at low cost as a mechanically robust membrane and can demonstrate a viable performance of a test cell with a  $\text{Li}^0$  anode and a variety of solid, liquid, and air cathodes. Prepare dense garnet membranes with  $\sigma_{\text{Li}} \approx 5 \times 10^{-4} \text{ S cm}^{-1}$  that have a reduced impedance for  $\text{Li}^+$  transfer across the oxide interface with a liquid electrolyte.

**COLLABORATIONS:** Li/S cell with A. Manthiram (UT Austin) and membrane characterization with K. Zaghib (Hydro-Québec.)

### Milestones

- 1) **Go-No/Go:** Polymer composite membrane project will stop if demonstration of a liquid cathode without crossover of the redox molecule and blocking of Li dendrites with a PEO/ $\text{Al}_2\text{O}_3$  membrane fails. **Criteria:** Suppression of drying of anolyte with an  $\text{Al}_2\text{O}_3$ /PEO membrane. Elimination of redox-molecule crossover to anolyte. Demonstration that Li dendrites are blocked. (Dec. 13) **Complete**
- 2) Determine TEM garnet surface structure in contact with a liquid electrolyte. Design of a surface coat of a garnet membrane to minimize impedance of  $\text{Li}^+$  transfer across garnet surface.(Mar. 14) **Partially completed; due Sep. 14**
- 3) Prepare dense garnet membrane with surface coatings to test impedance of  $\text{Li}^+$  transfer across garnet interface. (Jun. 14) **Ongoing**
- 4) Construct and test a Li/S cell with a solid  $\text{Li}^+$ -electrolyte separator. (Sep. 14) **Ongoing**

## Progress Report

The Li-ion conductors “ $\text{Li}_{6.5}\text{La}_3\text{Zr}_{1.5}\text{Ta}_{0.5}\text{O}_{12}$ ” (LLZT) and “ $\text{Li}_7\text{La}_3\text{Zr}_2\text{O}_{12}$ ” (LLZ) with garnet structure were prepared by solid-state reaction in an alumina crucible; their stability in water was investigated at room temperature.

The prepared LLZT and LLZ samples were crushed into powder for the ion-exchange reaction. The ion-exchange reaction was performed by placing 0.5 g of the garnet oxides in a flask containing 100 ml water of pH=7. The experiments were carried out under constant stirring at room temperature. The duration of the exchange process was 48 hours. The dried samples were characterized by TGA,  $^7\text{Li}$  and  $^{27}\text{Al}$  MAS NMR, neutron diffraction, and TEM.

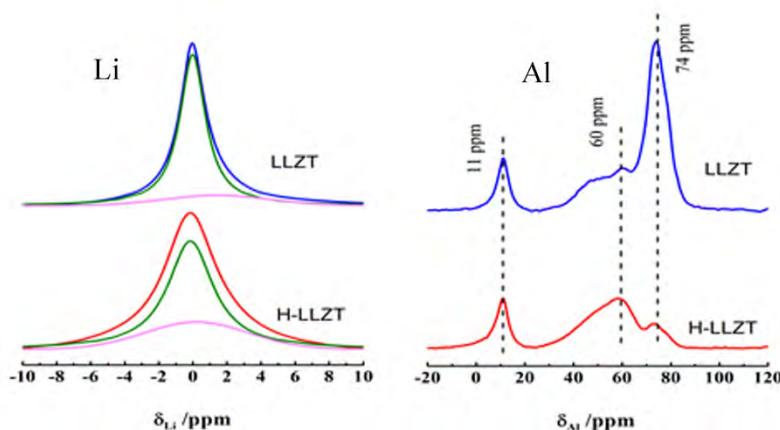


**Figure 1.**  $^7\text{Li}$  and  $^{27}\text{Al}$  MAS NMR spectra of LLZT and H-LLZT at room temperature, the line shape of  $^7\text{Li}$  is fit as a sum of broad and narrow component associated with slow and fast lithium ion domains.

It was found that both the bulk of garnet and grain-boundary phase are unstable in water. The exchanged protons distort the Li-O octahedra and reduce the occupancy of Li on the octahedral sites of the bulk phase. The amorphous phase  $\text{LiAlO}_2$  in the grain boundary is dissolved after ion exchange, which inhibits the Li transport in the grain boundary. The total (bulk+grain-boundary) conductivities of the garnets  $\text{Li}_{6.5-x}\text{H}_x\text{La}_3\text{Zr}_{1.5}\text{Ta}_{0.5}\text{O}_{12}$  at 25 °C is  $3.2 \times 10^{-5} \text{ Scm}^{-1}$  with an activation energy 0.38eV. The lowering of  $\sigma_{\text{Li}}$  and increase in  $E_a$  after reaction with water could be attributed primarily to a greater grain-boundary resistance.

## Task 5.1 - Robert Kosteckı (Lawrence Berkeley National Laboratory)

### Interfacial Processes

**PROJECT OBJECTIVE:** The main objective of this task is to obtain detailed insight into the dynamic behavior of molecules, atoms, and electrons at electrode/electrolyte interfaces of intermetallic anodes (Si) and high voltage Ni/Mn-based materials at a spatial resolution that corresponds to the size of basic chemical or structural building blocks. The aim of these studies is to unveil the structure and reactivity at hidden or buried interfaces and interphases that determine battery performance and failure modes. To accomplish these goals novel far- and near-field optical multifunctional probes must be developed and deployed *in situ*. The proposed work constitutes an integral part of the concerted effort within the BATT Program and it attempts to establish clear connections between diagnostics, theory/modeling, materials synthesis, and cell development efforts.

**PROJECT IMPACT:** This project provides a better understanding of the underlying principles that govern the function and operation of battery materials, interfaces and interphases, which is inextricably linked with successful implementation of high energy density materials such as Si and high voltage cathodes in Li-ion cells for PHEVs and EVs. This task also involves the development and application of novel innovative experimental methodologies to study and understand the basic function and mechanism of operation of materials, composite electrodes, and Li-ion battery systems for PHEV and EV applications.

**OUT-YEAR GOALS:** Design and employ novel and sophisticated *in situ* analytical methods to address the key problems of the BATT baseline chemistries. The proposed experimental strategies combine imaging with spectroscopy aimed at probing electrodes at an atom, molecular, or nanoparticulate level to unveil structure and reactivity at hidden or buried interfaces and determine electrode performance and failure modes in baseline LixSi-anodes and high-voltage LMNO cathodes. The main goal is to gain insight into the mechanism of surface phenomena on thin-film and monocrystal Sn and Si intermetallic anodes and evaluate their impact on the electrode long-term electrochemical behavior. Comprehensive fundamental study of the early stages of SEI layer formation on polycrystalline and single crystal face Sn and Si electrodes will be carried out. *In situ* and *ex situ* far- and near-field scanning probe spectroscopy will be employed to detect and monitor surface phenomena at the intermetallic anodes high-voltage (>4.3 V) model and composite cathodes.

**COLLABORATIONS:** Vince Battaglia (LBNL), Chunmei Ban (NREL)

#### Milestones

- 1) Determine the origin of fluorescent species that are produced at high-energy Li-ion cathodes. (Dec. 13) **Complete**
- 2) Resolve SEI layer chemistry of Si model single crystal anodes - collaboration with the BATT Anode Group. (Mar. 14) **Complete**
- 3) Characterize interfacial phenomena in high-voltage composite cathodes - collaboration with the BATT Cathode Group. (Jun. 14) **Ongoing**
- 4) Go/No-Go: Stop development of *in situ* near-field techniques, if the preliminary experiments fail to deliver adequate surface-bulk selectivity. Criteria: Demonstrate feasibility of *in situ* near-field techniques to study interfacial phenomena at Li-battery electrodes. (Sep. 14) **Ongoing**

## Progress Report

This quarter's focus was the influence of the electrolyte composition on the interfacial phenomena occurring on Si single crystal electrodes in organic carbonate electrolytes. The SEI formation on the facets (100), (110), and (111) was controlled electrochemically during the first potentiostatic charge in a three electrode cell from 2.5 V to 500 mV (before Si-Li alloying) and 10 mV vs. Li/Li<sup>+</sup>. The effect of VC and FEC additives was evaluated by using the following electrolyte compositions: 1 M LiPF<sub>6</sub>, EC/DEC (3:7), 1 M LiPF<sub>6</sub> 2% VC, EC/DEC (3:7), and 1 M LiPF<sub>6</sub> 10% FEC, EC/DEC (3:7). Composition, structure, and morphology of the SEI layer were investigated by a combination of *ex situ* FTIR, SEM-EDX, LIBS, and XPS.

The impact of the electrolyte composition on the chemical composition and morphology of the SEI on Si single crystal electrodes has been clearly demonstrated (Fig. 1). The SEI layer formation in the electrolyte with and without VC or FEC additives starts at a potential of *ca.* 2.2 V. Variations of the I-V polarization profiles and the charge consumed in the electrolyte reduction process indicate different mechanisms of the SEI layer formation and their passivating behavior. Consistently, the SEI morphology varies greatly with the electrolyte composition. Spectroscopic analysis of the SEIs revealed different ratios of LiF, alkyl carbonates, and Si-O-F (Fig. 1 D, E). However, the observed discrepancies between EDX and XPS data may indicate non-uniform decomposition products distributed at the surface and in the bulk of the SEI layers.

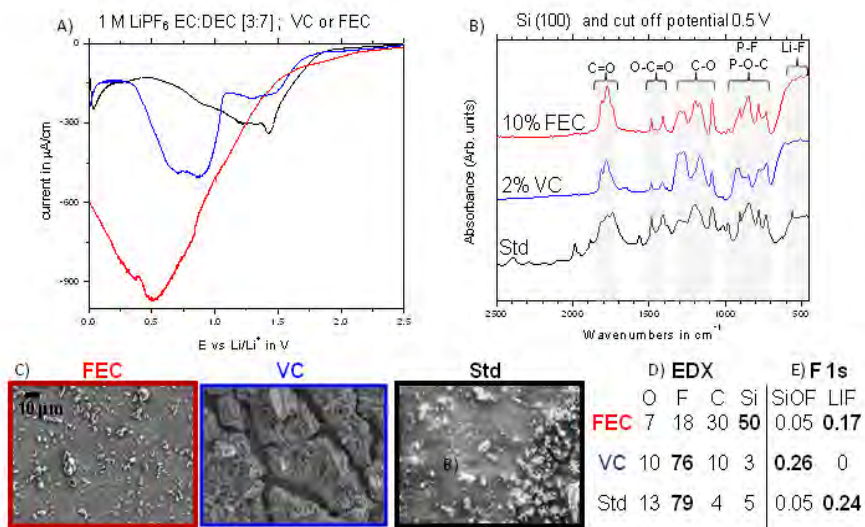


**Figure 1.** A) I-V polarization plots, B) FTIR spectra, C) SEM images, D) EDX and E) XPS analysis of the SEI layer on the Si (100) electrode in 1 M LiPF<sub>6</sub>, EC/DEC (3:7), electrolyte with VC or FEC additives.

The Si surface crystal orientation also affects strongly the electrochemical and spectroscopic response of the silicon in organic carbonate electrolytes. The composition of the SEI layer is quite dissimilar at Si (100), Si (110), and Si (001) particularly at the beginning of the electrolyte reduction process. Most importantly, these differences in the surface chemistry are still visible upon full lithiation of Si when the original surface crystal structure turned totally amorphous. A plausible explanation involves possible differences in Si surface reactivity, surface reconstruction effects, and Li-ion diffusion pathways. This completes efforts toward milestone 3.

Further investigations of the effect of fluorescent compounds formed on high voltage Ni/Mn-based materials on the Li<sup>+</sup> transport in the anode SEI layer (milestone 3) and developments of *in situ* LIBS and near-field IR techniques to study interfacial phenomena at Li-battery electrodes (milestone 4) are currently underway.

### Advanced *In Situ* Diagnostic Techniques for Battery Materials

**PROJECT OBJECTIVE:** The primary objective of this proposed project is to develop new advanced *in situ* material characterization techniques and to apply these techniques to support the development of new cathode and anode materials for the next generation of Li-ion batteries (LIBs) PHEVs. In order to meet the challenges of powering the PHEV, LIBs with high energy and power density, low cost, good abuse tolerance, and long calendar and cycle life must be developed.

**PROJECT IMPACT:** In the Multi Year Program Plan (MYPP) of Vehicle Technology Program (VTP), the goals for battery were described as: “Specifically, lower-cost, abuse-tolerant batteries with higher energy density, higher power, better low-temperature operation, and longer lifetimes are needed for the development of the next-generation of HEVs, PHEVs, and EVs.” If this project is successfully carried out, the knowledge learned from diagnostic studies and collaborations with US industries and international research institutions through this project will help US industries to develop new materials and processes for new generation of Li-ion batteries in their efforts to reach these VTP goals.

**OUT-YEAR GOALS:** For the Si-based anode materials, the capacity fading needs to be resolved, which is caused by the pulverization of the Si particles during cycling. In order to overcome these barriers, fundamental understanding of the physical and chemical changes of the cathode and anode materials in the bulk and at the surface are critical. This project will focus on applying integrated advanced *in situ* diagnostic characterization techniques to investigate these issues, through collaborative efforts with synthesis groups and industrial end users.

**COLLABORATIONS:** The BNL team will work closely with material synthesis groups at ANL (Mike Thackeray and Khalil Amine) for the high energy composite; at UT Austin (Ram Manthiram) for the high voltage spinel; and at PNNL (Jun Liu and Jason Zhang) for the Si-based anode materials. Such interaction between the diagnostic team at BNL and synthesis groups of these other BATT members will catalyze innovative design and synthesis of advanced cathode and anode materials. The team will also collaborate with industrial partners at General Motors (Bin Wu), Duracell (In Tae Bae), and Johnson Controls (Tony Cho and Frederic Bonhomme) to obtain feedback information as battery end users.

#### Milestones

- 1) Complete the studies of the kinetic properties of  $\text{Li}_{1.2}\text{Ni}_{0.15}\text{Co}_{0.1}\text{Mn}_{0.55}\text{O}_2$  [ $0.5\text{Li}(\text{Ni}_{0.375}\text{Co}_{0.25}\text{Mn}_{0.375})\text{O}_2 \bullet 0.5\text{Li}_2\text{MnO}_3$ ] high energy density cathode materials during constant current charge using x-ray absorption spectroscopy. (Dec. 13) **Complete**
- 2) Complete the development of using quick x-ray absorption spectroscopy technique to study the kinetic properties of  $\text{Li}_{1.2}\text{Ni}_{0.15}\text{Co}_{0.1}\text{Mn}_{0.55}\text{O}_2$  [ $0.5\text{Li}(\text{Ni}_{0.375}\text{Co}_{0.25}\text{Mn}_{0.375})\text{O}_2 \bullet 0.5\text{Li}_2\text{MnO}_3$ ] high energy density cathode materials during constant voltage charge. (Mar. 14) **Complete**
- 3) Complete the *in situ* XRD studies of Fe substituted high voltage spinel during charge-discharge cycling. (Jun. 14) **Ongoing**
- 4) Complete the *in situ* XAS studies of Fe substituted high voltage spinel during charge-discharge cycling. (Sep. 14) **Ongoing**

## Progress Report

In the 2nd quarter of FY2014, BNL used *in situ* synchrotron-based XAS to study structural changes of high energy density  $\text{Li}_{1.2}\text{Ni}_{0.15}\text{Co}_{0.1}\text{Mn}_{0.55}\text{O}_2$  cathode materials with layered structures. During a constant voltage hold, structural changes were monitored and related to rate capability towards the completion of milestone 2.

To elucidate the changes of the electronic transitions and local structure of the Li-rich layered  $\text{Li}_{1.2}\text{Ni}_{0.15}\text{Co}_{0.1}\text{Mn}_{0.55}\text{O}_2$  material, *in situ* XAS spectra at Mn, Co, and Ni K-edges were collected during the first full cycle and second charge under constant voltage at 5V. The comparative magnitudes of the Fourier transformed Ni, Co, Mn K-edge EXAFS spectra during a constant voltage hold at 5 V for a total of 900 seconds are plotted in a two-dimensional view in Fig. 1. (A color scale is used for displaying spectrum intensity.) For Ni, the first coordination peaks (Ni-O) show dramatic changes in both position and intensity within the first 100 seconds, which represent charge compensation occurring at the Ni sites. The peak intensities decreased first (from 0 to *ca.* 60 sec) due to the Jahn-Teller distortion caused by the oxidation of  $\text{Ni}^{2+}$  to  $\text{Ni}^{3+}$ , then increased with the further oxidation of  $\text{Ni}^{3+}$  to  $\text{Ni}^{4+}$ . The EXAFS features remained unchanged after 160 seconds, indicating that the oxidation of  $\text{Ni}^{2+}$  to  $\text{Ni}^{4+}$  was complete within the first three minutes. Compared to Ni, the evolutions of the local structure around Co and Mn sites caused by  $\text{Li}^+$  extraction are more straightforward as displayed in Fig. 1 – the first coordination shell peak (Co-O and Mn-O) intensities show a continuous decrease. No obvious Co-O peak intensity changes can be observed after 200 seconds at 5V charge while Mn-O peak intensities continued to decrease during the entire observation time scale (900 seconds), indicating a much slower delithiation kinetics around the Mn sites.

These results show that Mn sites have much poorer reaction kinetics both before and after initial "activation" of  $\text{Li}_2\text{MnO}_3$ , compared with Ni and Co, providing valuable guidance in designing various Li-rich layered materials with a desired balance of energy densities and rate capabilities for different applications.

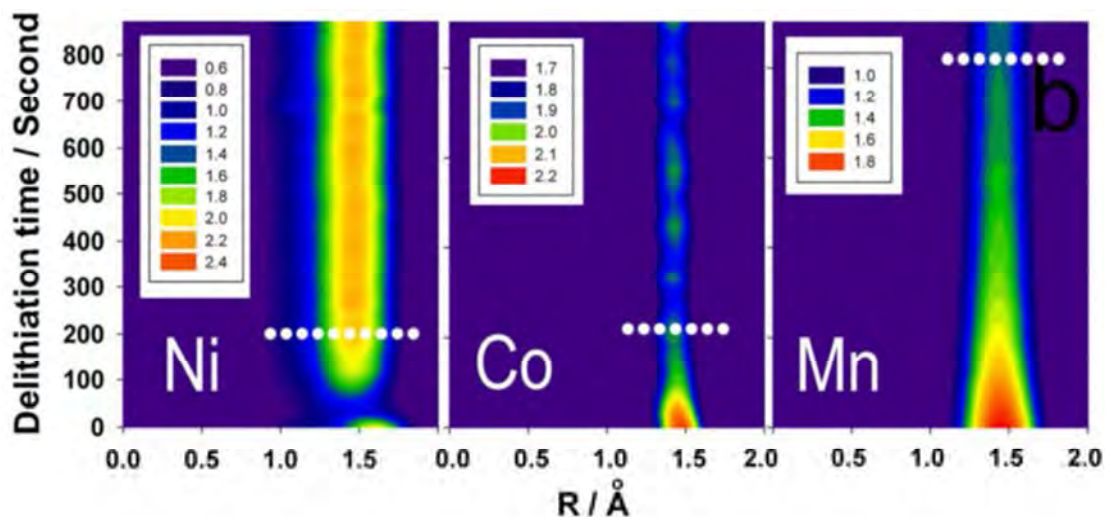


**Figure 1.** EXAFS spectra of  $\text{Li}_{1.2}\text{Ni}_{0.15}\text{Co}_{0.1}\text{Mn}_{0.55}\text{O}_2$  during constant voltage charging at 5 V. Ni, Co, and Mn reacted simultaneously using a time-resolved XAS technique. Projection view of corresponding Ni-O, Co-O, Mn-O peak magnitudes of the Fourier transformed K-edge spectra as functions of charging time.

### NMR and Pulse Field Gradient Studies of SEI and Electrode Structure

**PROJECT OBJECTIVE:** The formation of a stable SEI is critical to the long-term performance of a battery, since the continued growth of the SEI on cycling/aging results in capacity fade (due to Li consumption) and reduced rate performance due to increased interfacial resistance. Although arguably a (largely) solved problem with graphitic anodes/lower voltage cathodes, this is not the case for newer, much higher capacity anodes such as Si, which suffer from large volume expansions on lithiation, and for cathodes operating above 4.3 V. Thus it is essential to identify how to design a stable SEI. The objectives are to identify major SEI components, and their spatial proximity, and how they change with cycling. SEI formation on Si vs. graphite and high voltage cathodes will be contrasted. Li<sup>+</sup> diffusivity in particles and composite electrodes will be correlated with rate. The SEI study will be complemented by investigations of local structural changes of high voltage/high capacity electrodes on cycling.

**PROJECT IMPACT:** The first impact of this project will be an improved, molecular based understanding of the surface passivation (SEI) layers that form on electrode materials, which are critical to the operation of the battery. Second, we will provide direct evidence for how additives to the electrolyte modify the SEI. Third, we will provide insight to guide and optimize the design of more stable SEIs on electrodes beyond LiCoO<sub>2</sub>/graphite.

**OUT-YEAR GOALS:** The goals of this project are to identify the major components of the SEI as a function of state of charge and cycle number different forms of silicon. We will determine how the surface oxide coating affects the SEI structure and establish how the SEI on Si differs from that on graphite and high voltage cathodes. We will determine how the additives that have been shown to improve SEI stability affect the SEI structure and explore the effect of different additives that react directly with exposed fresh silicon surfaces on SEI structure. Via this program, we will develop new NMR based methods for identifying different components in the SEI and their spatial proximities within the SEI, which will be broadly applicable to the study SEI formation on a much wider range of electrodes. These studies will be complemented by studies of electrode bulk and surface structure to develop a fuller model with which to describe how these electrodes function.

**COLLABORATIONS:** Brett Lucht (U. Rhode Island), Kristin Persson (LBNL), Jordi Cabana (UICC), Stan Whittingham (SUNY Binghamton), Shirley Meng (UCSD), and Stephan Hoffman (Cambridge.)

#### Milestones

- 1) Identify major components (LiF, phosphates, carbonates and organics) in Si SEI by NMR methods. (Dec. 13). **Complete**
- 2) Correlate presence of SEI components with cycle number and depth of discharge of Si. Complete preliminary TOF-SIMS measurements to establish viability of approach. (Mar. 14) **Ongoing. Difficulties encountered with sample reproducibility and Si cracking (TOF-SIMS)**
- 3) Identify SEI components in the presence of FEC and VC in Si and determine how they differ from those present in the absence of additives. (Jun. 14) **Ongoing**
- 4) Go/No-Go: Stop Li<sup>+</sup> PFG diffusivity measurements of electrodes. Criteria: If experiments do not yield correlation with electrochemical performance. (Sep. 14) **Ongoing - PFG studies initiated.**

## Progress Report

A systematic study of Si nanoparticle coatings has been initiated. Experiments were performed with (3-aminopropyl)triethoxysilane (APTES), 2-cyanoethyltriethoxysilane, triethoxy(octyl)silane (TEOOS), (3-Glycidyloxypropyl)trimethoxysilane, and poly(methylvinylether-alt-maleic anhydride (Fig. 1) to examine how various surfaces affect SEI formation and the coulombic efficiencies observed on cycling 15 to 20 nm Si particles (Fig. 2). Small Si particles were chosen for initial experiments so as to maximize potential surface reactions. The low resolution TEM results indicate that the coating procedure resulted in increased particle agglomeration, with the coating surrounding the particle agglomerates. Control experiments will thus be required to separate effects from any morphological changes induced by the surface treatments from those due to the coatings themselves.

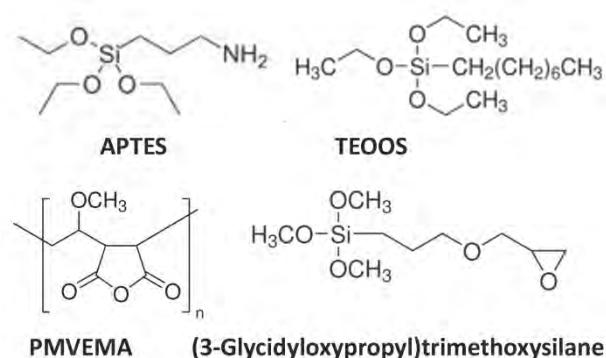


**Figure 1.** Molecules used for Si nanoparticle coating

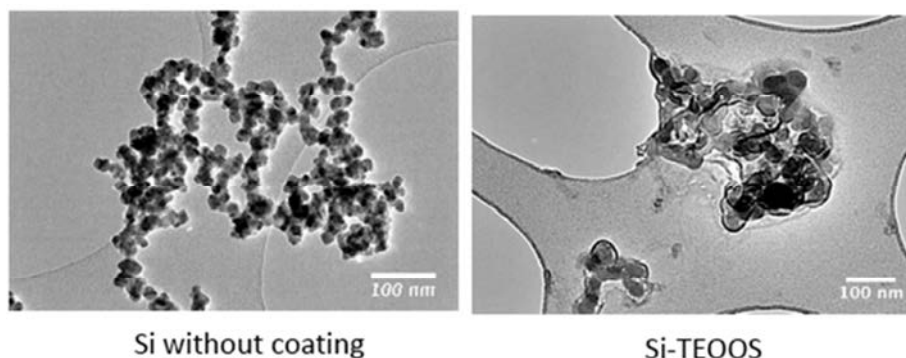


**Figure 2.** TEM results of the Si particles before (left) and after (right) Si-TEOOS coating.

Si electrodes, composed of 1/3 active Si nanoparticles, 1/3 carboxymethyl cellulose (CMC), and 1/3 super P carbon, were cycled vs. Li metal with 1M LiPF<sub>6</sub> in EC/DMC as the electrolyte. Noticeable improvements in coulombic efficiency were observed for all the coatings with APTES, which showed the best performance (Fig. 3). Improved rate performance was also observed, possibly due to the formation of a thinner SEI. NMR experiments were used to characterize (i) the nature of the coating both before and after electrochemical cycling and (ii) the nature of the SEI with and without the coating. Preliminary NMR experiments confirm that the SEI coating is less thick (as quantified *via* both <sup>1</sup>H and <sup>13</sup>C NMR). Experiments are ongoing to investigate the nature of the coating/grafting of molecules and how this affects SEI formation.

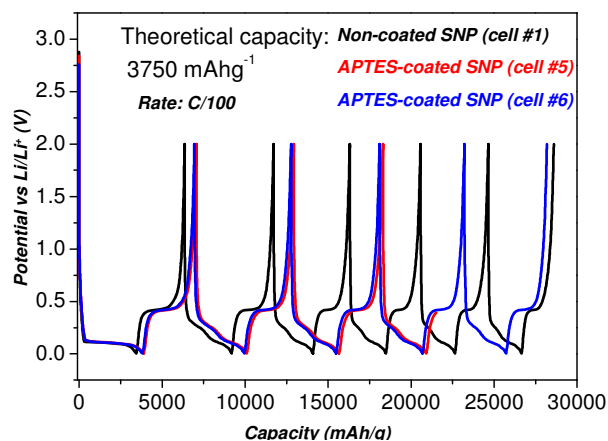


**Figure 3.** Cycling experiments performed with and without the APTES coating.

### Simulations and X-ray Spectroscopy of Li-S Chemistry

**PROJECT OBJECTIVE:** Lithium-sulfur cells are attractive targets for energy storage applications as their theoretical specific energy of 2600 Wh/kg is much greater than the theoretical specific energy of current lithium-ion batteries. Unfortunately, the cycle-life of Li-S cells is limited due to migration of species generated at the sulfur cathode. These species, collectively known as polysulfides, can transform spontaneously, depending on the environment, and it has thus proven difficult to determine the nature of redox reactions that occur at the sulfur electrode. The objective of this project is to use X-ray spectroscopy to track species formation and consumption during charge-discharge reactions in a Li-S cell. Molecular simulations will be used to obtain X-ray spectroscopy signatures of different polysulfide species, and to determine reaction pathways and diffusion in the sulfur cathode. The long-term objective of this project is to use the mechanistic information to build high specific energy Li-S cells.

**PROJECT IMPACT:** Enabling rechargeable Li-S cells has the potential to change the landscape of rechargeable batteries for large-scale applications beyond personal electronics due to: (1) high specific energy, (2) simplicity and low cost of cathode (the most expensive component of current Li-ion batteries), and (3) earth abundance of sulfur. The proposed diagnostic approach also has significant potential impact as it represents a new path for determining the species that form during charge-discharge reactions in a battery electrode.

**OUT-YEAR GOALS:** Year 1 Goals: Simulations of sulfur and polysulfides (PSL) in oligomeric polyethylene oxide (PEO) solvent. Prediction of X-ray spectroscopy signatures of PSL/PEO mixtures. Measurement of X-ray spectroscopy signatures PSL/PEO mixtures. Year 2 Goals: Use comparisons between theory and experiment to refine simulation parameters. Determine speciation in PSL/PEO mixtures without resorting to adhoc assumptions. Year 3 Goals: Build an all-solid lithium-sulfur cell that enables measurement of X-ray spectra *in situ*. Conduct simulations of reduction of sulfur cathode. Year 4 Goals: Use comparisons between theory and experiment to determine the mechanism of sulfur reduction and Li<sub>2</sub>S oxidation in all-solid Li-S cell. Use this information to build Li-S cells with improved life-time.

**COLLABORATIONS:** Tsu-Chien Weng, Dimosthenis Sokaras, and Dennis Nordlund (Stanford Synchrotron Radiation Lightsource, SLAC National Accelerator Laboratory)

#### Milestones

- 1) Complete simulations of PSL/PEO mixtures including calculation of solvation free energy and X-ray spectra; compare spectra with experimental measurements. (Dec. 13) **Complete**
- 2) Go/No-Go: Viability of the use of X-ray spectroscopy to study speciation of lithium sulfides in Li-S cells. Criteria: Determine speciation using X-ray spectra. (Mar. 14) **Complete**
- 3) Build *in situ* cell for generating polysulfides by electrochemically driven redox reactions and measuring X-ray spectra. (Jun. 14) **Ongoing**
- 4) Synthesize an electron- and ion-conducting polymer binder for the sulfur cathode. (Sep. 14) **Original target binder did not work. Working on synthesizing new binder.**

## Progress Report

**Milestone 1.** Previously, it was determined the first ever theoretical calculation of the Sulfur K-edge XAS of isolated  $\text{Li}_2\text{S}_x$  species solvated in tetraglyme.

**Milestone 2.** It was previously determined and shown using principal component analysis that XAS is capable of speciating Li polysulfides molecules. Calculations indicate that the ratio of the main-/pre-edge peak area, and not the peak intensities, can be used to differentiate dissolved Li polysulfides, as shown in Fig. 1.

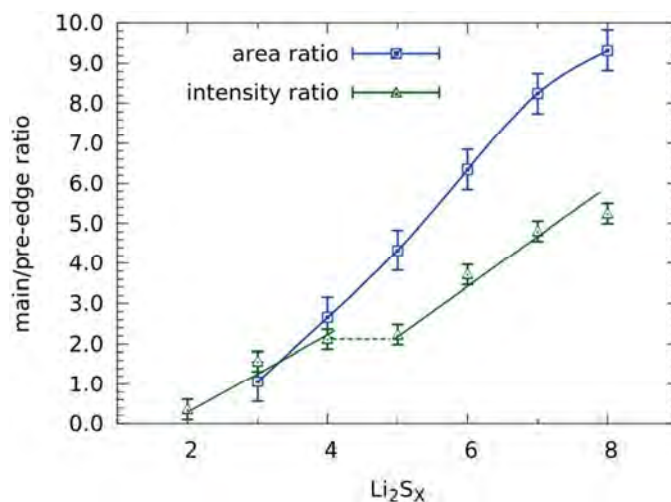


**Figure 1.** Plot of the main/pre-edge ratios *versus* x, the length of the  $\text{Li}_2\text{S}_x$  polysulfide chain.

**Milestone 3.** *In situ* Li-S cells for XAS measurement are still under development and testing. Recent efforts have also focused on development of heating stages that will be used to heat cells at XAS beamlines.

## Task 5.5 - Guoying Chen (Lawrence Berkeley National Laboratory)

### Design and Synthesis of Advanced High-Energy Cathode Materials

**PROJECT OBJECTIVE:** The successful development of next-generation electrode materials requires particle-level knowledge of the relationships between materials' specific physical properties and reaction mechanisms to their performance and stability. This single-crystal-based project was developed specifically for this purpose and it has the following objectives: 1) obtain new insights into electrode materials by utilizing state-of-the-art analytical techniques that are mostly inapplicable on conventional, aggregated secondary particles, 2) gain fundamental understanding on structural, chemical and morphological instabilities during Li extraction/insertion and prolonged cycling, 3) establish and control the interfacial chemistry between the cathode and electrolyte at high operating voltages, 4) determine transport limitations at both particle and electrode levels, and 5) develop next-generation electrode materials based on rational design as opposed to more conventional empirical approaches.

**PROJECT IMPACT:** This project will reveal performance-limiting physical properties, phase-transition mechanisms, parasitic reactions, and transport processes based on the advanced diagnostic studies on well-formed single crystals. The findings will establish rational, non-empirical design methods that will improve the commercial viability of next-generation  $\text{Li}_{1+x}\text{M}_{1-x}\text{O}_2$  (M=Mn, Ni and Co) and spinel  $\text{LiNi}_x\text{Mn}_{2-x}\text{O}_4$  cathode materials.

#### **OUT-YEAR GOALS:**

- Synthesize single-crystal samples of Li transition-metal oxide cathode materials.
- Characterize structural and morphological changes and establish their correlation to rate performance and cycling stability.
- Determine crystal-plane specific reactivity between cathode particles and the electrolyte.
- Measure Li-concentration dependent transport and kinetic properties.
- Define performance-limiting fundamental properties and mechanisms and outline mitigating approaches. Design, synthesize, and evaluate the improved electrode materials.

**COLLABORATIONS:** Robert Kostecki, Marca Doeff, Kristin Persson, Vassilia Zorba, Tolek Tyliczszak and Zhi Liu (LBNL), Clare Grey (Cambridge), Brett Lucht (URI), and Yet-Ming Chiang (MIT).

#### Milestones

- 1) Synthesize at least five new cathode crystal samples with at least two new morphologies. (Dec. 13) **Complete**
- 2) Characterize the interface between the high-voltage cathode and the electrolyte. Identify the role of particle surface planes in interfacial reactivity (Mar. 14) **Complete**
- 3) Complete the studies on structural evolution during initial Li extraction/insertion and extended cycling. Illustrate the impact of structural changes and phase transformation on rate capability and stability. (Jun. 14) **Ongoing**
- 4) Go/No-Go: Continue low-temperature based solvothermal synthesis. Criteria: If the crystal samples show similar quality and performance to those made at high temperatures. (Sep. 14) **Ongoing**

## Progress Report

**Effect of surface facets on cathode self-discharge:** One of the critical issues facing  $\text{LiMn}_{1.5}\text{Ni}_{0.5}\text{O}_4$  (LMNO) as a high-voltage cathode material is the severe self-discharge upon storage at a charged state. Previous mechanistic studies have largely attributed the phenomena to the oxidative decomposition of the electrolyte at high potentials, with the insertion capacity mostly reversible upon subsequent cycling. This, however, reduces calendar life and has a major impact on cycling performance and stability considering the limited amount of electrolyte available in commercial Li-ion cells. Several factors, including state of charge, storage temperature, and the choice of electrolyte, have been shown to influence the rate of cathode relithiation. In this quarter, the effect of surface facets on cathode relithiation during storage was investigated.

Micron-sized LMNO single crystals with predominant (112) and (111) surface facets (plates and octahedrons, respectively) were fully delithiated by chemical oxidation with a  $\text{NO}_2\text{BF}_4$  solution in acetonitrile and then aged at room temperature in a 1.0 M  $\text{LiPF}_6$  in EC:DEC (1:1) (% v/v) electrolyte for 5 weeks. In both cases, a light brown color gradually developed in the electrolyte but it was significantly darker in the solution containing the plate sample. Figure 1 shows the XRD patterns as well as the expanded view of (311), (400) and (440) peaks collected on the recovered crystals during various stages of storage. Pristine LMNO was composed of a single cubic phase with a lattice parameter of 8.168 Å (Phase I) and the fresh delithiated LMNO consists of a single cubic phase,  $\text{Mn}_{1.5}\text{Ni}_{0.5}\text{O}_4$  (MNO), with a lattice parameter of 8.008 Å (Phase III). Aging of MNO in the electrolyte leads to relithiation which is clearly shown by the appearance of a cubic phase with an intermediate Li content, previously determined to be  $\text{Li}_{0.5}\text{Mn}_{1.5}\text{Ni}_{0.5}\text{O}_4$ , with a lattice parameter of 8.089 Å (Phase II). For the plates, Phase II appeared during the first week of aging and then Phase I appeared after 3 weeks. The amount of both phases increased at the expense of Phase III, and after 5 weeks of storage, the plates were mostly composed of Phase I and II (Fig. 1a). Relithiation was also observed in the octahedrons, but the ratio between Phase III/II remained high and Phase I never appeared even after 5 weeks of storage (Fig. 1b). This suggests that the extent of Li reinsertion is much smaller in the latter case. Full-pattern Rietveld refinements of the XRD patterns were performed to estimate the Li content in the aged samples, which produced a Li content range of 0.2 to 0.3 for the plates and 0.1 to 0.2 for the octahedrons after 5 weeks (Fig. 2). The study suggests that relithiation may be used as a kinetic index for side reactions between cathode and electrolyte, and that particle morphology design is an important route to minimizing self-discharge.

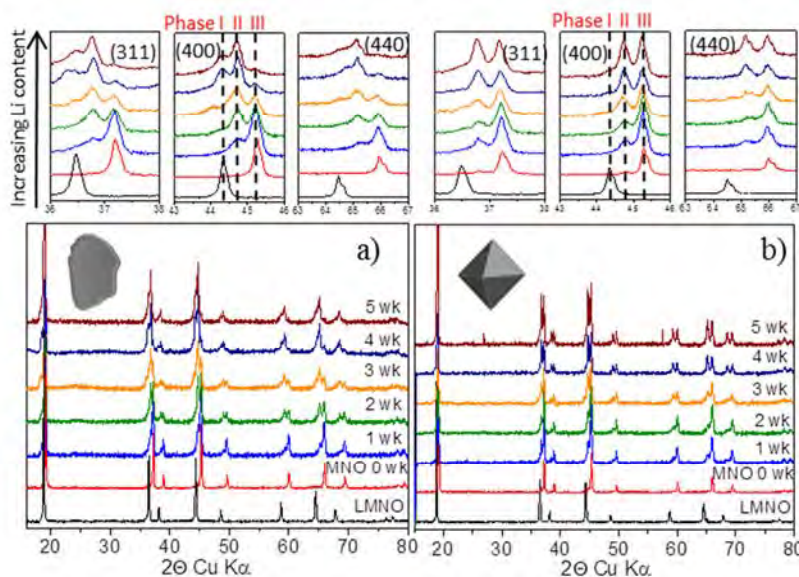


**Figure 1.** Evolution of the XRD patterns and the expanded view of (311), (400) and (440) peaks during room-temperature storage of fully delithiated  $\text{LiMn}_{1.5}\text{Ni}_{0.5}\text{O}_4$  in the electrolyte: a) plates and b) octahedrons.

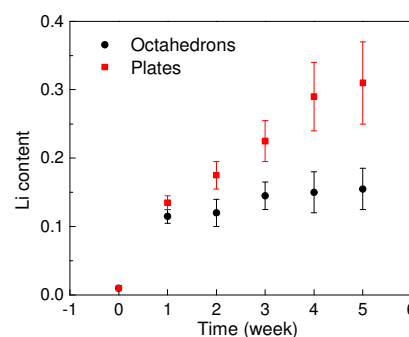


**Figure 2.** Li content in the crystal samples as a function of storage time.

### Optimization of Ion Transport in High-Energy Composite Cathodes

**PROJECT OBJECTIVE:** This project aims to probe and control the atomic-level kinetic processes that govern the performance limitations (rate capability and voltage stability) in a class of high energy composite electrodes. A systematic study with powerful suite of analytical tools (including atomic resolution scanning transmission electron microscopy (a-STEM) & Electron energy loss spectroscopy (EELS), X-ray photoelectron spectroscopy (XPS) and first principles (FP) computation) will be used to pin down the mechanism and determine the optimum bulk compositions and surface characteristics for high rate and long life, and to help the synthesis efforts to produce the materials at large scale with consistently good performance.

**PROJECT IMPACT:** If successful, this research will provide a major breakthrough in commercial applications of the class of high energy density cathode material for lithium ion batteries. Additionally, it will provide in-depth understanding of the role of surface modifications and bulk substitution in the high-voltage composite materials. The diagnostic tools developed here can also be leveraged to study a wide variety of cathode and anode materials for rechargeable batteries.

**OUT-YEAR GOALS:** Careful engineering of the surface (coating) and bulk compositions (substitution) of the high energy composite cathode materials can lead to significant improvement on ion transport and voltage stability. The goals are to establish the STEM/EELS and XPS as quantities diagnostic tools for surface and interface characterization and to enable quick identification of causes of surface instability (or stability) in various types of cathode materials. It is also planned to identify ways to extend the techniques for anode materials, such as Si anode.

#### **COLLABORATIONS:**

- Robert Kostecki and Gao Liu (LBNL) – on cathode electrolyte interface diagnosis and anode SEI diagnosis
- Se-Hee Lee (U. of Colorado, Boulder) – on surface coating of cathode materials.
- Michael Sailor (UCSD) – porous silicon and carbonization of Si-based anodes.

#### Milestones

- 1) Establish the initial suite of surface and interface characterization tools, including STEM/EELS, XPS and FP computation (Dec.13) **Complete**
- 2) Identify the surface coated materials ( $\text{AlF}_3$  and  $\text{Li}_3\text{PO}_4$ ) electrochemical performance matrices, including first cycle irreversible capacity, discharge energy density, voltage stability upon cycling and rate capabilities. (Mar. 14) **Complete/Initiated morphological control**
- 3) Go/No-Go: Stop and change the coating materials if the improvements for rate capability and voltage stability are not significant. Criteria: Characterize coated samples - coating thickness, compositions and morphology before, during and after cycling. (Jun. 14) **Ongoing**
- 4) Identify ways to extend the STEM/EELS and XPS techniques for anode materials, such as Si anode. (Sep. 14) **Ongoing**

## Progress Report

**Morphology control of  $L_{1.2}Ni_{0.2}Mn_{0.6}O_2$  cathode materials.** As shown in the previous report, a modified co-precipitation method was employed to synthesize  $L_{1.2}Ni_{0.2}Mn_{0.6}O_2$  (LNMO) particles with spherical morphology. This material preparation technique was found to improve capacity retention and reduce voltage fade. Figure 1a presents the 2<sup>nd</sup>, 20<sup>th</sup>, 40<sup>th</sup>, 60<sup>th</sup> and 80<sup>th</sup> dQ/dV profiles of the spherical LNMO material when cycled under a current density of  $25 \text{ mA g}^{-1}$  ( $C/10$ ) between 2.0 and 4.8 V. A discharge capacity *versus* cycle number demonstrates a steady rise in capacity for the first 30 cycles with spherical LNMO delivering an initial discharge capacity of  $220 \text{ mAh g}^{-1}$  and an 80<sup>th</sup> cycle discharge capacity of  $230 \text{ mAh g}^{-1}$ . The dQ/dV comparison shows that spherical LNMO shows remarkably stable electrochemical performance compared to the non-modified sample, suggesting that the co-precipitation technique holds promise for resolving the Li excess material's problems of capacity and voltage fading.

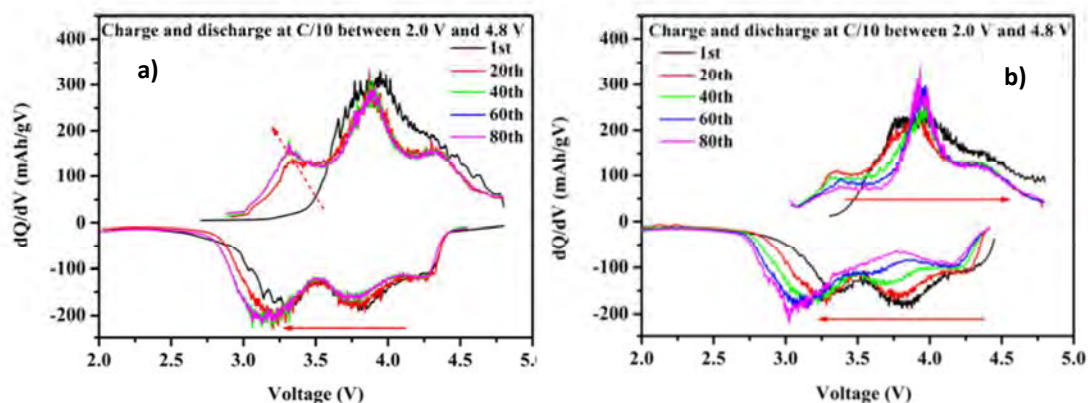


**Figure 1.** a) dQ/dV profiles for spherical LNMO cycled at a current density of  $25 \text{ mA g}^{-1}$  between 2.0 and 4.8 V, b) dQ/dV curves of the non-modified LNMO. The first cycle (not depicted) was conducted at a rate of  $C/20$ .

**Characterizing the Chemical Stability of Si Anodes.** The large irreversibility associated with the formative cycle of Si anodes is primarily due to mechanical pulverization and chemical degradation (*e.g.*, unstable SEI formation). It is not yet clear how to create a stable SEI between Si and the organic liquid electrolyte in order to improve electrode coulombic efficiency and reversibility. For this reason, the Meng group plans to conduct a fundamental compositional study of the SEI formed on amorphous-Si (*a*-Si) thin film electrodes fabricated by pulsed laser deposition and sputtering. The electrodes will be 50 to 80 nm thick in order to avoid cracking and eliminate any irreversibility due to mechanical pulverization.

In order to reveal the reactivity of native Si with the 1M  $\text{LiPF}_6$  in 1:1 EC:DEC electrolyte, the surfaces of an etched (110) Si wafer before and after dipping in electrolyte was examined (Fig. 2). Partial Si-H surface functionalization was achieved after etching. Nonetheless, after exposed in electrolyte, the highly reactive Si-H bonds disappear and a variety of new functionalities associated with electrolyte decomposition products are observed (blue.) Removal of the native Si oxide layer has been shown to improve the initial coulombic efficiency, however, the high reactivity etched Si promotes poor coulombic efficiency in subsequent cycles.

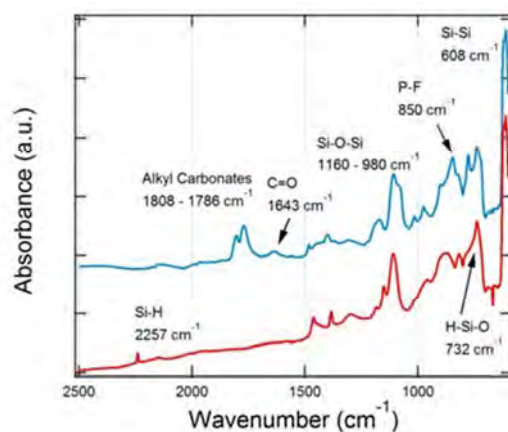


**Figure 2.** FTIR of etched Si wafer (red) compared to etched Si wafer that was exposed in EC:DEC electrolyte (blue).

## Analysis of Film Formation Chemistry on Silicon Anodes by Advanced *In Situ* and *Operando* Vibrational Spectroscopy

**PROJECT OBJECTIVE:** Understand the composition, structure, and formation/degradation mechanisms of the solid electrolyte interface (SEI) on the surfaces of Si anodes during charge/discharge cycles by applying advanced *in-situ* vibrational spectroscopies. Determine how the properties of the SEI contribute to failure of Si anodes in Li-ion batteries in vehicular applications. Use this understanding to develop electrolyte additives and/or surface modification methods to improve Si anode capacity loss and cycling behavior.

**PROJECT IMPACT:** A high capacity alternative to graphitic carbon anodes is Si, which stores 3.75 Li per Si versus 1 Li per 6 C yielding a theoretical capacity of 4008 mAh/g versus 372 mAh/g for C. But Si anodes suffer from large first cycle irreversible capacity loss and continued parasitic capacity loss upon cycling leading to battery failure. Electrolyte additives and/or surface modification developed from new understanding of failure modes will be applied to reduce irreversible capacity loss, improve long term stability and cyclability of Si anodes for vehicular applications.

**OUT-YEAR GOALS:** N/A

### **COLLABORATIONS:**

- Chunmei Ban (NREL) Functionalization of Si by Atomic Layer Deposition (ALD): Effect of functionalization on electrolyte reduction
- Gao Liu (LBNL) Surface electrochemistry of electrolyte additives on model Si electrodes

### Milestones

- 1) Develop method to attach Si nanostructures to the electrode substrate used in our spectroelectrochemical cell. (Dec. 13) **Delayed to Sep. 14**
- 2) Determine the oxidation and reduction potentials and products of at least one electrolyte additive provided by Gao Liu's group. (Mar.14) **Complete**
- 3) Determine role of the Si nanostructure on the SEI formation structure and properties. (Jun. 14) **Ongoing**
- 4) Go/No-Go: Feasibility of surface functionalization to improve SEI structure and properties. Criteria: Functionalize a model Si anode surface and determine how SEI formation is changed. (Sep-14) **Ongoing**

## Progress Report

In Q2, the additive effect (VC, FEC comparison) of Si nanoparticles on SEI film was investigated. The Si nanoparticles samples were prepared by Hui Zhao, a postdoc scholar in Gao Liu's group, LBNL. The samples are Si nanoparticles with CMC-based binder (loading is 50%, with 20% carboxymethyl cellulose and 5% polyvinyl alcohol as binder, 25% additive carbon), PVDF binder (loading is 90%, 10% PVDF as binder), and CMC/PVA paste on Cu foil (binder only). All the tests were run in the EC/DEC/LiPF<sub>6</sub> electrolyte (v/v=1:1).

As stated in the previous quarter, the major component formed on the coin cell Si anode under various additive conditions is lithium carbonate (Li<sub>2</sub>CO<sub>3</sub>). Although there is much literature that reports Li<sub>2</sub>CO<sub>3</sub> as an SEI component on binder-free Si anodes<sup>1,2</sup>, the exact mechanism of Li<sub>2</sub>CO<sub>3</sub> formation and how it is affected by additive are still not clear. Some literature attributed it to air exposure during handling, but no confirmed evidence was presented. Thus, it is important to determine the source of Li<sub>2</sub>CO<sub>3</sub> in the *ex situ* FTIR test, which will help us further understand the additive effect.

To isolate Si and binder degradation effects on the surface species formation, a series of experiments were performed using electrodes of Si anodes with CMC, PVDF as binder, as well as pure binder surface species for 3 cycles in the range of 1 to 0.05 V vs. Li/Li<sup>+</sup> at C/10 rate. All three spectra show very similar features. A large amount of Li<sub>2</sub>CO<sub>3</sub> (1400-1500 cm<sup>-1</sup>) and mixture of Li ethyl bicarbonate and oxalate (ca. 1650 cm<sup>-1</sup>) were observed on all three spectra, including the sample with CMC/PVA binder only. This implies that Si surface is not the only source of Li<sub>2</sub>CO<sub>3</sub>. The other control test is performed on Sn foil, cycling between 0 and 2 V, under the same condition in two different cells (coin cell and a homemade detachable cell made of Teflon.) Figure 1(b) shows that the surface signal on a Sn electrode in a coin cell test is primarily residual electrolyte and Li<sub>2</sub>CO<sub>3</sub>; however, the Li<sub>2</sub>CO<sub>3</sub> signal is absent on the Sn electrode surface in the detachable cell test. This could exclude the possibility of air exposure during IR test, since these parallel tests have been performed under the same IR and electrochemical test condition. Therefore, the possible reason for this abnormally large amount of Li<sub>2</sub>CO<sub>3</sub> could be mainly attributed to the coin cell operation process (the short circuit of the coin cell during opening will deposit Li on the anode, subsequently reacting with the remaining electrolyte). Further investigation on the correlation of the coin cell operation process and the formation of Li<sub>2</sub>CO<sub>3</sub> is ongoing, and more tests with homemade detachable cells to avoid possible contamination for IR testing will be done.

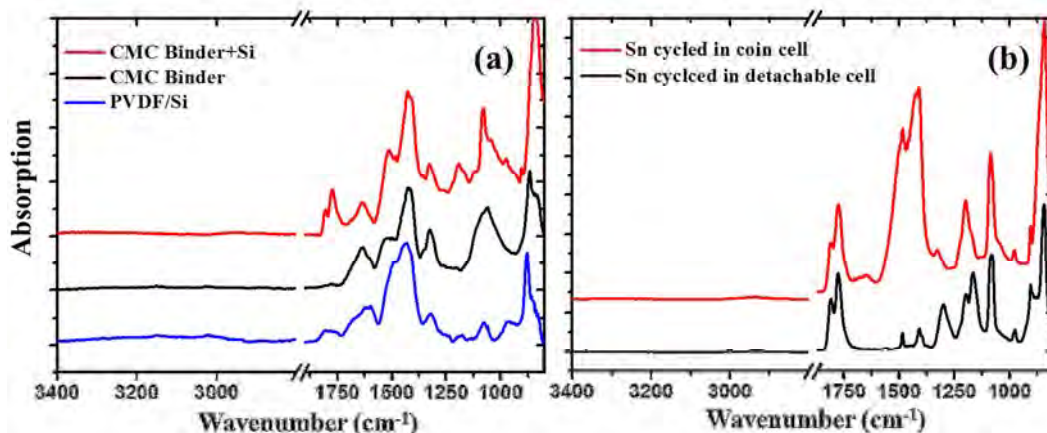


**Figure 1.** *Ex situ* ATR-FTIR spectra of: a.) Si anodes harvested from standard BATT coin cells comparing baseline composition with control samples having just binder (no Si) and Si with PVDF binder after rinsing with DMC to remove residual electrolyte (feature at ca. 1800 cm<sup>-1</sup>); b.) *ex situ* ATR-FTIR spectra of a Sn foil anode harvested from a standard BATT coin cell and an El-cell (type) not rinsed. Strongest features in all spectra except from El-cell is at ca. 1400 cm<sup>-1</sup> indicative of Li<sub>2</sub>CO<sub>3</sub>.

**References:** 1) S. Dalavi, P. Guduru and B. L. Lucht, *Journal of The Electrochemical Society*, 2012, **159**, A642-A646, 2) M. Nie, D. P. Abraham, Y. Chen, A. Bose, and B. L. Lucht, *J. Phys. Chem. C*, 2013, **117**, 13403–13412

### Electrode Materials Design and Failure Prediction

**PROJECT OBJECTIVE:** The goal of this project is to use continuum-level mathematical models along with controlled experiments on model cells to (i) understand the performance and failure models associated with next-generation battery materials, (ii) design battery materials and electrodes to alleviate these challenges. The focus of the research will be on two systems, Si-based anodes and Li-S cells. In Si anodes, the challenges associated with the large volume change and the associated stress effects will be studied. In the Li-S system, the focus will be on the concept of using ceramic single-ion conducting glass layers for lithium protection, along with quantification of the losses associated with such a design and its impact on the performance of the chemistry. A theoretical study of the impact of polarization losses on the energy density will be conducted.

**PROJECT IMPACT:** Si-anode-based Li-ion cells and Li-S cells promise to increase the energy density and decrease the cost of batteries compared to the state-of-the-art. If the performance and cycling challenges can be alleviated, these systems hold the promise for meeting the *EV Everywhere* targets.

**OUT-YEAR GOALS:** At the end of this project, a mathematical model will be developed that can address the power and cycling performance of next-generation battery systems. The initial focus will be on Si anodes and Li-S cells, although the project will adapt to newer systems, if appropriate. The models will serve as a guide for better design of materials, including mechanical properties to reduce stress in Si anodes, and the kinetics and solubility needed to decrease the morphological changes in S cells and increase the power performance.

**COLLABORATIONS:** None this quarter.

#### Milestones

- 1) **Go/No-Go:** Stop materials testing. **Criteria:** Stop materials testing if unsuccessful at obtaining reproducible results for mechanical property values of binder and conductive material composites saturated in electrolyte. (Dec. 13) **Go for materials testing.**
- 2) Incorporate material property values and behavior measured for binders saturated with electrolyte into simulations of model systems. (Feb. 14) **Complete**
- 3) Quantify polarization losses at liquid/SIC interface for different electrolytes. (Mar. 14) **Complete**
- 4) Determine possible reasons for dynamic nature of polarization loss in liquid/SIC interface (e.g., interfacial vs. bulk.) (Jun. 14) **Ongoing**
- 5) Quantify the impact of the interfacial polarization loss between the liquid/SIC by estimating the energy density of a Li-S cell for a given power to energy ratio. (Sep. 14) **Ongoing**

## Progress Report

### Quantifying polarization loss at single-ion conductor/liquid electrolyte interface:

Next-generation chemistries like Li-S have much higher theoretical energy densities than current Li-ion batteries. To prevent polysulfide migration to the Li anode and to limit dendrite growth, the use of single-ion conductors (SICs) has been proposed. SICs act as a physical barrier that prevents dendrites from propagating and also prevents transfer of polysulfides. It is therefore necessary to quantify the polarization loss at the SIC/liquid electrolyte interface. In Q1, a novel methodology to account for the polarization loss at the SIC/liquid electrolyte was developed. Constant current cycling experiments were first performed in a custom Li-Li symmetric diffusion cell in the absence of the SIC. Thereafter, the SIC was incorporated in the cell such that it was sandwiched between two electrolyte chambers. Polarization loss at the SIC/liquid electrolyte interface was then extracted from these two sets of experiments after accounting for Ohmic drop in the SIC and concentration polarization effects in the liquid electrolyte, using a mathematical model. In Q2, polarization loss at the SIC/liquid electrolyte was measured for different concentrations of  $\text{LiPF}_6$  in three different solvents (Fig. 1): ethylene carbonate/diethyl carbonate (1:1), dimethyl sulfoxide (DMSO), and propylene carbonate (PC). Figure 1 shows that irrespective of the solvent, polarization losses at the interface are substantial. This will lead to a decrease in cell voltage at high currents. In the next quarter, possible reasons for polarization loss will be explored. This completes the Mar. 2014 milestone.

**Stress and strain in Si electrodes:** Equipment developed in the previous quarter for mechanical testing of binder materials submerged in solvent has been refined this quarter as the testing procedure has matured. Together with improved sample fabrication procedures, these updates have improved test consistency. Samples of PVDF of two different thicknesses, and with and without conductive additive, have been tested when dry and when submerged in a EC/DEC 1:1 solution. Results suggest that sample thickness, presence of additive, and exposure to solvent can all have a significant effect on mechanical behavior.

For the present, Hooke's law has been retained in the simulation code developed last year as a description of binder stress-strain response. A procedure for extracting Young's modulus values from the raw material testing data has been automated; the values calculated for samples containing conductive additive and immersed in solvent, which are expected to best represent conditions within an actual cell, differ significantly from the mechanical properties of dry PVDF taken from the literature and used in earlier simulations. A set of simulations incorporating the newly measured values has been performed. This fulfills the Feb. 2014 milestone.

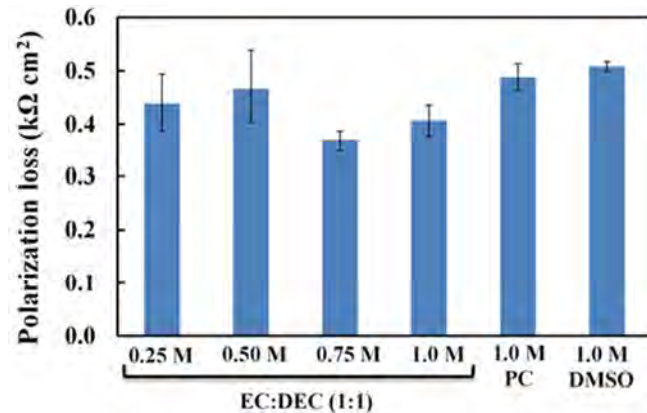


**Figure 1.** Polarization loss for different concentrations of  $\text{LiPF}_6$  in various solvents: ethylene carbonate: diethyl carbonate [EC:DEC(1:1)], dimethyl sulfoxide (DMSO) and propylene carbonate (PC).

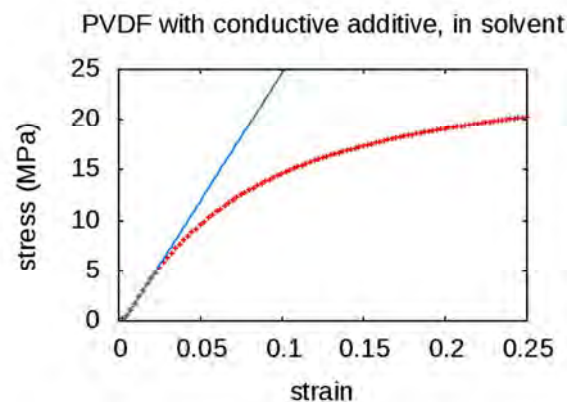


**Figure 2.** Stress-strain curve (red) and automated linear fit (blue) for binder sample containing conductive additive and immersed in solution.

### Predicting and Understanding Novel Electrode Materials from First-Principles

**PROJECT OBJECTIVE:** The aim of the project is model and predict novel electrode materials from first-principles focusing on 1) understanding the atomistic interactions behind the behavior and performance of the high-capacity Li excess and related composite cathode materials and 2) predict new materials using the recently developed Materials Project high-throughput computational capabilities at LBNL. More materials and new capabilities will be added to the Materials Project Lithium Battery Explorer App ([www.materialsproject.org/apps/battery\\_explorer/](http://www.materialsproject.org/apps/battery_explorer/)).

**PROJECT IMPACT:** The project will result in a profound understanding of the atomistic mechanisms underlying the behavior and performance of the Li-excess as well as related composite cathode materials. The models of the composite materials will result in prediction of voltage profiles and structural stability – the ultimate goal being to suggest improvements based on the fundamental understanding that will increase the life and safety of these materials. The Materials Project aspect of the work will result in improved data and electrode properties being calculated to aid predictions of new materials for target chemistries relevant for ongoing BATT experimental research.

**OUT-YEAR GOALS:** During year 1-2, the bulk phase diagram will be established – including bulk defect phases in layered  $\text{Li}_2\text{MnO}_3$ , layered  $\text{LiMO}_2$  ( $M = \text{Co}, \text{Ni}, \text{and Mn}$ ) and  $\text{LiMn}_2\text{O}_4$  spinel to map out the stable defect intermediate phases as a function of possible transition metal rearrangements. Modeling of defect materials (mainly  $\text{Li}_2\text{MnO}_3$ ) under stress/strain will be undertaken to simulate effect of composite nano-domains. The composite voltage profiles as function of structural change and Li content will be obtained. In year 2-4, the project will focus on obtaining Li activation barriers for the most favorable TM migration paths as a function of Li content as well as electronic DOS as a function of Li content for the most stable defect structures identified in year 1-2. Furthermore, stable crystal facets of the layered and spinel phases will be explored, as a function of  $\text{O}_2$  release from surface and oxygen chemical potential. Within the Materials Project, hundreds of novel Li intercalation materials will be calculated and made available.

**COLLABORATIONS:** Gerbrand Ceder (MIT), Clare Grey (U Cambridge, UK), Mike Thackeray (ANL), and Guoying Chen (LBNL).

#### Milestones

- 1) Finalize low T phase diagram including relevant bulk Li, O and Mn and defect phases in layered  $\text{Li}_x\text{MnO}_2$ , spinel  $\text{Li}_x\text{MnO}_3$  and spinel  $\text{Li}_x\text{Mn}_2\text{O}_4$  (Dec. 13) **Complete**
- 2) Over-charge mechanism processes: oxygen migration paths and activation barriers obtained in lowest energy defect structures; oxygen redox potentials obtained (Mar. 14) **Complete**
- 3) Go/No-Go: On over-charge mechanism. Criteria: Oxygen release, migration or oxygen redox process; process down select based on data. (Jun. 14) **Ongoing**
- 4) Composite voltage profiles as function of structural change and Li content obtained (Sep. 14) **Ongoing**

### Progress Report

To elucidate the activation process as well as the structural evolution of  $\text{Li}_2\text{MnO}_3$  as a function of charge and discharge, the role of oxygen was investigated, using first-principles methods and a ternary cluster expansion.

For every extracted Li ion in  $\text{Li}_x\text{MnO}_3$ , the charge of one electron should be compensated. To analyze whether these electrons are primarily originating from orbitals associated with Mn and/or O, the charge of each ion from the magnetic moment was calculated. Cognizant of the fact that the chosen DFT functional determines the degree of localization and charge sharing between the cations and anions, we employed both the GGA, GGA+U and the HSE scheme for a range of structures near the convex hull. A priori, we would expect that the GGA+U and the more computationally expensive HSE scheme, which uses Hartree-Fock hybrid functionals to provide better representations of the electron distribution in a Mn-O system, compared to the GGA.

Indeed, a high level of consistency exists between the GGA+U and HSE results which lends credibility to the results. Using both descriptions of the many-body electron interactions, it was observed that Mn remains largely in the 4+ state and the majority of the redox activity occurs on orbitals primarily associated with the O species.

Oxygen release has been suggested as another possible mechanism for charge compensation in  $\text{Li}_2\text{MnO}_3$  during delithiation. To examine the thermodynamic stability of O, the O vacancy formation enthalpy was calculated (Fig. 1). For each chosen composition ( $0 < x < 2$ ) we examined the formation of an  $\text{O}^{2-}$  or  $\text{O}^{1-}$  (if applicable) vacancy as a function of the local cation environment and symmetry and present only the lowest energy, most favorable, case. Figure 1 shows that O vacancy formation, e.g. evolution from the material, is indeed favorable for  $x < 1$  and hence provides another possible mechanism for the material to compensate the charging process.

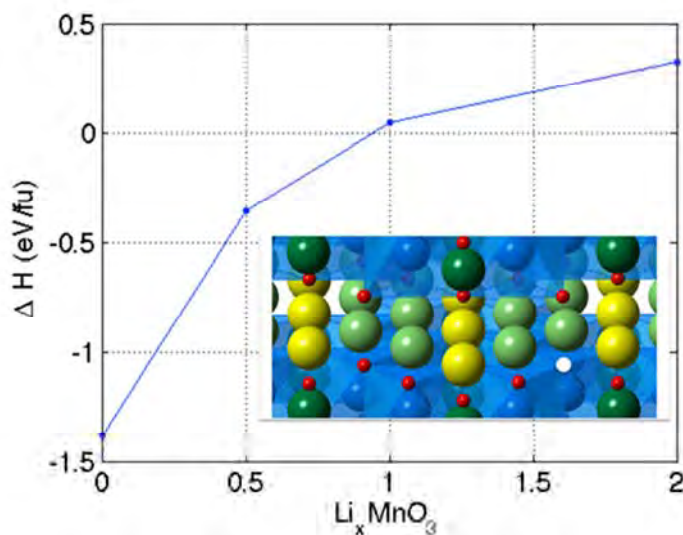


**Figure 1.** The lowest oxygen formation enthalpy as a function of charge state in  $\text{Li}_x\text{MnO}_3$ . Inset illustrates one possible vacancy in the lattice (white circle).

### First Principles Calculations of Existing and Novel Electrode Materials

**PROJECT OBJECTIVE:** Identify the structure of layered cathodes that leads to high capacity. Clarify the role of the initial structure as well as structural changes upon first charge and discharge. Give insight into the factors that control the capacity and rate of Na-intercalation electrodes, and make suggestions for novel Na-intercalation cathode materials. Generate insight into the behavior of alkali-intercalating electrode materials.

**PROJECT IMPACT:** The project will lead to insight in how Li excess materials work and ultimately to higher capacity cathode materials for Li-ion batteries. The project will also lead to definite conclusions as to whether Na-ion batteries can exceed Li-ion batteries in energy density.

**OUT-YEAR GOALS:** Higher capacity Li-ion cathode materials, and novel chemistries for higher energy density storage devices.

**COLLABORATIONS:** Kristin Persson (LBNL)

#### Milestones

- 1) Identify at least three ordered states in  $\text{Na}_x\text{MO}_2$  compounds that can be verified with experiments. (Dec. 13) **Complete**
- 2) Obtain computed voltage curve of  $\text{Li}_2\text{MO}_3$  compound where  $\text{M} = \text{Mn}$  or other metal. (Mar. 14) **Complete**
- 3) Go/No-Go: If voltage curves of Na compounds with less than 0.5V error cannot be modeled. Criteria: Obtain voltage curves for all the  $\text{O}_3$   $\text{Na}_x\text{MO}_2$  compounds where  $\text{M}$  is at least five distinct 3d metals. (Jun. 14) **Ongoing**
- 4) Complete ground state study in Li-Ni-Mn-O and Li-Co-Mn-O system. (Sep. 14) **Ongoing**

## Progress Report

The structure evolution in cation-disordered  $\text{Li}_{1.211}\text{Mo}_{0.467}\text{Cr}_{0.3}\text{O}_2$  (LMCO) upon cycling was investigated. While LMCO forms as a layered rock salt, it transforms to a disordered rocksalt after just a few charge-discharge cycles (Fig. 1A) [1]. In general, disordering leads to poor electrochemical performance in rock salt-like materials [2]. Nevertheless, LMCO cycles remarkably well upon disordering (*ca.* 265  $\text{mAh g}^{-1}$ , Fig. 1C), which was attributed to the percolation of a certain type of active diffusion channels in disordered Li-excess materials [1].

Through *ex situ* X-ray diffraction (XRD), it was found that the change in lattice parameters and volume during charge and discharge is negligible in cation-disordered LMCO. The unit cell volume only varies by *ca.* 0.12% (Fig. 2), which is much less than in layered materials. In layered materials, the c-lattice parameter tends to decrease substantially upon high delithiation, leading to limited Li diffusion at highly charged states [3], and thus makes it challenging to achieve very high specific capacities. In contrast, the stable topology of disordered structures can allow for facile Li diffusion even at highly charged states so that very high capacities can be achieved. Furthermore, such stable structures result in reduced mechanical stress in the electrodes, which in turn extends the cycle-life in Li-ion batteries.

Inspired by our new insight, the search for new cation-disordered materials with 3d transition metal ions as redox centers for high-energy density Li-ion battery cathodes has begun.

[1] J. Lee *et al.*, *Science* **343** (2014) 519-523.

[2] M.N. Obrovac, O. Mao, and J.R. Dahn, *Solid State Ion.* **112** (1998) 9-19.

[3] A. VanderVen and G. Ceder, *Electrochem. Solid-State Lett.* **3** (2000) 301-304.

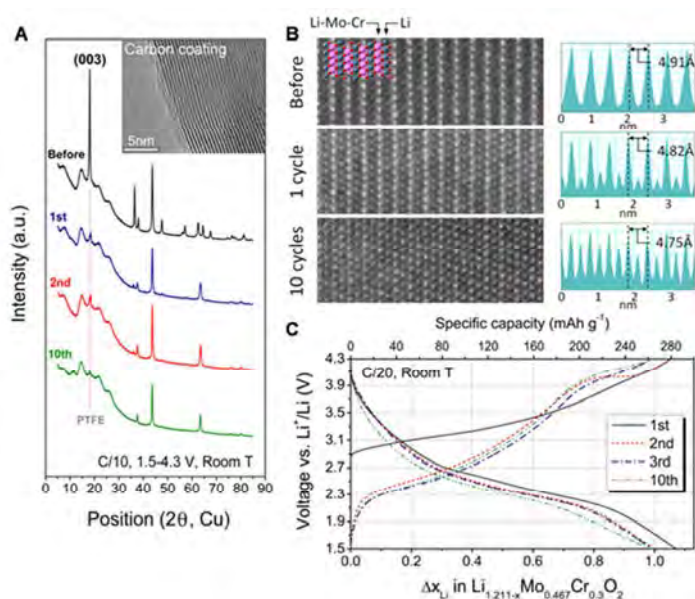


**Figure 1.** (A) XRD pattern of  $\text{Li}_{1.211}\text{Mo}_{0.467}\text{Cr}_{0.3}\text{O}_2$  (LMCO) before and after 1, 2 and 10 cycles. (B) Scanning transmission electron microscopy images of LMCO particles before and after 1 and 10 cycles. (C) The voltage profile of carbon-coated LMCO. The figure has been reproduced from Ref. [1].

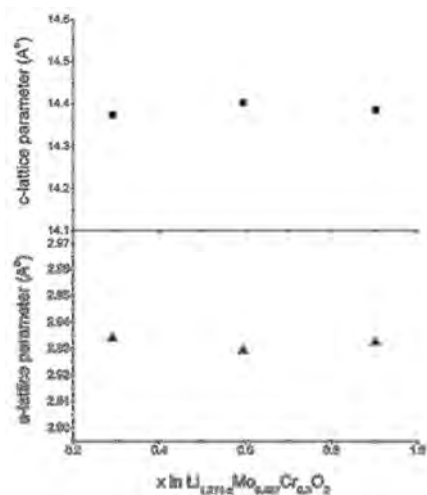


**Figure 2.** The c- and a-lattice parameter in disordered-LMCO upon delithiation.

### First Principles Modeling of SEI Formation on Bare and Surface/Additive Modified Silicon Anode

**PROJECT OBJECTIVE:** This project aims to develop fundamental understanding of the molecular processes that lead to the formation of a SEI layer due to electrolyte decomposition on Si anodes, and to use such new knowledge in a rational selection of additives and/or coatings. The focus is on SEI layer formation and evolution during cycling and subsequent effects on capacity fade through two concatenated problems: 1) SEI layers formed on lithiated Si surfaces, and 2) SEI layers formed on coated surfaces. Key issues that this project addresses include the dynamic evolution of the system and electron transfer through solid-liquid interfaces.

**PROJECT IMPACT:** Finding the correspondence between electrolyte molecular properties and SEI formation mechanism, structure, and properties will allow the identification of new/improved additives. Studies of SEI layer formation on modified surfaces will allow the identification of effective coatings able to overcome the intrinsic deficiencies of SEI layers on bare surfaces.

**OUT-YEAR GOALS:** Investigating the SEI layer formed on modified Si surfaces involves analysis of the interfacial structure and properties of specific coating(s) deposited over the Si anode surface, characterization of the corresponding surface properties before and after lithiation, especially how such modified surfaces may interact with electrolyte systems (solvent/salt/additive), and what SEI layer structure, composition, and properties may result from such interaction. This study will allow identification of effective additives and coatings able to overcome the intrinsic deficiencies of SEI layers on bare surfaces. Once the SEI layer is formed on bare or modified surfaces, it is exposed to cycling effects that influence its overall structure (including the anode), chemical, and mechanical stability. Elucidating such effects using a molecular level approach will help establish their relationship with capacity fading, which will lead to revisiting additive and/or coating design.

**COLLABORATIONS:** Work with Chunmei Ban (NREL) consists in modelling the deposition-reaction of trimethylaluminum and glycerol on Si surfaces and their reactivity. Work with Brett Lucht (URI) relates to finding the best additives for optimum SEI formation on Si anodes. Reduction of solvents and additives on Si surfaces were studied in collaboration with Kevin Leung and Susan Rempe (Sandia National Labs.)

#### Milestones

- 1) Identify reaction pathways and activation energies for electrolyte reduction on lithiated Si surfaces, both clean and covered with surface oxides and/or with selected SEI products. (Dec. 13) **Complete**
- 2) Quantify electron transfer from a lithiated Si surface covered by a model SEI layer to the electrolyte; develop theory/algorithms accounting for voltage effect on electrolyte reduction reactions. (Mar. 14) **Electron transfer studies completed; voltage effect in progress (to be completed in Sept 14).**
- 3) Characterize reactivity of additives; identify reaction pathways and interactions of reaction products with electrolyte components; assess aggregation effects. (Jun. 14) **Ongoing**
- 4) Go/No-Go: Development of a coarse-grained Kinetic Monte-Carlo approach for assessing long-time evolution (order of days) of SEI films. Criteria: Continuation will be based on the demonstrated effectiveness of the technique. (Sep. 14) **Ongoing**

## Progress Report

**Milestone 1.** Work on solvent reduction mechanisms was summarized and published in three articles. In the first one, the ethylene carbonate (EC) reduction mechanisms were analyzed on intermediates and high degrees of lithiation of the Si surface ( $\text{LiSi}_4$ ,  $\text{LiSi}_2$ ,  $\text{LiSi}$ , and  $\text{Li}_{13}\text{Si}_4$ ). The second article discussed reduction of the additive fluoroethylene carbonate (FEC) on  $\text{Li}_{13}\text{Si}_4$ , and the third one referred to EC and FEC reductions at an ultra-low degree of lithiation ( $\text{LiSi}_{15}$ ). Differences were found regarding the adsorption mode of the solvent molecules to the surface showing formation of Si-O bonds at low lithiation and Si-C bonds at higher lithiation. The location of Li-ions also differs substantially, since at low lithiation Li is adsorbed over the plane of the surface, whereas at higher lithiation Li atoms are located on the surface or subsurface plane; thus dramatically affecting the reduction mechanisms.

**Milestone 2.** Electrodes were modeled through various degrees of lithiation: Si,  $\text{LiSi}$ ,  $\text{Li}_{13}\text{Si}_4$ , and Li. *Ab initio* Molecular Dynamics (AIMD) simulations demonstrated the rapid formation of LiF on the surface of lithiated Si anodes having an irregular structure in the initial stages of nucleation, and showed the possible continuation of the EC reduction on parts of the surface that were not covered by LiF. Based on structures obtained from the AIMD simulations, model SEI layers made of LiF fragments were constructed in various thicknesses and configurations, and by analogy,  $\text{Li}_2\text{O}$ , and  $\text{Li}_2\text{CO}_3$  model films were also built. The presence of surface oxides ( $\text{SiO}_2$  and  $\text{Li}_2\text{Si}_2\text{O}_5$ ) revealed a maximum conductivity followed by a decay as a function of oxide thickness. At the same thicknesses and similar configurations, the trend of conductivity showed the order  $\text{Li}_2\text{O} > \text{LiF} \sim \text{SiO}_2 > \text{Li}_2\text{CO}_3 > \text{Li}_2\text{Si}_2\text{O}_5$ . In each case, the resistance of the films is also larger as porosity increases. Thus, this analysis proves useful for testing electron transfer through various SEI configurations. Future reports will address the effect of the SEI cluster geometry and composition. The effect of voltage on electrolyte reductions on Si anodes will be completed by Sep. 2014. The deferral is due to a delay in establishing the DOE subcontract with SNL, and the topic will be addressed in collaboration with K. Leung (SNL).

**Milestone 3.** Reduction mechanisms for VC and FEC additives were identified as a function of the degree of lithiation of the Si anode using static DFT and AIMD simulations. In the case of VC, a two-electron mechanism was observed for  $\text{LiSi}_2$  and  $\text{LiSi}$  surfaces, resulting in an adsorbed  $\text{VC}^{2-}$  anion with a broken C1-O2 bond. Two more electrons are transferred to this species on the  $\text{Li}_{13}\text{Si}_4$  surface, which generates  $\text{CO}_2^{\text{(ads)}}$  and  $\text{OC}_2\text{H}_2\text{O}^{2-}$ . No direct formation of  $\text{CO}_2$  was observed upon reduction of VC on  $\text{Li}_x\text{Si}_y$  surfaces. However, spontaneous reactions between VC and EC-reduction species studied in liquid phase revealed that  $\text{CO}_2$  can be released upon reaction of VC with  $\text{CO}_3^{2-}$ , present in the liquid phase after EC reduction, in agreement with experimental observations. Reduction of FEC on  $\text{Li}_x\text{Si}_y$  surfaces was found to be independent of the degree of lithiation, and taking place through three different mechanisms. One of them leads to the adsorbed  $\text{VC}^{2-}$  anion upon release of HF from the FEC molecule. This is a very interesting finding showing that in some cases the reduction of FEC and VC leads to the exact same reduction products, and explaining similarities in SEI layers formed in the presence of these additives. However, FEC molecules can be also reduced through two other mechanisms, involving the transference of four electrons to the molecules and resulting in either formation of  $\text{CO}_2^{2-}$ ,  $\text{F}^-$ , and  $\text{CH}_2\text{CHO}^-$  or  $\text{CO}^{2-}$ ,  $\text{F}^-$ , and  $\text{OCH}_2\text{CHO}^-$ . These latter reduction products, which are different to the ones produced from VC reduction, may oligomerize and form SEI layers with different components to that formed in the presence of VC. Additionally, in every FEC decomposition pathway observed, the F atom leaves the FEC molecule forming LiF moieties on the anode surface. This is in agreement with experimental observation of increased LiF concentration on SEI layers formed in the presence of FEC. Results obtained in this work agree with experimental reports of chemical structure of SEI layers formed in the presence of FEC and VC additives. This demonstrates that detailed studies of reduction mechanisms of different components of the electrolyte can be used to elucidate the formation process of SEI layers on Si anodes. Future work will focus on elucidating further reaction and/or polymerization of FEC and VC reduction products. The results will be the basis for a coarse-grained model to be developed in the near future (Milestone 4).

### A Combined Experimental and Modeling Approach for the Design of High Current Efficiency Si Electrodes

**PROJECT OBJECTIVE:** The use of high-capacity Si-based electrode has been hampered by its mechanical degradation due to the large volume expansion/contraction during cycling. Nanostructured Si can effectively avoid Si cracking/fracture. Unfortunately, the high surface to volume ratio in nanostructures leads to unacceptable amount of SEI formation and growth, thereby low current/coulombic efficiency and short life. Based on mechanics models we demonstrate that the artificial SEI coating can be mechanically stable despite the volume change in Si, if the material properties, thickness of the SEI, and the size/shape of Si are optimized. Therefore, the objective of this project is to develop an integrated modeling and experimental approach to understand, design, and make coated Si anode structures with high current efficiency and stability.

**PROJECT IMPACT:** The validated model will ultimately be used to guide the synthesis of surface coatings and the optimization of Si size/geometry that can mitigate SEI breakdown. The optimized structures will eventually enable a negative electrode with a 10x improvement in capacity (compared to graphite) while providing a >99.99% coulombic efficiency, which could significantly improve the energy/power density of current LIB.

**OUT-YEAR GOALS:** To develop a well-validated mechanics model that directly import material properties either measured from experiments or computed from atomic simulations. The predicted SEI induced stress evolution and other critical phenomena will be validated against *in situ* experiments in a simplified thin-film system. This comparison will also allow fundamental understanding of the mechanical and chemical stability of artificial SEI in electrochemical environments and the correlation between the coulombic efficiency and the dynamic process of SEI evolution. Thus the size and geometry of coated Si nanostructures can be optimized in order to mitigate SEI breakdown, thus provide high current efficiency.

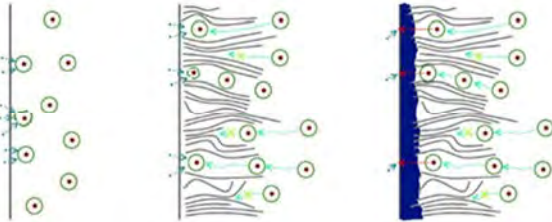
**COLLABORATIONS:** LBNL, PNNL.

#### Milestones

- 1) Compare the basic elastic properties of ALD coatings (e.g.,  $\text{Al}_2\text{O}_3$ ) computed from MD simulations with ReaxFF and measured by AFM and acoustic wave for method validation. (Dec. 13) **Complete**
- 2) Predict the interface strength of given coatings on Si substrate from QM calculations and compare with nanoindentation and scratch tests. (Mar. 14) **Complete**
- 3) Develop a continuum frame work to model SEI deformation and stability on Si film and compare with *in situ* MOSS measurement. (Jun. 14) **Ongoing**
- 4) Go/No-Go: Stop hard coating core-shell structure design. Criteria: If no mechanically stabled coating can be identified after searching in ALD coating property design space using the continuum model. (Sep. 14) **Ongoing**

## Progress Report

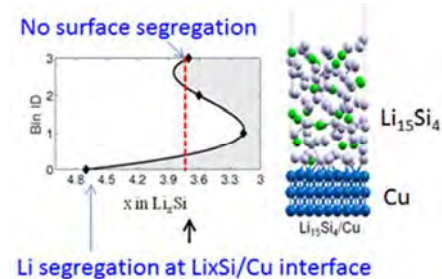
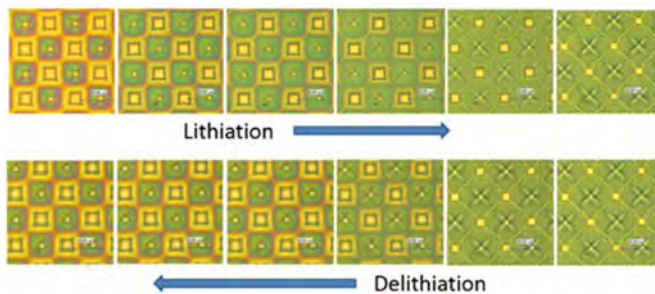
- 1) **Developed SEI growth model:** (a) SEI decomposition at higher potential, resulting in more organic products; (b) Continuing decomposition increases the SEI thickness and decreases meso-porosity, which reduces the growth rate as the solvation complex now has to diffuse to the electrode through SEI that is thicker and denser (ultimately larger complexes are unable to reach the surface at all); (c) At lower voltage a dense SEI forms, which allows Li-ion diffusion but passivates by limiting both electrolyte diffusion and electrical conductivity.



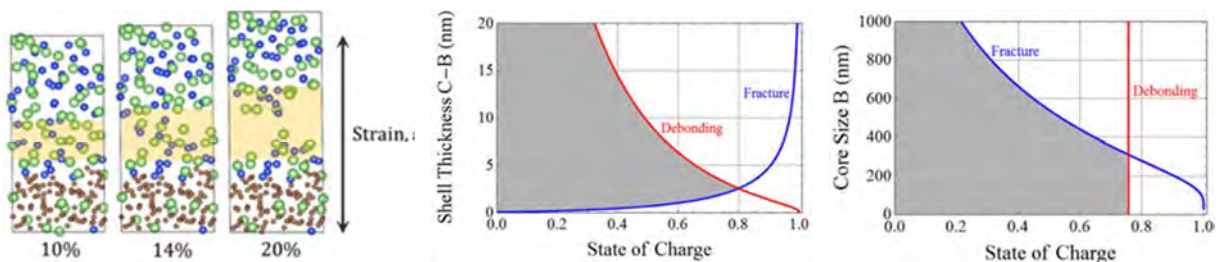
$$\frac{dh}{dt} \approx \frac{V_m c^s}{\left[\frac{1}{k} + \frac{h}{D}\right]} + \frac{V_m c_{et}^s}{\left[\frac{1}{k_{et}} + \frac{h}{D_{et}}\right]}$$

SEI growth limited by electrolyte transport (short times) and electron conduction (long times)

- 2) Developed a model Si pattern thin-film system to connect coating/SEI failure mechanism and electrochemistry performance in order to reveal SEI failure mechanism. The Si islands can slide biaxially and can provide sufficient strain to break SEI.



- 3) A multiscale modeling approach was developed to predict the mechanically stable size of the Si-C core-shell structure. First, *ab initio* simulations were used to calculate interface properties for lithiated a-Si/a-C interface structures and combine these results with linear elasticity expressions to model conditions that will avert fracture and debonding in core-shell structures. The a-Si/a-C interface was found to retain good adhesion even at high stages of lithiation. For average lithiated structures, it has been observed that the strong Si-C bonding averts fracture at the interface; instead, the structure ruptures within the lithiated a-Si. The predicted safe zone for Si-C core-shell structures is when the thickness of the core is less than 200 nm and the thickness of the shell is approximately 10 nm.



- 4) Li diffusion mechanisms are calculated in common SEI components (such as LiF) and typical surface layers (such as SiO<sub>2</sub> and Al<sub>2</sub>O<sub>3</sub>). The results are compared with previous studies on Li<sub>2</sub>CO<sub>3</sub>.

### Predicting Microstructure and Performance for Optimal Cell Fabrication

**PROJECT OBJECTIVE:** This work uses microstructural modeling coupled with extensive experimental validation and diagnostics to understand and optimize fabrication processes for composite particle-based electrodes. The first main outcome will be revolutionary methods to assess electronic and ionic conductivities of porous electrodes attached to current collectors, including heterogeneities and anisotropic effects. The second main outcome is a particle-dynamics model parameterized with fundamental physical properties that can predict electrode morphology and transport pathways resulting from particular fabrication steps. These two outcomes will enable the third, which is an understanding of the effects of processing conditions on microscopic and macroscopic properties of electrodes.

**PROJECT IMPACT:** This work will result in new diagnostic tools for rapidly and conveniently interrogating electronic and ionic pathways in porous electrodes. A new mesoscale 3D microstructure prediction model, validated by experimental structures and electrode-performance metrics, will be developed. The model will enable virtual exploration of process improvements that currently can only be explored empirically.

**OUT-YEAR GOALS:** This project was initiated April 2013 and concludes March 2017. Goals by fiscal year are as follows.

1. Fabricate first-generation micro-four-line probe and complete associated computer model.
2. Assess conductivity variability in electrodes; characterize microstructures of multiple electrodes.
3. Fabricate four-line ionic conductivity probe; complete first-gen dynamic particle packing (DPP) model.
4. Fabricate N-line probe for anisotropic film conductivity; validate DPP model; assess effect of processing variables.
5. Use conductivity predictions in full electrochemical model; evaluate effect of innovative processing conditions.

**COLLABORATIONS:** Karen Thomas-Alyea (A123) and Andrew Jansen (ANL) both provided battery materials. Transfer of technology to A123 to improve their electrode production process is in process. A modeling collaboration with Simon Thiele (University of Freiburg) was continued.

#### Milestones

- 1) Measure variability and average electronic conductivity for five candidate electrode compositions using four-line probe. (Dec. 13) **Complete**
- 2) Measure microstructure of three candidate electrodes using SEM/FIB. (Mar. 14) **Complete**
- 3) Determine appropriate set of descriptors or metrics that effectively characterize previously observed microstructures. (Jun. 14) **Ongoing**
- 4) **Go/No-Go:** Discontinue current four-line probe geometry. **Criteria:** If measurement variability is not significantly less than sample-to-sample variability. (Sep. 14) **Ongoing**

## Progress Report

### Completion of Milestone 2

The microstructures of three electrode samples, Toda 523 (ANL), Toda HE5050 (ANL), and Graphite Anode (A123), were examined using SEM/FIB. The ion beam was used to mill sequentially through the sample; at each stage an SEM image is taken to later produce a cross section. One advantage of SEM/FIB over other X-ray tomography is the unambiguous identification of carbon/binder domains. Figure 1a and 1c each shows one sample 2D cross-section image of a sample microstructure. Analysis of the cross-sectional samples includes segmentation, in which each pixel is assigned to active, carbon/binder, and pore domains.

To date, the Toda 523 (ANL) cathode sample has been analyzed most deeply. First, since the shape of the active material in this case is similar to a sphere, an algorithm was used to measure the diameter of each active material, allowing us to determine an appropriate size distribution of active material, which will be used in subsequent modeling of this electrode material. Second, segmentation of all the 2D images has been completed manually (using image editing software), leading to a 3D reconstructed microstructure of this sample. Figure 1b shows a sample segmentation corresponding to the image in Fig. 1a; black represents active material, gray represents nanoporous carbon/binder, and white represents larger pores. Third, a preliminary algorithm has been developed to automatically segment each 2D image using Matlab Image Processing tools.

Analysis of the 3D structures will continue as part of the next milestone.

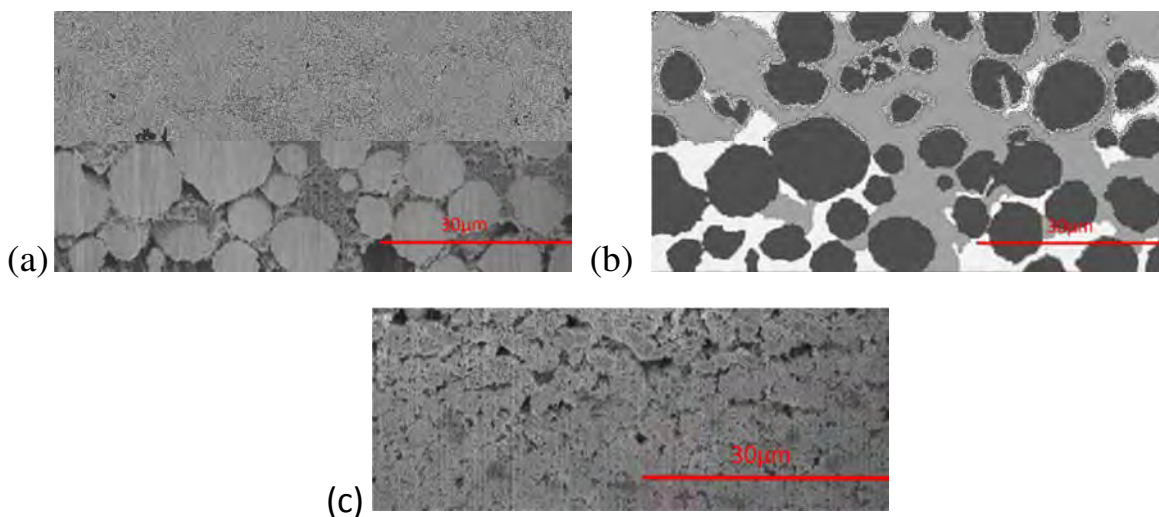


**Figure 1.** (a) FIB/SEM image of Toda 523 NMC cathode (size 81.0µm x 40.7µm); (b) corresponding segmented FIB/SEM image of Toda 523; (c) FIB/SEM image of Toda HE5050 (size 62.98µm x 24.5µm).